ELECTROCHEMICAL ANALYSIS OF SELECTED POLYCHLORINATED BIPHENYLS AND CONTAMINATED WATER REMEDIATION USING POLYANILINE COATED SAWDUST

OKUMU FREDRICK OLUOCH

Cape Peninsula
University of Technology

Electrochemical analysis of selected polychlorinated biphenyls and contaminated water remediation using polyaniline coated sawdust

by

OKUMU FREDRICK OLUOCH

B.Sc. (University of Nairobi)

Thesis submitted in fulfilment of the requirements for the degree

Master of Technology: (Chemistry)

In the Faculty of Applied Sciences

At the Cape Peninsula University of Technology

Supervisor: Dr. M. C. Matoetoe

Co-supervisor(s): Prof. O. S. Fatoki

Prof. T. A. Akenga

Cape Town

November 2012

DECLARATION

I, **Okumu Fredrick Oluoch**, declare that the contents of this thesis represent my own unaided work, and that the thesis has not previously been submitted for academic examination towards any qualification. Furthermore, it represents my own opinions and not necessarily those of the Cape Peninsula University of Technology.

Signed.....**Date**.....18/04/2013.....

ABSTRACT

Polychlorinated biphenyls (PCBs) are known harmful chemicals which require urgent remediation, monitoring and assessment in the environment. The predominant current methods used to analyze PCBs involve expertise and are cost intensive. Most of these methods are chromatographic based techniques which are difficult to sustain in Africa due to the expensive nature of the instrument, costly running expenses and skilled labour required. These limitations face Africans, who are the most affected by the presence of PCBs in their environment as a result of improper disposal and usage of these compounds.

An alternative electrochemical method of selected polychlorinated biphenyl congeners (PCB 28, PCB 52 and PCB 101) was investigated using square wave voltammetry. The PCB square wave voltammograms were characterized by irreversible redox reactions when scanned from 500 mV to -2500 mV. The irreversible reaction occurred at E_{pc1} = -719 mV and E_{pc1} = -1907 mV, for PCB 28 reduction, while for PCB 52 reduction was observed at E_{pc1} = -625 mV and E_{pc2} = -1610 mV and PCB 101 reduction at E_{pc1} = -637 mV and E_{pc2} = -2112 mV. The analytical parameters of the square wave voltammetry (SWV) method, using the glassy carbon electrode at the scan speed and pulse amplitude of 20 mV/s and 25 mV respectively gave lower calculated limits of detection (LODs) within the range of 6.8×10^{-9} M to 1.3×10^{-7} M with remarkable reproducibility range of 7.5 % to 1.5 %. The method had a linear dynamic graph that ranged from 10^{-8} to 10^{-5} M. Sensitivity values obtained in this method ranged from 224.37 µM to 1.33 µM.

Chemical and morphological spectroscopic characterisation of the composites indicated that the polyaniline (PANI) backbone is maintained .Small variations in surface appearances, porosity and chemical composition in the presence of dopants (sawdust and TiO_2) were observed. The colour of PANIs synthesised ranged from blue to cream and their morphology studies by scanning electron microscopy (SEM) and transmission electron microscopy (TEM) depicted a variety of shapes such as honeycombed, rods and cauliflower for PANI, polyaniline coated sawdust (PANI/SD) and functionalised polyaniline coated sawdust (PANI/SD/TiO_2) respectively. They appeared as homogeneous; condensed well defined powders except in the presence of TiO_2 where aggregates were observed.

The UV-visible and fourier transform infrared (FTIR) spectroscopic spectra of these polymers yielded useful information of the electronic band gaps of the polymers relative to each other, which could be directly linked to the redox states of the polymer. The results revealed that the polymers exhibited three UV-visible absorption bands (294, 386 and 526 nm),

corresponding to the absorption of benzenoid and quinoid groups respectively, which are in the polymer structure. The FTIR spectra of PANI showed characteristics peaks at 805 cm^{-1}, 1193 cm^{-1} and 1280 cm^{-1} which was observed in all the composites. The intensity of the peaks increased in the composites. Addition of TiO_2 and SD particles caused significant reductions in the intensity of the aromatic out of plane bending peak 805 cm^{-1}. This indicates that the aromatic rings of the polymer structure have become more stable. Therefore the PANI backbone remained intact in the composites.

Powder X-Ray diffraction (PXRD) investigations indicate that the PANIs synthesized were amorphous with Bragg diffraction peaks for $2\theta \sim 26$ °. The inclusion of TiO_2 and SD had minimum change in the PANI backbone structure. However thermogravimetric analysis (TGA) showed that PANI/SD/TiO_2 adsorbent material was more stable relative to pristine PANI. The thermostability measurements showed an increase in the order PANI < PANI/SD < PANI/SD/TiO_2 < PANI/TiO_2.

This electroanalytical method was used in the feasibility batch adsorption studies of functionalized polyaniline adsorbent material (PANI/SD/TiO_2) to remove PCBs from contaminated solutions. The Langmuir isotherm was found to fit data for both PCB 28 and PCB 101 with Freundlich isotherm fitting PCB 52 adsorption. Adsorption kinetic models was found to vary across the PCB congeners with PCB 28 and PCB 52 favoured by pseudo second order model while PCB 101 was favoured by intraparticle diffusion model.

ACKNOWLEDGEMENTS

First and foremost, I dearly thank the Almighty God for His grace in the period over which I carried out this study.

To my supervisor and academic advisor Dr. M.C. Matoetoe, thank you so much for the progressive evaluation of this work and for giving me the opportunity to work with this project. It is an honour for me to work with you, and to learn from your work ethics. This thesis would not have been possible without your guidance, and your encouragement. I also want to thank you for being very patient with me and assisting me until the very end. My co-supervisors; Prof. O.S. Fatoki and Prof. T.A. Akenga, thank you so much for the facilitation that ensured successful completion. Kindly feel highly appreciated.

To Prof. Emmanuel Iwuoha am so grateful for the assistance and contribution to this work. Feel much appreciated. The sensor lab (UWC) colleagues (Godfrey Fuku, Nwabisa Jijana, Stephen Nzioki, Dr. Peter Ndangili and Dr. Rasaq Wale) and all my friends including Erick Jondiko (CPUT), Maureen Ahawo and Alvin Ouko, your support and motivation are highly appreciated.

To the Centre for Postgraduate Studies (CPGS), the financial assistance of the Cape Peninsula University of Technology (CPUT) towards this research is hereby acknowledged.

Much appreciation to my family members for their love and care during the period of study. My sister and brothers: Pauline Akinyi Okumu, Michael Onyango Okumu (the late), Gregory Ochieng Okumu, each time you assured me of your moral support while studying, I felt highly encouraged and loved. Thank you so much.

Lastly, to my parents Mrs. Monica A. Okumu and Mr. Benedict M. Okumu, this is for you. Thank you very much for your love, care, education and upbringing.

DEDICATION

This is dedicated to me and the entire Okumu family. I would not have done it without their love and support.

- I thank God Almighty for all the blessings and for keeping up with me through all the hard times.

- To Prof. Beatrice Anyango, your tremendous effort is gracefully appreciated thank you so much and may God bless you abundantly.

- To my late brother Michael Onyango Okumu, thank you very much for the support and the hard times we shared.

TABLE OF CONTENTS

DECLARATION ii
ABSTRACT iii
ACKNOWLEDGEMENTS v
DEDICATION vi
TABLE OF CONTENTS vii
LIST OF FIGURES x
LIST OF TABLES xii
LIST OF SCHEMES xiii
APPENDICES xiv
GLOSSARY xv
CHAPTER ONE 1
INTRODUCTION 1
1.1 Background 1
1.2 Research problem 3
1.3 Research questions 5
1.4 Objectives of the research 5
1.5 Thesis outline 6
1.6 References 7
CHAPTER TWO 9
LITERATURE REVIEW 9
2.1 General characteristics of Polychlorinated biphenyls (PCBs) 9
2.2 Physicochemical properties of PCBs 11
2.3 Mechanisms of action of PCBs and Health effects 12
2.4 Sources of exposure 13
2.5 Transport and distribution 14
2.6 Production and use of PCBs 15
2.7 Monitoring and analytical techniques 16
2.8 Remediation techniques for PCBs 18
2.8.1 Bioremediation methods 19
2.8.2 Physical and chemical remediation methods 20
2.9 Polymers as adsorbents 22
2.9.1 Polyaniline 24
2.9.2 Properties of Polyaniline 24
2.9.3 Use of PANI as a remediator 25
2.10 Characterization: Morphological and structural analysis techniques 25

2.10.1 Microscopy techniques....26
2.10.2 Spectroscopic techniques....27
2.10.3 Other techniques....29
2.11 Electroanalytical techniques....31
2.11.1 Cyclic voltammetry (CV)....31
2.11.2 Square wave voltammetry (SWV)....36
2.12 Conclusion....37
2.13 References....38
CHAPTER 3....52
ELECTROCHEMICAL ANALYSIS OF PCBs....52
3.1 Introduction....52
3.2 Experimental method....53
3.2.1 Instrumentation....53
3.2.2 Reagents and materials....54
3.2.3 Electrode preparation....54
3.2.4 Suitability of solvent used as supporting electrolyte....54
3.3 Preparation of PCB analyte....55
3.4 Electrochemical property of PCBs at GC electrode surface....55
3.4.1 Effect of scan rate....58
3.5 Development of the PCBs square wave analysis method....61
3.6 Interferences to PCB detection....65
3.7 Conclusion....68
3.8 References....69
CHAPTER FOUR....71
SYNTHESIS AND CHARACTERIZATION OF POLYANILINES....71
4.1 Introduction....71
4.2 Experimental method....74
4.2.1 Reagents and materials....74
4.2.2 Synthesis of Polyanilines....74
4.2.3 Instrumentation....74
4.2.4 Preparation of PANI composites for UV-visible studies....75
4.2.5 Preparation of PANI composites for FTIR studies....75
4.2.6 Preparation of PANI composites for SEM studies....75
4.2.7 Preparation of PANI composites for TEM studies....75
4.2.8 Preparation of PANI composites for XRD studies....76
4.2.9 Preparation of PANI composites for TGA/DSC studies....76
4.3 Results and discussion....76
4.3.1 Chemical synthesis of PANIs....76

4.3.2 Spectrophotometric characterization of Polyanilines 78
4.3.3 Morphological properties 81
4.3.4 X-ray Diffraction patterns (XRD) 87
4.3.5 Thermal properties 89
4.4 Conclusion 92
4.5 References 94
CHAPTER 5 97
EXTRACTION STUDIES 97
5.1 Introduction 97
5.2 Material and Reagents 99
5.3 Materials and Instrumentation 99
5.4 Extraction procedures 100
5.5 Results and Discussion 100
5.5.1 Kinetics of adsorption 102
5.5.2 Adsorption equilibrium 105
5.6 Conclusion 106
5.7 References 108
CHAPTER 6 111
CONCLUSION AND RECOMMENDATION 111
6.1 Conclusion 111
6.2 Future work and Recommendation 112

LIST OF FIGURES

Figure 2.1: Chemical structure of polychlorinated biphenyls and numbering in the biphenyl ring system.....9

Figure 2.2: Chemical structures of three polychlorinated biphenyl congeners used for the present analysis.....10

Figure 2.3: Global consumption of polymer absorbents and adsorbents (Sources: BCC research).....22

Figure 2.4: Excitation waveform of square wave voltammetry (Curve a) and response obtained by square wave voltammetry (Curve b).....37

Figure 3.1: Cyclic voltammetry of blank and PCB analytes in 0.1 M TBAP/ACN/PBS 80:20 v/v solution at 20 mV/s.....56

Figure 3.2 : Square wave voltammetry of (a) Peak 2 for PCB 28 at concentration 2.5 x 10^{-5} M, (b) Peak 1 for PCB 52 at concentration 1.7 x 10^{-7} M (c) Peak 1 for PCB 101 at concentration 3.1 x 10^{-6} M at different scan rates in glassy carbon electrode in 0.1 M TBAP/ACN/PBS 80:20 v/v solution.....59

Figure 3.3 : Dependence of current (I_p) on the square root of scan rate ($V^{1/2}$) (Randles plot) for peak 1 of PCB 52, PCB 101 and peak 2 for PCB 28 in 0.1 M TBAP/ACN/PBS 80:20 v/v solution.----------.....60

Figure 3.4 : Square wave voltammetry of blank and PCB analytes in 0.1 M TBAP/ACN/PBS 80:20 v/v solution at 20 mV/s.....61

Figure 3.5: SWV curve of (a) Peak 2 of PCB 28, (b) Peak 1 of PCB 52 (c) Peak 1 for PCB 101 different concentrations with glassy carbon electrode in 0.1 M TBAP/ACN/PBS 80:20 v/v solution.....63

Figure 3.6 : SWV calibration curves of (a) Peak 2 current vs. PCB 28, Peak 1 vs. PCB 52 (b) Peak 1 current vs. PCB 101 concentration with glassy carbon electrode in 0.1 M TBAP/ACN/PBS 80:20 v/v solution.....63

Figure 3.7: SWV of PCBs interferences in 0.1 M TBAP/ACN/PBS (80:20 v/v) solution in presence of (a) PCB 28 alone and a mixture of PCB 101 and interference (b) PCB 52 alone and a mixture of PCB 52 and interference, (c) PCB 101 alone and a mixture of PCB 101 and interference.....67

Figure 4.1: General structure of PANI 72

Figure 4.2: Images of SD, PANI, PANI/SD and PANI/SD/TiO_2 after synthesis.....77

Figure 4.3: Various colour changes during polyaniline synthesis.....77

Figure 4.4: FTIR spectra of (a) (i) PANI, (ii) PANI/TiO_2; (b) (i) PANI/SD (ii) PANI/SD/TiO_2 composites.....79

Figure 4.5: UV spectra of (a) PANI, (b) (i) PANI/SD, (ii) PANI/SD/TiO_2 and (c) PANI/TiO_2 ...80

Figure 4.6 : SEM micrographs of (a) PANI (b) acid treated SD (c) PANI/SD, (d) PANI/TiO_2 and (e) PANI/SD/TiO_2. 82
Figure 4.7 : TEM micrograh of, (a) acid treated SD (b) pure PANI, (c) PANI/SD (d) PANI/TiO_2 and (e) PANI/SD/TiO_2 particles. Micrographs obtained at 100 keV at a magnification of 100 nm. 85
Figure 4.8 : X-ray diffraction patterns of acid treated SD, PANI/SD, PANI, PANI/TiO_2 and PANI/SD/TiO_2 composite. 88
Figure 4.9: Thermogravimetric curves (TG curves) and corresponding differential scanning curves (DSC curves) for (a) pure PANI, (b) PANI/SD, (c) PANI/TiO_2 and (d) PANI/SD/TiO_2 composites. 90
Figure 4.10: Comparison of thermal degradation of (a) PANI, (b) PANI/SD, (c) PANI/SD/TiO_2 and (d) PANI/TiO_2. 92
Figure 5.1: Effect of contact time on adsorption of PCBs onto PANI/SD/TiO_2 (0.05 g PANI/SD/TiO_2, ... 101
25 °C, 1.75 h). 101
Figure 5.2: Comparison of SW voltammogram before and after adsorption studies for each PCB used. 101
Figure 5.3: Graphical representation of various adsorption kinetic models used. 103
Figure 5.4: Langmuir and Freundlich isotherms as applied to the PCB adsorption. 106

LIST OF TABLES

Table 2.1: Summary of physical and chemical properties representative of PCBs 12
Table 2.2: Summary of reversible and irreversible electrochemical processes..... 35
Table 3.1: Electrochemical analysis of PCBs 65
Table 3.2: Interference studies of 2,4-dichlorophenol and 2,4,6-trichlorophenol on PCB 28, PCB 52 and PCB 101 detection..... 67
Table 4.1: Comparison of FTIR absorption bands of PANI and PANI composites synthesized in this study. 80
Table 4.2: Summary of the degradation products during thermal analysis 91
Table 5.1: Summary of the kinetic and isotherm parameters for adsorption of PCBs..... 104

LIST OF SCHEMES

Scheme 2.1: Representation of electrochemical reduction of polychlorinated biphenyls 18
Scheme 2.2: Schematic representation of an electrochemical cell consisting of three electrodes: (1) working electrode; (2) auxiliary electrode; (3) reference electrode..... 32
Scheme 3.1: Mechanism of electrochemical reduction of polychlorinated biphenyls. 57
Scheme 4.1: Overall polymerization of aniline in the presence of a dopant or counter ion (A-), where A- can either be a cation, anion, biomass (surface functional groups) or organic compounds such as dyes. 73

APPENDICES

Appendix A: EDX spectrum for PANI/TiO_2 113
Appendix B: EDX spectrum for PANI/SD 113
Appendix C: EDX spectrum for PANI/SD/TiO_2 114
Appendix D: EDX spectrum for PANI 114
Appendix E: EDX spectrum for acid treated sawdust 115

GLOSSARY

Terms/Acronyms/Abbreviations	Definition/Explanation
HPLC	High performance liquid chromatography
PANI	Polyaniline
PCBs	Polychlorinated biphenyls
POPs	Persistent organic pollutants
IR	Infrared radiation
XRD	X-ray diffraction
ECD	Electron capture detector
FID	Flame ionization detector
MS	Mass spectrometry
Ah	Aryl hydrocarbon
PAHs	Polycyclic aromatic hydrocarbon
CV	Cyclic voltammetry
UV-Vis	Ultraviolet-visible light
TEM	Transmission electron microscope
SEM	Scanning electron microscope
SWV	Square wave voltammetry
XRD	X-ray diffraction
FTIR	Fourier transform infrared
TGA	Thermogravimetric analysis
GC	Gas chromatography
ACN	Acetonitrile

CHAPTER ONE
INTRODUCTION

1.1 Background

Environmental pollution is one of the biggest challenges the world faces today. It is an issue that impacts economically, physically and everyday of our lives. Firstly, there is no doubt that living in polluted environment is harmful to our health since the contamination of the environment is linked to some of the diseases that affect us. Pollution is an ever increasing problem that needs to be taken care of as soon as possible, not only for the good of the environment but also for the people that live in it. There are many issues contributing to environmental pollution in the world some of which if well addressed would definitely help both the environment and man. Persistent bio-accumulative pollutants are among the pollutants that pose the greatest chemical threat to sustainability. They can be grouped into two classes; toxic elements: These are the prototypical persistent pollutants such as long-lived radioactive elements which are especially dangerous. New toxicities are continuously being discovered for biologically uncommon elements. The second class consists of degradation-resistant molecules: Many characterized examples originate from the chlorine industry and are also potently bioaccumulative. For example, polychlorinated dibenzo-dioxins and furans (PCDDs and PCDFs) are deadly, persistent organic pollutants. They can form in the bleaching of wood pulp with chlorine-based oxidants, the incineration of chlorine-containing compounds and organic matter, and the recycling of metals.

The United Nations Environmental Program (UNEP), in their international agreement on persistent organic pollutants, list 12 "priority" pollutant compounds and classes of compounds for global phase-out. All are organochlorines. Some of the notable persistent organic pollutants (POPs) are the polychlorinated biphenyls (PCBs). As pollutants, they are of great concern because some of them have been identified to be carcinogenic, mutagenic and teratogenic. These pollutants require constant environmental monitoring and evaluation. Polychlorinated biphenyls (PCBs) are some of the most persistent and ubiquitous pollutants in the environment. Their physicochemical properties are variable owing to the different number of chlorines attached to the biphenyl molecule. The functional properties that make PCBs ideal for "open" applications (e.g., heat insulators, transformers and dielectric fluids) result from the fact that commercial grade PCBs are mixtures or Aroclors (Baker, 1980). Because of their potential carcinogenicity, since the late 1970s the commercial products have not been manufactured on a large scale (Harrad *et al.*, 1994). However, environmental recycling has led to worldwide distribution of PCBs. Measurable levels of PCBs have been

documented universally in ambient air, soils, rivers, sediments and tissues of organisms (EPA, 1976). Once released into the environment, PCBs initially tend to adsorb to organic matter in sediment, bioaccumulate in fatty tissues and subsequently transfer via diet to higher organisms in the food web. Additionally, sediments control concentrations and distributions of PCBs in the water column through re-suspension in the short term while burial is the ultimate fate of PCBs in the long term (Ko and Baker, 1995; Jonsson and Carman, 2000).

The exposure to small doses of PCBs when prolonged over time affects the general population and this is a potential public health problem which has been the subject of many toxicological studies aimed at investigating their possible harmful effects. As a result of these studies, the International Agency for Research on Cancer (IARC) classified PCBs as "probably carcinogenic to humans" (2A group) and the majority of OCPs as "possibly carcinogenic to humans" (2B group) (IARC, 1987; 1991). It is therefore not surprising that various epidemiological studies have been tried in recent years to evaluate the scope of these potential harmful effects, both carcinogenic and non-carcinogenic, in humans (Adami *et al.,* 1995; Porta *et al.,* 1999; Hoyer *et al.,* 2000; Furberg *et al.,* 2002; Engel *et al.,* 2007; Wolff *et al.,* 2007; USEPA, 2008), and that their number is increasing. The effects of PCBs mentioned are an indication that the mechanism and magnitude of PCBs spreading after application continues to be dangerous and thus an active area of research.

Some of the health effects related to PCBs exposure are mainly neurobehavioral changes, endocrine disruption and carcinogenicity. Owing to their toxicity, PCBs as well as other persistent organic pollutants (POPs) can pose a threat to humans and the environment. Since May 2004, a list of 12 toxic POPs are covered by the international treaty called the Stockholm Convention aimed at restricting and ultimately eliminating their production, use, release and storage (UNEP, 2005). Restrictions were established in most European countries during the 1980s, including Spain in 1989. Nevertheless, although its production was banned, an exception was made to allow continued use of PCB-containing equipment, notably electrical transformers and capacitors, until 2025; the recovered PCBs must be treated and eliminated by 2028 (Abdul and Aberuagba, 2005). On the other hand, it is believed that large surfaces of water may release significant amounts of PCB residues from previous uses into the atmosphere. Thus, given the ability of PCBs to move long distances in air and water, the elimination of PCBs becomes an international problem, not dependent only on the effectiveness of national measures (WHO, 2003). The United Nations Environment Programme Governing Council included PCBs among the 12 persistent organic pollutants (POPs) identified for remedial international action (UNEP, 2005).

Comprehensive surveillance and monitoring of human exposure to PCBs are scarce. Even though current levels are on average lower than those measured in the past, this is hardly a reason to disregard monitoring, considering that PCBs continue to be present in the food chain and that most populations have experienced exposure to such compounds for long periods. Adverse health effects in aquatic biota and humans that have accumulated hydrophobic organic contaminants (HOCs) such as polychlorinated biphenyls (PCBs) and polyaromatic hydrocarbons (PAHs) are well documented (NRC, 2001). These have resulted into restrictive use, production and even banning of these chemicals globally. The presence of PCBs in an aquatic ecosystem impacts directly or indirectly to biota and human beings, which results in an ever-increasing demand for the detection of organochlorine contaminants.

The most challenging aspect of these pollutants is discovering how to eliminate them from the environment and where to focus remediation efforts. Even pollutants no longer in production persist in the environment, and bioaccumulate in the food chain. Most methods of PCBs analysis consist of an extraction step, a clean-up step, and a final quantification step. Despite great efforts and expenditure of resources to develop both technically and economically effective cleanup processes of PCB/PAH-contaminated soils/sediments, no widely accepted methods have been found and further research is still needed (GAO, 1996). Nevertheless, recent developments show that the number of available treatment methods will probably increase in the near future (Akgerman *et al.*, 1997; Ekhtera *et al.*, 1997).

1.2 Research problem

Polychlorinated biphenyls (PCBs) are known to be persistent harmful chemicals. Due to this, their remediation, monitoring and assessment in the environment have been researched extensively for years. The predominant current methods used to analyze PCBs involve expertise and are cost intensive. Most of these methods are chromatographic based techniques which are difficult to sustain in Africa due to the expensive nature of the instrument, involve costly running expenses and skilled labour required. These limitations face Africans, who are the most affected by the presence of PCBs in their environment as a result of improper disposal and usage of these compounds.

In view of the above challenges for our environment, human and wildlife, there is no doubt that monitoring of the level of polychlorinated biphenyls with carcinogenic activities, is mandatory, with special emphasis on remediation and detection methods. The common techniques used for detection of polychlorinated biphenyls are gas chromatography (GC), liquid chromatography (LC) and high performance liquid chromatography (HPLC). However,

these methods require long pre-treatment, are time consuming, complex, and involve utilization of expensive and toxic reagents. Thus, preference is given to electroanalytical techniques because they are time saving, have fast response time, use cheap instrumentation and are robust techniques with potential to be used in analyses of PCBs contamination at the point source. Therefore, there is need to develop a method that is user friendly, cost effective and applicable for onsite analysis. Low cost materials can also be used in remediation; as a result their application in monitoring and remediation of PCBs is investigated in this study.

Various electrochemical techniques have been used in the detection of different pollutants notably cyclic voltammetry (CV) and square wave voltammetry (SWV) techniques which have been applied in various contaminants detection. For example, for the determination of heavy metals, square wave anodic stripping voltammetry (SWASV) is widely recognized as an effective analytical technique at low cost (Achterberg and Braungardt, 1999; Jia *et al.,* 2008). This research focused on the electrochemical analysis of selected PCB congeners and contaminated water remediation using titanium dioxide (TiO_2) functionalized polyaniline coated sawdust (PANI/SD/TiO_2. The techniques used in this study involved electroanalysis of selected PCB congeners through development of a method of evaluating and assessing the amount of PCBs in water. Further techniques employed involved use of low cost PANI/SD/TiO_2 material as a possible remediator for PCBs in a contaminated water sample. Various methods have been proven to be effective when applied to analysis and remediation of PCBs in various matrices. However, in this case, an electrochemical method was developed as a low cost alternative that is applicable in any matrix and the TiO_2 functionalized polyaniline coated sawdust was used as a low cost material for remediating PCBs in any matrix. This research was carried out in order to optimize the monitoring and remediation levels of the pollutant from artificial contaminated sites with the aim of *in situ* remediation of real contaminated sites. PCB congeners 28, 52 and 101 were used as pollutants which are normally commercialised by the Company Monsanto USA. To achieve effective monitoring and remediation, various parameters were considered in electrochemical method development and remediation steps.

1.3 Research questions

i. Are the present methods of determination of polychlorinated biphenyl suitable for investigating them in the various sample matrices?

ii. What are the best conditions to employ in the remediation of polychlorinated biphenyls?

iii. To what extent the titanium dioxide (TiO_2) functionalized polyaniline coated sawdust adsorbent remediate polychlorinated biphenyls?

iv. Are there variations in the methodology between the developed electroanalytical method of PCBs analysis and the existing acceptable method?

1.4 Objectives of the research

i. To develop an effective electroanalytical method of analysis for selected PCB congeners namely; 2,4,4'-trichlorobiphenyl (PCB 28), 2,2',5,5'-tetrachlorobiphenyl (PCB 52) and 2,2',4,5,5'-pentachlorobiphenyl (PCB 101) found in water.

ii. To validate the developed method using either a reference sample, comparison with data obtained from high performance liquid chromatography/mass spectroscopy which is the currently adopted PCB analysis method or use of recovery experiments.

iii. To chemically synthesize titanium dioxide (TiO_2) functionalized polyaniline coated sawdust.

iv. To characterize the low cost material by transmission electron microscopy (TEM), scanning electron microscopy (SEM), Fourier transform infrared (FTIR), UV-Visible spectrometry, thermogravimetric analysis (TGA) and X-ray diffraction (XRD).

v. To optimize the remediation studies for selected PCBs using functionalized polyaniline coated sawdust and application of the optimum conditions to real samples.

1.5 Thesis outline

This thesis attempts to develop an electrochemical approach to PCBs analysis and to apply functionalized polyaniline coated sawdust as a possible remediator. Here are the outlines of the remaining chapters in this thesis.

- **Chapter two** of the thesis is for literature review that is introducing theoretical backgrounds of PCBs and characterization methods and tools including: voltammetry and polymers.

- **Chapter three** deals with development of an electrochemical method of analysis of selected polychlorinated biphenyl congeners.

- **Chapter four** of this thesis concentrates on the general experimental procedures for the chemical synthesis of PANI and PANI composites and the characterization of the synthesized polymers. The interaction between the PANI reported in this work with sawdust and titanium dioxide particles with respect to spectroscopic behaviour and structural properties are discussed.

- **Chapter five** examines the application of the TiO_2 functionalized polyaniline coated sawdust in PCB remediation.

- **Chapter six** summarizes the main conclusions and recommendation of the thesis.

1.6 References

Abdul, A. and Aberuagba, F. 2005. Comparative study of the Adsorption of Phosphate by Activated Carbon from Corncobs. Groundnut shell and Rice-husk. *AU. J. T.,* 9(1): 59-63.

Achterberg, E.P. and Braungardt, C. 1999. Stripping voltammetry for the determination of trace metal speciation and *in-situ* measurements of trace metal distributions in marine waters. *Anal. Chim. Acta,* 400: 381-397.

Adami, H.O., Lipworth, L., Titus-Ernstoff, L., Hsieh, C.C., Hanberg, A., Ahlborg, U., Baron, J. and Trichopoulos, D. 1995. Organochlorine compounds and estrogenrelated cancers in women. *Cancer Cause Control,* 6: 551-566.

Akgerman, A. 1997. Supercritical fluids in environmental remediation and pollution prevention. *ACS Symp. Ser.,* Abraham, M.A., Sunol, A.K. (eds), ACS: Washington DC: 670: 208-231.

Baker, R.A. 1980. Contaminants and Sediments: Analysis, Chemistry, Biology. 1st ed. Ann Arbor Science, Ann Arbor, Michigan. ISBN: 0250403072: 627.

Ekhtera, M.R., Mansoori, G.A., Mensinger, M.C., A. Rehmat, A. and Deville, B. 1997. Supercritical fluid extraction for remediation of contaminated soil, *ACS Symp. Ser.,* Abraham, M.A., Sunol, A.K. (eds). ACS: Washington DC: 670: 208-231.

Engel, S.M., Berkowitz, G.S., Barr, D.B., Teitelbaum, S.L., Siskind, J., Meisel, S.J., Wetmur, J.G. and Wolff, M.S. 2007. Prenatal organophosphate metabolite and organochlorine levels and performance on the Brazelton neonatal behavioural assessment scale in a multiethnic pregnancy cohort. *Am. J. Epidemiol.*, 165: 1397-1404.

Environmental Protection Agency. 1976. PCBs in the United States Industrial Use and Environmental Distribution. 1st ed. EPA: Washington: 334.

Furberg, A.S., Sandanger, T., Thune, I., Burkow, I.C. and Lund, E. 2002. Fish consumption and plasma levels of organochlorines in a female population in Northern Norway. *J. Environ. Monitor.,* 4: 175-181.

Government Accountability Office (GAO)/Resources, Community, and Economic Development (RCED)-96-13, GAO. 1996. Report on soil remediation technologies.

Harrad, S.J., Stewart, A.P., Alcock, R., Boumphrey, R. and Burnett, V. 1994. Polychlorinated biphenyls (PCBs) in the British environment: Sinks, sources and temporal trends. *Environ. Pollut.,* 85: 131-146.

Hoyer, A.P., Jorgensen, T., Grandjean, P. and Hartvig, H.B. 2000. Repeated measurements of organochlorine exposure and breast cancer risk (Denmark). *Cancer Cause Control,* 11: 177-184.

International Agency for Research on Cancer. 1987. Polychlorinated biphenyls. IARC Monographs on the Evaluation of Carcinogenic Risks to Humans. Overall Evaluations of Carcinogenicity: An Updating of IARC Monographs, vols. 1 to 42, Supplement 7, Lyon, France: 321-325.

International Agency for Research on Cancer. 1991. Occupational Exposures in Insecticide Applications, and Some Pesticides. IARC Monographs, vol. 53. IARC Press, Lyon, France.

Jia, J.B., Cao, L.Y., Wang, Z.H. and Wang, T.X. 2008. Properties of poly(sodium 4-styrenesulfonate)-ionic liquid composite film and its application in the determination of trace metals combined with bismuth film electrode. *Electroanalysis*, 20(5): 542-549.

Jonsson, A. and Carman, R. 2000. Distribution of PCBs in Sediment from Different Bottom Types and Water Depths in Stockholm Archipelago, Baltic Sea. *Ambio.,* 29: 277-281.

Ko, F.C. and Baker, J.E. 1995. Partitioning of hydrophobic organic contaminants to resuspended sediments and plankton in the mesohaline. Chesapeake Bay. *Mar. Chem.,* 49: 171-188.

National Research Council. 2001. A Risk Management Strategy for PCB-Contaminated Sediments. NRC: National Academy Press, Washington, DC.

Porta, M., Malats, N., Jariod, M., Grimalt, J.O., Rifa, J., Carrato, A., Guarne, R.L., Salas, A., Santiago-Silva, M., Corominas, J.M., Andreu, M. and Real, F.X. 1999. Serum concentrations of organochlorine compounds and K-ras mutations in exocrine pancreatic cancer. *Lancet*, 354: 2125-2129.

United Nations Environment Programme Chemicals. 2005. Ridding the World of POPs: A Guide to the Stockholm Convention on Persistent Organic Pollutants, UNEP: Geneva, Switzerland.

US Environmental Protection Agency. 2008. Health Effects of PCBs. USEPA: http://www.epa.gov/epawaste/hazard/tsd/pcbs/pubs/effects.html [24 April 2012].

Wolff, M.S., Engel, S., Berkowitz, G., Teitelbaum, S., Siskind, J., Barr, D.B. and Wetmur, J. 2007. Prenatal pesticide and PCB exposures and birth outcomes. *Pediatr. Res.*, 61: 243-250.

World Health Organization. 2003. *Health Risks of Persistent Organic Pollutants from Lon-range Transboundary Air Pollution*, The Regional Office for Europe of the World Health Organization, (WHO): Copenhagen, Denmark.

CHAPTER TWO
LITERATURE REVIEW

2.1 General characteristics of Polychlorinated biphenyls (PCBs)

Polychlorinated biphenyls (PCBs) are a group of persistent organic contaminants that were mass produced and released into the environment either inadvertently through spills or by poor disposal practices (ATSDR, 2000). PCBs were introduced in 1929 and were manufactured in different countries under various trade names (e.g., Aroclor, Clophen, and Phenoclor). Polychlorinated biphenyls are normally created by heating benzene, a by-product of gasoline refining, with chlorine. Peak production occurred in the early 1970s, and was banned or restricted in several countries afterwards (IARC, 1978). Several hundred million of kilograms were released into the environment. Due to their hydrophobic properties, PCBs tend to become adsorbed by natural organic matter in soil, sediments and sludges. The majority of the PCBs released into the aquatic environment have, therefore, partitioned into aquatic sediments (Wiegel and Wu, 2000). The chemical formulae of polychlorinated biphenyl is $C_{12}H_{(10-n)}Cl_n$, where n is within the range of 1-10. The basic structure of PCB is illustrated below;

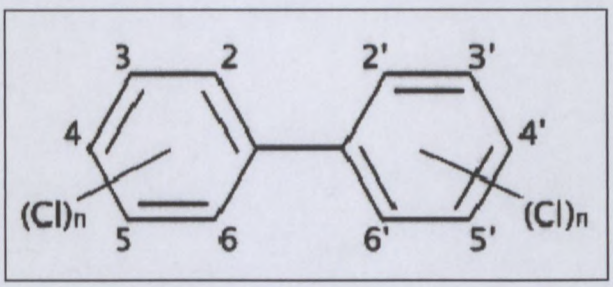

Figure 2.1: Chemical structure of polychlorinated biphenyls and numbering in the biphenyl ring system.

There are 209 polychlorinated biphenyl congeners that persist worldwide in the environment and food chain (Centi *et al.,* 2006). These congeners are divided into three classes based upon orientation of chlorine moieties, i.e., coplanar, mono-ortho coplanar, and non-coplanar (Duffy *et al.,* 2002; Kim *et al.,* 2004). However, only about 130 of these are likely to occur in commercial products. For this study, the selected PCBs congeners are shown in Figure 2.2.

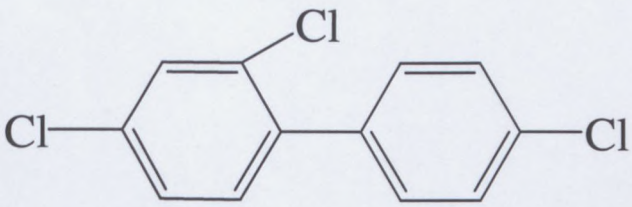

PCB 28 (2, 4, 4'-trichlorobiphenyl)

7012-37-5

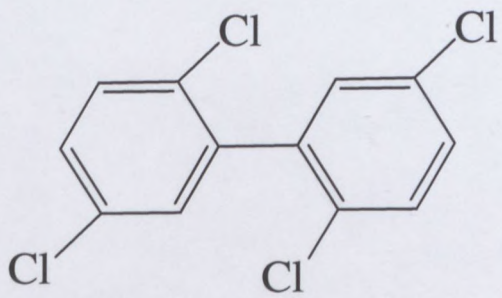

PCB 52 (2, 2', 5, 5'-tetrachlorobiphenyl)

35693-99-3

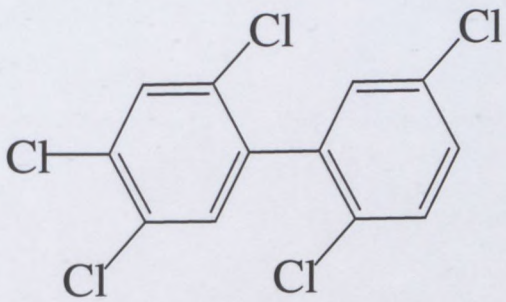

PCB 101 (2, 2', 4, 5, 5'-pentachlorobiphenyl)

37680-73-2

Figure 2.2: Chemical structures of three polychlorinated biphenyl congeners used for the present analysis.

The full chemical notation for these 209 possible PCB congeners is inconvenient, and therefore various shorthand notations have been developed and adopted (Erickson, 1997, 2001). Ballschmiter and Zell, 1980, originally introduced a system (BZ) in which congeners were arranged in ascending numerical order based on the number of chlorine atoms and their substitution pattern on the biphenyl base structure (shown in brackets Figure 2.1). Minor theoretical discrepancies in the BZ naming system were later corrected (Ballschmiter *et al.,* 1992; Guitart *et al.,* 1993). The BZ system of PCB shorthand notation was subsequently recognized by the International Union of Pure and Applied Chemistry (IUPAC) (USEPA, 2003) and is the generally accepted notation used by scientists who perform congener-specific PCB research. According to this IUPAC nomenclature the structure of PCB's constitute two rings; one ring in the biphenyl assembly is assigned an unprimed number and the other biphenyl assembly as primed numbers (Figure 2.1). Later efforts were made by Frame *et al.,* 1996, where they classified the PCBs based on the chemical abstracts service (CAS) registry number (Figure 2.2 underlined numbers) for ease of reference.

In terms of structural relationship to toxicity, PCBs fall into 2 distinct categories, referred to as coplanar or non-*ortho*-substituted arene substitution patterns and noncoplanar or *ortho*-substituted congeners (Kim *et al.,* 2004). The coplanar group members have a fairly rigid structure, with the 2 phenyl rings in the same plane. This gives the molecule a structure similar to polychlorinated dibenzo-*p*-dioxins (PCDDs) and polychlorinated dibenzofurans (PCDFs), and allows it to act in the same way as these molecules as an agonist of the aryl hydrocarbon receptor (AhR) in organisms. These types of PCBs are considered as contributors to overall dioxin toxicity, and the term dioxin is often used interchangeably when the environmental and toxic impact of these compounds is considered. Noncoplanar PCBs, with chlorine atoms at the ortho positions, have not been found to activate the AhR, and are not considered part of the dioxin group. However, studies have indicated some neurotoxic and immunotoxic effects, but at levels much higher than normally associated with dioxins, and thus of much less concern to regulatory bodies (Winneke *et al.,* 1998).

2.2 Physicochemical properties of PCBs

Although the physical and chemical properties vary widely across the class, PCBs have low water solubilities -0.0027-0.42 ng/L for Aroclors, (UNEP, 1997) and low vapour pressures at room temperature, but they have high solubilities in most organic solvents, oils, and fats. Most PCB congeners are colourless, odourless, tasteless crystals, the commercial mixtures are clear to pale-yellow, viscous liquids (highly chlorinated mixtures are more viscous and deeper yellow). They are formed by electrophilic chlorination of biphenyl with chlorine gas. They have high dielectric constants, very high thermal conductivity, (UNEP, 1997) high flash points from 170 to 380 °C (UNEP, 1997) and are chemically fairly inert, being extremely resistant to oxidation, reduction, addition, elimination, and electrophilic substitution (Boate *et al.,* 2004). The density varies from 1.182 to 1.566 kg/L (UNEP, 1997) and their mean molecular weight varies from 188.7 for $C_{12}H_9Cl$ to 498.7 for $C_{12}Cl_{10}$. As the degree of chlorination increases, melting point and lipophilicity increase, and vapour pressure and water solubility decrease (UNEP, 1997). Because of their high thermodynamic stability, all degradation mechanisms are difficult, and environmental and metabolic degradation is generally very slow. PCBs are characterized by their stability, semi-volatility and high lipophilicity. These properties enable PCBs to be highly persistent, to accumulate in the food chain and predispose them to long-range transport. Thus, currently PCBs are found in at least trace amounts worldwide in most compartments of the ecosystem and human tissues (WHO, 2003). Furthermore, PCBs have a long half life (8 to 10 years) which contributes to their stability (Mahan, 1998). PCBs readily penetrate skin, PVC (polyvinyl chloride), and latex (natural rubber) (ANZECC, 1997). PCB-resistant materials include Viton, polyethylene, polyvinyl acetate (PVA), polytetrafluoroethylene (PTFE), butyl rubber, nitrile rubber, and

Neoprene (ANZECC, 1997). Other general properties of PCBs are listed in the following table.

Table 2.1: Summary of physical and chemical properties representative of PCBs

Property	Information	References
Molecular weight	292.0 to 360.9	HSDB, 2009
Specific gravity	1.44 at 30°C	HSDB, 2009
Melting point	340°C to 375°C	HSDB, 2009
Log K_{ow}	7.1	ChemIDplus, 2009
Water solubility	0.0007 g/L at 25 °C	ChemIDplus, 2009
Vapour pressure	0.000494 mm Hg at 25 °C	SRC, 2009

2.3 Production and use of PCBs

Prior to the public outcry concerning the apparent link between PCBs and widespread environmental problems and the discovery of their detrimental health effects, PCBs were produced commercially in the United States from 1929 until 1977. The total global production of PCBs between 1930 and 1993 has been estimated to be 1.324 million tonnes (Breivik *et al.,* 2002). However, about 2.1 x 10^8 kg of PCBs, one-third of the total quantity produced, has been released into water, sediments and soil (Hutzinger and Verrkamp, 1981; Fava *et al.,* 2003 and Kastanek *et al.,* 2004). The global spatial and temporal consumption pattern of individual PCBs is considered essential information for the interpretation of global PCB contamination patterns.

Prior to 1976, PCBs were used both for nominally closed applications (e.g., capacitor and transformers, heat transfer and hydraulic fluids) and in open-end applications (e.g., flame retardants, inks, adhesives, microencapsulation of dyes for carbonless duplicating paper, paints, pesticide extenders, plasticizers, polyolefin catalyst carriers, slide-mounting mediums for microscopes, surface coatings, wire insulators and metal coatings (IARC, 1978; Safe, 1984). The main use of PCBs has been as dielectric insulating material in electrical equipment such as capacitors and transformers.

Due to their wide applications, they were mass produced and released into the environment either inadvertently through spills, usage or by poor disposal practices (ATSDR, 2000). Unfortunately, a lack of flammability translates to antioxidant behaviour, which explains why

the PCBs are so persistent when released into the environment (Rajashwar and Ibanez, 1997) and also why they are commonly known as a group of persistent organic contaminants. Even though the production of these contaminants has stopped, PCBs continue to be detected in environmental samples from around the world e.g. (Iwata *et al.,* 1994; AMAP, 1998).

2.4 Sources of exposure

Polychlorinated biphenyls have been released to the environment solely by human activity. The European PCBs emission inventory for 1990 (Berdowski *et al.,* 1997) enumerates the following sources: coal combustion, steel smelting (open-hearth, converter, electric), sintering, waste incineration, electrical equipment (capacitors and transformers) as sources of exposures to polychlorinated biphenyls. Apart from certain occupational settings and release from PCB-containing waste sites, food is the main source of exposure for the general population. This is of great concern as the nutritional role of fish as a part of a healthy diet has notably increased in recent years. In food samples of animal origin the most persistent congeners PCB 138 and 153 show the highest levels, whereas the easier metabolizable PCBs 28 and 52 show the lowest levels. PCBs 101 and 180 exhibit an intermediate level (Kunz *et al.,* 2006). The lower chlorinated congeners, PCBs 28, 52 and 101 are present at somewhat higher levels in cereals, fruit, vegetables and vegetable oil compared to food of animal origin. Because of their volatility, PCBs 28 and 101 also play a role as pollutants in indoor and outdoor air (Buehler *et al.,* 2002; Herrick *et al.,* 2004). In indoor air the volatile congeners mainly escape from sealants of doors and windows and remain rather in the gaseous phase than bind to particulate matter. Liebl *et al.,* 2004, reported elevated levels of PCBs 28, 52 and 101 in blood of pupils exposed to high indoor levels of PCBs in a contaminated school.

Because PCBs are no longer manufactured or imported in large quantities, significant releases of newly manufactured or imported materials to the environment do not occur. Rather, PCBs predominantly are redistributed from one environmental compartment to another (e.g., soil to water, water to air, air to water, sediments to water) (Larsson, 1985; Swackhamer and Armstrong, 1986; Lin and Que Hee, 1987; Mackay, 1989; Eisenreich *et al.,* 1992). Thus, for example, the majority of PCBs in air result from volatilization of PCBs from soil and water. Some PCBs may be released to the atmosphere from uncontrolled landfills and hazardous waste sites; incineration of PCB-containing wastes; leakage from older electrical equipment in use; and improper disposal or spills (Murphy *et al.,* 1985; Eisenreich *et al.,* 1992; Wallace *et al.,* 1996; Hansen *et al.,* 1997; Bremle and Larsson, 1998). PCBs may be released into water from accidental spillage of PCB-containing hydraulic fluids;

improper disposal; combined sewer overflows (CSOs) or storm water runoff; and from runoff and leachate from PCB-contaminated sewage sludge applied to farmland (Gan and Berthouex, 1994; Gunkel *et al.,* 1995; Shear *et al.,* 1996; Pham and Proulx, 1997).

2.5 Transport and distribution

Polychlorinated biphenyls are globally circulated and are present in all environmental media. Atmospheric transport is the most important mechanism for global dispersion of PCBs. Biphenyls with 0-1 chlorine atom remain in the atmosphere, those with 1-4 chlorines gradually migrate toward polar latitudes in a series of volatilization/deposition cycles, those with 4-8 chlorines remain in mid-latitudes, and those with 8-9 chlorines remain close to the source of contamination (Wania and Mackay, 1996). The lower chlorinated PCBs (IUPAC No. 18, 28 and 52) constitute up to 40 % of the total PCBs (Jones *et al.,* 1992). Studies on PCB congener distribution analysis of PCB 52 and 101 has been reported using trophodynamic analysis where most of the differential PCB fractionation seemed to occur at the lower end of the food chain (water to plankton to mysid). At the higher trophic levels (mysid to smelt to salmonid), the PCBs seemed to be distributed as a uniform composition mixture (Oliver *et al.,* 1988). PCBs enter the atmosphere from volatilization from both soil and water surfaces (Hansen, 1999). Once in the atmosphere, PCBs are present both in the vapour phase and sorbed to particles. PCBs in the vapour phase appear to be more mobile and are transported further than particle-bound PCBs (Wania and Mackay, 1996). Wet and dry depositions remove PCBs from the atmosphere (Dickhut and Gustafson, 1995; Nelson *et al.,* 1998). The dominant source of PCBs to surface waters is atmospheric deposition; however, redissolution of sediment-bound PCBs also accounts for water concentrations (Hansen, 1999). PCBs in water are transported by diffusion and currents. PCBs are removed from the water column by sorption to suspended solids and sediments as well as by volatilization from water surfaces. Higher chlorinated congeners are more likely to sorb, while lower chlorinated congeners are more likely to volatilize (Eisenreich *et al.,* 1992; Pearson, 1996). PCBs also leave the water column by concentrating in biota. PCBs accumulate most in higher trophic levels through the consumption of contaminated food, a process referred to as biomagnification (Willman *et al.,* 1999). PCBs in soil are unlikely to migrate to groundwater because of strong binding to soil (Sklarew and Girvin, 1987). Volatilization from soil appears to be an important loss mechanism; it is more important for the lower chlorinated congeners than for the higher chlorinated congeners (Hansen, 1999). Vapour-phase PCBs accumulate in the aerial parts of terrestrial vegetation and food crops by vapour-to-plant transfer (Bohm *et al.,* 1999).

2.6 Mechanisms of action of PCBs and health effects

Polychlorinated biphenyls exhibit a wide range of toxic effects. These effects may vary depending on the specific PCB. Similar to dioxin, toxicity of coplanar PCBs and mono-ortho PCBs are thought to be primarily mediated via binding to aryl hydrocarbon receptor (AhR) (Safe and Hutzinger, 1984; Safe *et al.,* 1985). Because AhR is a transcription factor, abnormal activation may disrupt cell function by altering the transcription of genes. Due to their high binding affinity to the aryl hydrocarbon (Ah) receptor, coplanar congeners are potentially the most toxic (Silkworth *et al.,* 1984) and have been also shown to impact the immune system suppressing immunocompetence. The concept of toxic equivalency factors (TEF) is based on the ability of a PCB to activate aryl hydrocarbon receptor (AhR). However, not all effects may be mediated by the AhR receptor, and PCBs do not alter estrogen concentrations to the same degree as other ligands of the AhR receptor, such as polychlorinated dibenzodioxins (PCDD) and polychlorinated dibenzofurans (PCDF) (Wang *et al.,* 2006). Examples of other actions of PCBs include di-ortho-substituted non-coplanar PCBs interfering with intracellular signal dependent on calcium; this may lead to neurotoxicity (Simon *et al.,* 2007). Ortho-PCBs may disrupt thyroid hormone transport by binding to transthyretin (Chauhan *et al.,* 2000).

These mechanisms of action result in health effects related to PCB exposure which are mainly neurobehavioral changes, endocrine disruption and carcinogenicity (Longnecker *et al.,* 2003). PCB 52 has been reported to result in tumour promotion (Oesterle and Deml, 1981; Buchmann *et al.,* 1986; Sargent *et al.,* 1991). Past studies have also reported PCBs to inhibit oestrogen sulfotransferase, the enzyme responsible for the inhibition of oestrogen metabolism (Kester *et al.,* 2000). It has been reported that the non-coplanar PCB 52 increased DNA damage as assessed in the comet assay in acutely cultured human lymphocytes (Sandal *et al.,* 2008) while PCB 28 have been found to suppress aromatase activity in vitro (Woodhouse *et al.,* 2004).

PCBs can also be toxic to higher plants, marine biota, and birds. PCBs may interfere with the overall growth of some plant species, by inhibiting cell division, and also interfere with photosynthesis in some plants. PCBs can induce mixed function oxidase (MFO) enzymes and can inhibit ATPases in marine biota. PCBs are known to effect hormones in fish, and in birds, they can cause teratogenic and behavioral effects (Waid, 1986b). PCBs can also be toxic to some microorganisms, including the fresh-water, marine and soil microorganisms (WHO, 1993). PCBs may affect respiration and photosynthesis in some algae, whereas, they can reduce the micelial growth and increase the relative RNA content of the mycelium in some fungi (WHO, 1993).

Therefore PCBs are generally toxic and due to this, they are a threat to humans and the environment. This was further emphasized by the United Nations Environment Programme Governing Council resulting in inclusion of PCBs among the 12 persistent organic pollutants (POPs) identified for remedial international action (UNEP, 2005).

2.7 Monitoring and analytical techniques

It is of paramount importance to monitor and study the behaviour of PCBs to establish a better understanding of their trends and impacts in the surrounding environment. For these reasons, reliable analytical methods are required. There are various monitoring techniques done for PCBs. Most of which are analytical based and involve field or laboratory tests. A number of analytical tests are available for determining the presence of PCBs in various media, for example simple methods and laboratory analytical methods (UNEP, 1999). Simple methods cannot quantify the concentration of PCBs or provide complete verification of PCB presence. They are used as preliminary steps. Laboratory analytical methods can be divided into two categories: non-specific and specific methods (Finch, 1990). Non-specific methods identify classes of compounds, such as chlorinated hydrocarbon, to which PCB belong. Specific methods test particularly for PCB molecules. The main challenges of monitoring studies include volatility and the insolubility properties of the PCBs and the fact that PCBs are found in very low concentrations. This shows the need for highly sensitive techniques that are robust.

Current PCB analysis methods are based on complex laboratory-based instrumental techniques, mainly high performance liquid chromatography (HPLC) and gas chromatography (GC) coupled with different detection techniques such as mass spectrometry (MS), electron capture detector (ECD), and flame ionization detector (FID). Routine analysis of PCBs in environmental matrices is typically done through gas chromatography coupled with mass spectrometry (GC/MS) and different extraction techniques (Muir and Sverko, 2006). These conventional methods are generally time-consuming and expensive and typically require sample preparation before the chromatographic separation (Ferrario *et al.,* 1997). Along with the preconcentration studies, these procedures often take up most of the total analysis time, contributing highly to the total cost of analysis, and greatly influencing the reliability and accuracy of the analysis. In addition to this, most of the analyses involve the use of organic solvents, the techniques are not user friendly and they are generally performed at centralized laboratories (Lin *et al.,* 2008).

Alternative methods based on immunoassays have also been used to detect PCBs. Among the high number of immunoassay techniques, the enzyme-linked immunosorbent assays

(ELISA) combined with a colorimetric end point measurement are the most widely used (Fillman *et al.,* 2002). Disposable magnetic beads have also been used as immunosensors for monitoring polychlorinated biphenyl (PCBs) pollutants (Centi *et al.,* 2006). However, this technique requires expensive instrumentation, which is not suitable for on-site analysis, and usually the analysis procedure is time-consuming (Del Carlo *et al.,* 1997). Other studies have shown PCB 101 detection using the membrane of fluorophore phenyl isothiocyanate immobilized porous anodic aluminium oxide which exhibited dynamic fluorescence detection (Wang *et al.,* 2011).

Recently the electroanalytical methods have become the preferred choice over other methods as they are simple and have rapid procedures with a potential for a wide range of applications in food and clinical chemistry (Kotani *et al.,* 2002) amongst other applications. Electrochemical reduction constitutes a simple, effective and elegant method for the analysis of polychlorinated biphenyls. The merit of electrochemical reduction is that it is safe; it needs no potentially dangerous reagents and is easy to control. The electrochemical reduction of polychlorobiphenyls involves the dissociation of the C-Cl bonds. The decomposition of each C-Cl bond in polychlorinated biphenyls follows one of the two different mechanisms (i) stepwise and (ii) concerted (Muthukrishnan *et al.,* 2012). The relative rates of the two steps of the reduction (electron transfer vs. the bond breaking step) determine the mechanism of the reduction (Muthukrishnan *et al.,* 2012). If the bond breaking step is slow relative to the electron transfer, the reaction follows the stepwise mechanism, and analogously, if the bond breaking step is faster, the concerted mechanism is inferred. The neutral radical formed after dissociation of chloride anion undergoes reduction at a lower potential than the parent compound and leads to the formation of the anion. The anion abstracts a proton predominantly from solvent (Webster, 2004) thereby yielding the completely dechlorinated compounds (Scheme 2.1).

Other examples of electroanalytical studies include electrochemical dechlorination of polychlorinated biphenyls (PCBs) using mediators (Matsunaga and Yasuhara, 2005) which has been reported in PCB analysis involving mainly electrochemical reduction steps. PCB 52 has also been analyzed through electrochemical reduction in a bicontinous microemulsion media (Huang and Rusling, 1995). In contrast, reductive methods offer relatively mild conditions for the selective dechlorination of such compounds. Thus, metallic sodium (Suzuki, 1997), solvated electrons (Brown, 1996) or biphenyl radical anions (Oku *et al.,* 1978) have been successfully used as reducing reagents.

Thus, while this review attempts to summarize the current best practices for analysis of PCBs, a major focus is the need for low-cost methods that can be easily implemented in developing countries.

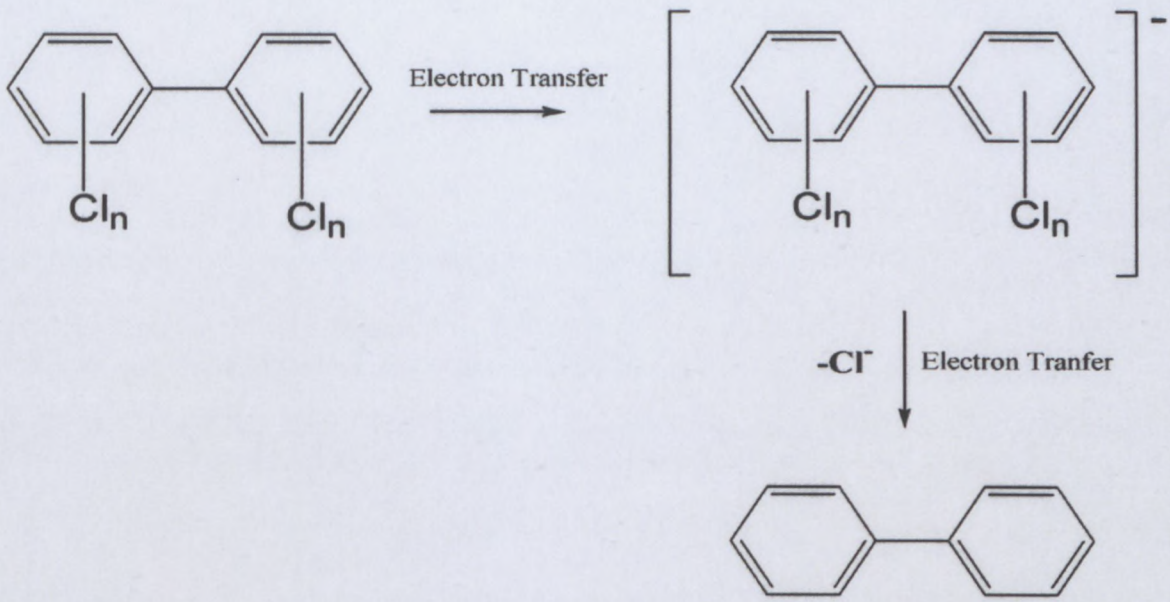

Scheme 2.1: Representation of electrochemical reduction of polychlorinated biphenyls

2.8 Remediation techniques for PCBs

Removal and monitoring of PCB's in the environment is vital to maintain human health. This is achieved by remediation and analysis of at risk environmental samples. Remediation involves destruction or physical removal of the PCBs in the sample. However, PCBs destruction by chemical, thermal, and biochemical processes is extremely difficult and present risk of generating extremely toxic dibenzodioxins and dibenzofurans through partial oxidation. Intentional degradation as a treatment of unwanted PCBs generally requires high heat or catalysis. Therefore, various methods are used to carry out remediation, reduction and cleanup of these persistent organic pollutants which are threatening the environment. Remediation methods can be subdivided into two categories; degradation and adsorption predominantly in water and soil. Degradation is carried out using microorganism (biodegradation) or using chemicals especially catalysts (catalytically) while adsorption is basically done using adsorbents such as activated carbon (Sotelo *et al.,* 2002).

The remediation of PCB contaminated water has focused on biological, physical and chemical methods. Biological methods are called bioremediation. These are treatment

processes which use microorganisms such as fungi and bacteria to degrade hazardous substances into nontoxic substances (Mori and Kondo, 2002). The microorganisms break down the organic contaminants into harmless products; mainly carbon dioxide and water. Bioremediation may be a lucrative and environmentally beneficial alternative that could produce economic profit (Iranzo *et al.,* 2001). However, some drawbacks occurs during aerobic and anaerobic processes of breaking down the original contaminants as a result of production of intermediate products that are less, equally, or more toxic than the original contaminants (Kulkarni *et al.,* 2008). In addition to this the bioremediation steps do not completely destroy the pollutants. Other disadvantages are the bioremediation regulations, which has resulted in some design engineers avoid bioremediation processes (Boopathy, 2000).

Physical methods have mainly focused on adsorption processes which involve use of adsorbents such as activated carbon to extract pollutants from mainly water and soil while chemical methods involve the use of chemical reagents and media for the decomposition of polychlorinated aromatic compounds in soil and water. Among diverse methods of removal of pollutants, adsorption remains the most commonly practised method (Sotelo *et al.,* 2002) since it is found to be superior compared to other techniques in terms of initial cost, flexibility and simplicity of design, ease of operation and insensitivity to toxic pollutants. Moreover, adsorption does not result in the formation of harmful substances (Gayatri and Ahmaruzzaman, 2010). Chemical processes, such as advanced oxidation processes, photocatalysis, degradation, reductive dehalogenation in the presence of metals, supercritical water oxidation and hybrid methods, as well as physical processes like sorption on activated carbon and ultrafiltration have given very good results and high PCB removal, but they do not appear cost-effective.

2.8.1 Bioremediation methods

Bioremediation of PCB involves usage of fungi, bacteria in presences or absence of oxygen. The microorganisms can be used alone or in combination with chemicals or physical methods. Contaminated soil remediation has been suggested using a combination of anaerobic and aerobic treatments. For example, aerobic treatments would metabolize the lower chlorinated homologs (e.g., biphenyl; mono- and di-ortho chloro-substituted chloro biphenyls) produced in soil from anaerobic dechlorination processes (Tiedje *et al.,* 1993). Numerous bacterial and some fungal isolates have been reported to aerobically biodegrade PCBs (Abramowitz, 1990). Experiments with both pure and mixed microbial cultures have shown that some congeners of PCBs, usually containing one to four chlorine substituents, are readily biodegraded aerobically (Abramowitz, 1990), although biodegradation of

congeners containing up to six or seven chlorine atoms have been shown under enrichment conditions (Gibson *et al.,* 1993).

Other diverse techniques used for the degradation of PCBs include biochemical degradation using bacteria (Ye *et al.,* 1995; Furukawa *et al.,* 2004). The ability of plant cells to metabolize PCBs has also been demonstrated eg. *Brassica nigra* directly contributed to accelerated PCB removal in Aroclor 1242 contaminated soil (Singer *et al.,* 2003). *Carex aquatalis* and *Spartina pectinata* are predicted to be the most effective plant treatments for phytoremediation of PCBs (Smith *et al.,* 2007). Alfalfa, black nightshade, and particularly tobacco grown in soil with a long-time PCB contamination have a positive effect on the rate of PCB degradation (Ryslava *et al.,* 2003). Biomass materials such as mushroom have also been applied in bioremediation (Adenipekun and Lawal, 2012).

2.8.2 Physical and chemical remediation methods

The most widely practiced physical treatment method for PCBs in aqueous wastes is activated carbon adsorption. This method is suitable insofar as PCBs are very apolar pollutants (Sotelo *et al.,* 2002). Due to the high cost of activated carbon, researchers have investigated usage of biomass and polymers. Some of the notably practised methods include incineration. For example, Baukal *et al.,* 1994 reported waste incineration using oxy-fuel technology in simulated soils containing 1 % PCBs and oil containing up to 40 % PCBs, more than 99.99 % of the PCBs were destroyed. The general acceptance of incineration as a means of disposal for PCB-contaminated materials has declined because of concerns about incomplete incineration and the possible formation of highly toxic dioxins and dibenzofurans if the combustion temperature is not held sufficiently high (Arbon *et al.,* 1994; Chuang *et al.,* 1995). These limit application of incinearation since there is a need to carefully control the reaction conditions. Solutions to these limitations have been treatment with metallic sodium which was suggested for PCB wastes because it yielded low molecular weight polypropylene and sodium chloride which are less undesirable than products from incineration (IRPTC, 1985).

Other physical methods reported include application of various technologies such as thermal desorption, solvent extraction, wet air oxidation, and an incineration process known as anaerobic thermal process (ATP) to PCB-contaminated sediment. Timberlake and Garbaciak, 1995, reported both thermal desorption and solvent extraction technologies indirectly separated contaminants from a solid matrix and concentrated them into smaller volumes of treatable oily residues. Wet air oxidation process which use elevated temperatures and pressure to oxidize the organic constituents, was reported not very

effective in destroying PCBs (Timberlake and Garbaciak, 1995). Zhang and Rusling, 1995, investigated electrochemical catalytic dechlorination as a method for decontaminating soils and reported 94 % dechlorination level using a lead cathode and a micro emulsion of didodecylmethylammonium bromide, dodecane, and water containing 6.5 % organic matter and contaminated with 14 % Aroclor 1260 (84 mg of PCB). Other examples of physical methods involved use of fly ash which was found to be effective for the removal of PCBs from an aqueous solution. It could be an alternate adsorbent to commercially available carbon due to its low cost and good efficiency. Further example involves both reverse osmosis (RO) and ultrafiltration (UF) membrane which has been used in removal of PCBs with a consistent achievement of > 99.5 % removal (Wu *et al.,* 1998).

The conventional chemical methods have been used in the decomposition of polychlorinated biphenyls such as reduction, hydrogenation, and dechlorination (Ross and Lemay, 1987; Hawari, 1992; Roth *et al.,* 1994; Chu *et al.,* 2005; Agarwal *et al.,* 2007). Chemical destruction method has been used for the treatment of PCBs in contaminated dielectric liquids or soil based on the reaction of a polyethylene glycol/potassium hydroxide mixture with PCBs (De Filippis *et al.,* 1997). This method was used successfully for the destruction of higher chlorinated PCBs with an efficiency of > 99 %, but was found to be unsuitable for the treatment of di- and trichlorobiphenyls due to low destruction efficiencies (Sabata *et al.,* 1993). Irradiation of PCBs in isooctane and transformer oil has been achieved using γ-radiation which resulted in degradation of PCBs to less chlorinated PCBs and PCB-solvent adducts (Arbon *et al.,* 1996). Hofelt and Shea, 1997, demonstrated the use of semi permeable membrane devices to accumulate PCBs from New Bedford Harbor, Massachusetts water.

Another method showing some promise for the treatment of PCBs in water, soil, and sediment is titanium dioxide-catalyzed photodecomposition with sunlight (Zhang *et al.,* 1993; Zhang and Rusling, 1995; Hong *et al.,* 1998). Catalytic vacuum distillation/hydrotreatment technology (Brinkman *et al.,* 1995) has been used to degrade PCBs in used lubricating oils and petroleum products. Degradation of PCB 28, PCB 52 and PCB 101 have also been reported by oxidation using hydroxyl ions (OH's), generated with Fenton's reagent in aqueous solutions (Sediak and Andren, 1991). Other examples include; thermal oxidative degradation at high temperatures (Manlon *et al.,* 1985); hydrogenation of PCBs using bimetallic surfaces (Agarwal *et al.,* 2007); photochemical decomposition (Hawari *et al.,* 1992; Chu *et al.,* 2005) and decomposition of polychlorobiphenyls using supercritical water containing NaOH into phenol, biphenyl, and CO_2 (Sako *et al.,* 2000).

All of these chemical compounds pose a significant threat to the health and environment. The elimination of wide ranges of pollutants and wastes from the environment is therefore an absolute requirement to promote a sustainable development of our society with low environmental impact. Due to the magnitude of this problem and the lack of a reasonable solution, rapid cost-effective environmentally friendly methods of clean-up are greatly needed.

2.9 Polymers as adsorbents

In the past few decades, permanently porous polymeric adsorbents have become effective for the removal of organic pollutants from aqueous streams due to its controllable pore structure, stable physical and chemical properties, and regenerability on site as well as vast surface area comparable to activated carbons (Long *et al.,* 2011). Research has shown that the growing interest in use and application of polymer adsorbents is increasing rapidly as depicted in Figure 2.3. The 2007 forecasts of the global market suggested that the polymer sorbents will increase from $3.8 million in 2007 to an estimated $ 4.2 million in 2008 and $7.0 million in 2013, for a compound annual growth rate (CAGR) of 11.0 % (BCC Research).

Figure 2.3: Global consumption of polymer absorbents and adsorbents (Sources: BCC research)

Generally, polymeric adsorbents can effectively trap many of the ubiquitous organic pollutants, namely, phenolic compounds (Abburi, 2003, Otero *et al.,* 2005), organic acids (Otero *et al.,* 2005), aromatic or polyaromatic hydrocarbons, alkanes and their derivatives

(Lee *et al.,* 2005). Upon regeneration, the adsorbed organic chemicals are desorbed and may be recovered for further use (Pan, 1999).

To further improve adsorption performance of a given polymeric adsorbent toward other pollutants such as highly water-soluble compounds (e.g., sulfonated pollutants) and heavy metal ions, surface modification or functionalization has proved to be an effective approach because the functional groups bound to the polymeric matrices are expected to provide specific interaction with the target pollutants (Pan *et al.,* 2005; Zheng *et al.,* 2007).

Of the porous polymers, hypercrosslinked polymeric adsorbent, which is produced by further cross-linking polymers in a good solvent presents a class of predominantly microporous organic materials with large specific surface area and high micropore volume (Davankov and Tsyurupa, 1990; Tsyurupa and Davankov, 2006). Recently, a few studies have proven that hypercrosslinked polymeric adsorbent has a good sorption capacity for volatile organic compounds (VOCs) and is a promising adsorbent for removing and recovering VOCs from polluted gas streams (Simpson *et al.,* 1996; Baya *et al.,* 2000; Liu *et al.,* 2009; Long *et al.,* 2010).

Polymer modification has been reported to enhance selectivity and efficiency, easy handling, availability of different synthetic and natural adsorbents. In addition they are cost effective as a result there has been an increase in usage of polymer modified biomass (Kumar *et al.,* 2008; Ansari and Mosayebzadeh, 2010; Mansour *et al.,* 2011). One of the notable biomass materials is sawdust. A major disadvantage of adsorbents usage in remediation is the production of excessive solid waste material. Therefore it is mandatory to study the adsorbent chemical and physical properties in order to find effective safe disposal of spent material.

More recently, polymer/inorganic hybrid adsorbents have emerged as a new class of adsorbent materials for deep removal of trace pollutants from waters. Generally speaking, these hybrid adsorbents can be fabricated by irreversibly dispersing inorganic nanoparticles (e.g., metal oxides, inorganic ion exchangers, zero valent Fe) within different polymeric supports (Pan *et al.,* 2009). For example, solid polymer beads have been used in PCBs biodegradation from soil (Rehmann and Daugulis, 2008). One of the basic reasons for designing these new hybrid adsorbents relies on the fact that fine or ultrafine inorganic particles are unusable in fixed beds or any flow-through systems because of excessive pressure drops and poor mechanical strength, though most of them exhibit specific affinity toward target pollutants in waters (Pan *et al.,* 2009). For example, metal (hydr) oxides namely Fe(III) (Jang and Dempsey, 2008), Mn(IV) (Trivedi *et al.,* 2001), and Al(III) (Fan *et al.,*

2005) oxides offer specific adsorption affinity toward charged pollutants like heavy metal ions (Fan *et al.,* 2005) and phosphate or arsenate (Jang and Dempsey, 2008). In addition, zero-valence Fe can effectively decontaminate some of the disinfection by-products (DBPs) (Gopal *et al.,* 2007) in drinking waters. Thus, they have to be impregnated into porous supports of larger particle size to overcome the technical bottleneck, and porous polymeric materials seem more attractive than activated carbon (Jang *et al.,* 2008), cellulose (Guo and Chen, 2005), alginate (Chen *et al.,* 2007), diatomite (Jang *et al.,* 2007), and sand (Hansen *et al.,* 2001) due to their excellent mechanical strength and adjustable surface chemistry.

2.9.1 Polyaniline

Conducting polymers have attracted great interest in the world of research due to their various physical and chemical properties and their numerous possible applications (Skotheim, 1986). One of these polymers is polyaniline (PANI). It is one of the most extensively used and studied conducting polymers (Yue *et al.,* 1990; Unde *et al.,* 1996; Liu *et al.,* 1999) due to their well-behaved electrochemistry, easy protonation reversibility, excellent redox properties, good environmental stability, electrochromism, ease of doping, and ease of preparation. PANI has received a great deal of attention as an adsorbent due to its unique physicochemical behaviour (Bhadra *et al.,* 2009) and great promise in various practical applications in field-effect transistors, intergrated circuits, batteries, electrical or optoelectronics devices, and development of amperometric chemical sensors (Waryo *et al.,* 2009) due to its air-moisture stability. It can be prepared by chemical or electrochemical polymerization of aniline.

2.9.2 Properties of Polyaniline

Polyaniline exists in a variety of forms that differ in chemical and physical properties (Furukawa, 1988). The three principal forms are: leucoemeraldine (LE; closed valence, shell reduced form, benzenoid structure), emeraldine (EM; combination of quinoid and benzenoid structure), and pernigraniline (PE; quinoid structure) (Xu, 2009). The colour change during the redox transformations is as follows: yellow-green-blue (Inzelt, 2008). The green protonated emeraldine has semiconductor behaviour with conductivity between 8.4 and 10^{-7} Scm^{-1}, depending on the polymerization method and the film preparation conditions (Jang, 1995). Protonated PANI can be converted to a nonconducting blue emeraldine base (In het Panhuis, 2005). The ease of protonation of the insulating emeraldine base (PANI-EB) polymer into a conductive emeraldine salt (PANI-ES), results in a delocalization of the positive charges over the polymeric backbone of the PANI (Dimitriev, 2004). PANI can have structures that consist of four types of constitutional units: imino-1, 4-phenylene (IP), its salt

(IP +), nitrilo-2, 5-cyclohexadiene-1, 4-diylidenenitrilo-1, 4-phenylene (NP), and the radical cation of IP (IP·+). The high electrical conductivity of polyaniline is due to the presence of "modified quinone diimine" (semiquinone radical cation) structures over which the delocalization of p electrons occurs.

2.9.3 Use of PANI as a remediator

Polyaniline has been used widely because it carries large amounts of amine and imine functional groups, this makes the polymer to have interactions with some metal ions having strong affinity to nitrogen (Tang *et al.,* 2009). This has been proven to be true by, Li's group that has developed the polyaniline derivatives adsorbents for removal of metal ions (Hg^{2+}, Pb^{2+}, Ag^{+}) (Li *et al.,* 2004; Li *et al.,* 2005; Lu *et al.,* 2007; Karthikeyan *et al.,* 2009). Recently PANI has been used in the removal of indigo dye (Okumu and Matoetoe, 2012). Other research groups have reported successful usage of PANI derivatives or composites in removal of anions (Karthikeyan *et al.,* 2009; Wang *et al.,* 2009) and dyes (Mahanta *et al.,* 2008; Ai *et al.,* 2010; Ayad and Abu El-Nasr, 2010) from aqueous solutions. These adsorbents have stronger absorbability, faster adsorption rate, and lower costs than traditional adsorbents. To date, many methods have been used for the preparation of micro/nanostructure PANI (Reddy *et al.,* 2008; Reddy *et al.,* 2009 and Jing *et al.,* 2006; Bicak *et al.,* 2006). Many studies by Trivedi, 1999, have established that the macromolecular structural, morphological and electrical properties of PANI are found to be dependent on the nature of dopant ion inserted into the polymer.

2.10 Characterization: Morphological and structural analysis techniques

Characterization of a material is an important step after its synthesis because it gives useful parameters in determining the properties of polymers and optimization of the existing materials. This section will review three categories of characterization namely physical, thermal and microscopic. Physical characterization consists of spectroscopic analysis using Fourier transform infrared (FTIR), UV-visible spectroscopy and analysis of X-ray diffraction (XRD) patterns of a material. Thermal characterization of synthesized materials includes thermogravimetric analysis (TGA/DSC). Microscopic characterization involves use of transmission electron microscopy (TEM) and scanning electron microscopy (SEM). The techniques used for the characterization of polyaniline and its composites are described in following sections.

2.10.1 Microscopy techniques

Microscopy studies are used to investigate the morphology of the polymers and for estimation of their sizes. This section describes the principles involved in use of transmission electron microscopy (TEM) and scanning electron microscopy (SEM) during characterization of materials.

2.10.1.1 Transmission Electron Microscopy (TEM)

The transmission electron microscope (TEM) has evolved over many years into a highly sophisticated instrument that has found widespread application across scientific disciplines. Because the TEM has an unparalleled ability to provide structural and chemical information over a range of length scales down to the level of atomic dimensions, it has developed into an indispensable tool for scientists who are interested in understanding the properties of nanostructured materials and in manipulating their behaviour (Augus and John, 2007).

The main application of transmission electron microscopy (TEM) is in the determination of the size, distribution and the morphology of synthesized nanoparticles. The principle of TEM works in much the same way as an optical microscope. A beam of electrons, generated by the high voltage electron emitter situated at the top of the lens column, interacts with the sample as it passes through the entire thickness of the sample and a series of magnifying magnetic lenses, where they are ultimately focused at the viewing screen at the bottom of the column. The TEM image is basically a projection of the entire item, including the surface and the internal structures. In this work TEM was used to determine the size, morphology and the elemental composition of the synthesized materials.

2.10.1.2 Scanning Electron Microscopy (SEM)

Scanning electron microscopy (SEM) is a versatile imaging technique capable of producing three-dimensional images of material surfaces. SEM is one of the most frequently used instruments in material research today because of the combination of high magnification, large depth of focus, greater resolution and ease of sample observation. The basic operation in SEM entails the interaction of an accelerated highly monoenergetic electron beam, originating from the cathode filament, with the atoms at the sample surface. The electron beam is focused into a fine probe which is rastered over the sample. The scattered electrons are collected by a detector, modulated and amplified to produce an exact reconstruction of the sample surface and particle profile (Cherstiouk *et al.*, 2003). A requirement for effective performance is that the surface of the samples should be electrically conductive. During

operation electrons are deposited onto the sample. These electrons must be conducted away to earth, thus conductive materials such as metals and carbon can be placed directly into the SEM whereas non-metallic samples have to be coated with a gold metal layer to be observed. Many scanning electron microscopes have an energy dispersive spectrometer (EDX) detection system, which detects and displays most of the spectra of the elements contributing to the sample composition. In this work SEM was used to determine morphology of the synthesized materials.

2.10.2 Spectroscopic techniques

The common spectroscopic characterization of polymers includes techniques, such as fourier transform infrared (FTIR) and UV-Visible spectroscopy which have been used to provide qualitative indication of the intrinsic redox states of conducting polymers and to predict successful doping (Cataldo and Maltese, 2002). UV-Visible spectroscopy gives the energy band gap and defect states, while IR spectroscopy identifies and confirms the structure and presence of various linkages in the polymer.

2.10.2.1 Fourier Transform Infrared (FTIR) Spectroscopy

Fourier transform infrared (FTIR) spectroscopy bases its functionality on the principle that almost all molecules absorb infrared light. Only the monatomic (He, Ne, Ar, etc) and homopolar diatomic (H_2, N_2, O_2, etc) molecules do not absorb infrared light. Molecules only absorb infrared light at those frequencies where the infrared light affects the dipolar moment of the molecule. In a molecule, the differences of charges in the electronic fields of its atoms produce the dipolar moment of the molecule. Molecules with a dipolar moment allow infrared photons to interact with the molecule causing excitation to higher vibrational states. The homopolar diatomic molecules do not have a dipolar moment since the electronic fields of its atoms are equal. Monatomic molecules do not have a dipolar moment since they only have one atom. Therefore, only homopolar diatomic molecules and monatomic do not absorb infrared light (Meyer, 2009).

FTIR analysis is a technique that provides information about the chemical bonding or molecular structure of materials, whether organic or inorganic. It is used in the identification of unknown materials as well as conformation of the synthesized chemical sample. The technique works on the fact that bonds and groups of bonds vibrate at characteristic frequencies. A molecule that is exposed to infrared rays absorbs infrared energy at frequencies which are characteristic to that molecule. During FTIR analysis, a spot on the specimen is subjected to a modulated infrared (IR) beam. The specimen's transmittance and

reflectance of the infrared rays at different frequencies is translated into an IR absorption plot consisting of reverse peaks. It involves the dispersive method, which entails creating a spectrum by collecting signals at each wave number separately. The resulting FTIR spectral pattern is then analyzed and matched with known signatures of identified materials in the FTIR spectrum. Unlike SEM inspection or energy dispersive X-ray (EDX) analysis, FTIR spectroscopy does not require a vacuum, since neither oxygen nor nitrogen absorbs infrared rays. FTIR analysis can be applied to minute quantities of materials, whether solid, liquid, or gaseous (Silicon, 2005). Currently, FTIR has almost totally replaced the dispersive method because FTIR has a much higher signal-to-noise ratio than that of dispersive method (Yang, 2008) and it is the most widely used vibrational spectroscopic technique.

2.10.2.2 Ultraviolet-Visible spectroscopy

It is a spectroscopic technique that involves the spectroscopy of photons in the UV-visible region. It uses light in the visible and adjacent ultraviolet (UV) and near infrared (NIR) ranges). In UV-visible spectroscopy, one can monitor the colour of a material. The colour monitored is the wavelength at which the maximum of the absorption band (s) occurs, λ_{max}, together with the absorbance at each of these wavelengths. The optical absorbance, *Abs*, is defined according to the equation:

$$Abs = \log_{10} T \quad \text{.....Equation 1}$$

Where, T is the transmittance of light following its passage through the cell. Any changes in the absorbance relates to the amount of electroactive material as converted by the flow of current. The absorption spectrum tells us the nature of the material generated. It is a major technique that is used in the quantitative determination of solutions of transition metal ions and highly conjugated compounds. For example, if a material absorbs UV-visible light, then we can monitor its concentration using the Beer-Lambert relationship;

$$Abs = \varepsilon C_0 l \quad \text{.....Equation 2}$$

Where the absorbance is determined at fixed wavelength λ, ε is the extinction coefficient (cited at the same value of λ), and *l* is the optical path length. If the magnitude of the extinction coefficient at λ is known, then the amount of analyte (C_0) can be quantified simply by determining the optical absorbance and inserting the values into equation (2). Most of the analytical techniques are not particularly useful for telling us what 'something' is, but are excellent at telling us how much of that 'something' is present, or has been formed or has been changed. However, UV-visible spectroscopy is one of the best ways of identifying an analyte. This is because each specific analyte absorbs energy in the form of photons at

different wavelengths (Monk, 2001). Hence one is able to identify a certain analyte. It is a complementary technique to fluorescence spectroscopy in that it deals with transitions from the ground state to the excited state while fluorescence spectroscopy measures transitions from the excited state to the ground state (Skoog, 2007).

2.10.3 Other techniques

2.10.3.1 X-Ray Diffraction (XRD)

X-ray diffraction (XRD) is a versatile, non-destructive technique that reveals detailed information about the chemical composition and crystallographic structure of natural and manufactured materials. It is an indispensable method for material characterization. XRD is a powerful tool in the study of crystallinity and atomic structure of materials and forms an integral part of the comprehensive characterization study of the consolidated composite carbon material. It is used extensively in the determination of the Bravais lattice types and unit cell dimensions. X-ray diffraction methods can be classified into two types: spectroscopic and photographic. The spectroscopic technique known as the X-ray powder diffractometry, or simply X-ray diffractometry, is the most widely used diffraction method. Because spectroscopic methods can replace most photographic methods, photographic techniques are not widely used as diffractometry in modern laboratories. However, photographic methods are used to determine unknown crystal structures (Yang, 2008). In XRD, crystalline solids are bombarded with a collimated X-ray beam which causes crystal plane atoms, serving as diffraction gratings, to diffract X-rays in numerous angles. Each set of crystal planes or Miller indices (hkl) with interplanar spacing (d_{hkl}) can give rise to diffraction at only one angle. The diffraction angle is defined from Bragg's law (equation 3), where the intensities of the diffracted X-ray are measured and plotted against the corresponding Bragg angles (2θ) to produce a diffractogram.

$$n\lambda = 2d\sin\theta \quad \text{.....Equation 3}$$

Where: λ = wavelength of the X-rays, d = spacing of the planes in the crystal, 2θ = angle of diffraction. The intensities of the diffraction peaks are proportional to the densities of the abundance of the corresponding crystal facets in the material lattice. Diffractograms are unique for different materials and can therefore qualitatively be used in material identification. For the purpose of this study XRD was used to investigate the crystallinity of the PANI and its composites synthesized.

2.10.3.2 Thermogravimetric Analysis (TGA)

This involves thermal analysis which consists of a group of techniques in which a physical property of a substance is measured as a function of temperature, during which the substance is subjected to a programmed temperature. Various thermoanalytical methods which have been used are differential scanning calorimetry (DSC), thermogravimetric analysis (TGA) and analytical pyrolysis (Py) (Sharypov *et al.,* 2002; Renneckar *et al.,* 2004; Araujo *et al.,* 2008; Reichert and Korte, 2009; Windt *et al.,* 2011). DSC can be used to identify a polymer based on its melting point whereas TGA is useful to determine thermal stability and degradation behaviour of a polymer or composite (Ehrenstein *et al.,* 2003). TGA measurements of individual components provide information regarding their thermal degradation behaviour and also quantitative measure of all the changes which occur in the weight of a sample as a function of temperature (Wesolwski, 1995). Reichert and Korte, 2009, used DSC measurements and showed that on the basis of the peak area of the melting point, quantification of the polymer fraction is possible. The peak height is measured by the difference between the heat flow at the peak and at the DSC curve baseline.

Data from a thermogravimetric analysis (TGA) experiment originate from the mass loss of a sample suspended from a vacuum balance during a programmed heating while a carrier gas is flowing around the sample. The heated sample undergoes a vaporization reaction producing gaseous species. Sample mass is lost by two mechanisms: (1) diffusion of gaseous species away from the sample, and (2) transport of gaseous species in the carrier gas. The pressures in the apparatus are near atmospheric pressure and are such that the transport of gaseous species (Oniyama and Wahlbeck, 1995) is by gaseous viscous flow. Thermal decomposition of polymer composites depends on particle size, moisture content, quantity and type of polymers and other additives.

Thermal analysis techniques such as thermogravimetric analysis (TGA) have been widely used because they provide rapid quantitative methods for the examination of processes under isothermal or non-isothermal conditions (Seo *et al.*, 2010) and allow for the estimation of effective kinetic parameters for various decomposition reactions. Thermogravimetric analysis may be coupled with differential thermal analysis (DTA) to distinguish the physical phenomena of changes in state from the chemical phenomena responsible for the changes in sample weight (Dufaure *et al.,* 1999).

In the present study, thermogravimetric analysis of pure PANI and its composites: PANI/SD, PANI/TiO_2 and PANI/SD/TiO_2 have been conducted by using TGA and DSC to investigate the stability of the composites during decomposition and to monitor occurrence of PANI

composite transformations during the heating process. The results of this study could enhance the understanding of the heat resistance properties of PANI composites for adsorption application. In this study, experiments are carried out under a nitrogen atmosphere at a heating rate of 10 °C/min. The knowledge of thermal stability and degradation behaviours is useful in the application of PANI/SD/TiO_2 as an adsorbent in this study.

2.11 Electroanalytical techniques

Electrochemistry has always provided analytical techniques characterized by instrumental simplicity, moderate cost and portability (Bard and Faulkner, 2001; Mirceski *et al.*, 2007). The techniques used in this study are mainly voltammetric which include cyclic and square wave voltammetry. Detailed discussions of these techniques are mentioned in the next sections.

2.11.1 Cyclic voltammetry (CV)

Cyclic voltammetry (also called linear scan voltammetry) is an electrochemical technique that is classified under sweep techniques. In cyclic voltammetry, the root of the word voltammetry, "voltam-", refers to both potential ("volt-") and current ("am-"). During the voltammetric experiment some applied potential at a working electrode is varied at some scan rate in both forward and reverse directions while the current is simultaneously monitored. The basic instrumentation for the cyclic voltammetry analysis requires controlled potential equipment (potentiostat) and an electrochemical cell consisting of three electrodes. The analysis is normally carried out using an electrochemical analyser connected to a three electrode cell, containing the working electrode, reference electrode and auxiliary electrode as represented in Scheme 2.2.

The electrode where the reaction of interest takes place is called the working electrode. The common materials used for working electrode include platinum, gold and carbon (carbon can be in the form of graphite, glassy carbon, or diamond). These electrodes are generally encased in a rod of inert insulator with a disk exposed at one end and should not be susceptible to oxidation or reduction. In addition, it is very important that material used as a working electrode should not oxidise any ions in solution. The reference electrode provides a stable potential compared to the working electrode. Reference electrodes are used because their potentials are constant. There are different types of reference electrodes and the commonly used ones are the saturated calomel electrode (SCE), and the silver/silver chloride electrode Ag/AgCl. The counter electrode, also called the auxiliary or secondary

electrode, can be made with any material which conducts easily and will not react with the bulk solution. The auxiliary electrode is usually made of platinum wire.

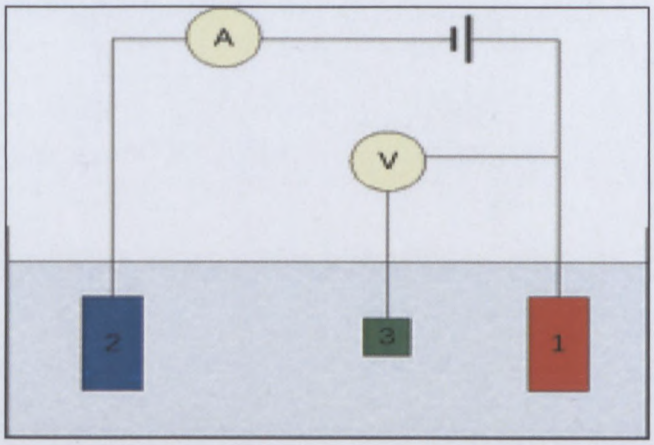

Scheme 2.2: Schematic representation of an electrochemical cell consisting of three electrodes: (1) working electrode; (2) auxiliary electrode; (3) reference electrode.

In cyclic voltammetry the potential is ramped from an initial potential (E_i) and at the end of its linear sweep, the direction of the potential scan is reversed, usually stopping at the initial potential. The potential may commence with additional cycles. The potential at which the change in direction occurs is also known as the switch potential (E_λ). The scan rate between E_i and E_λ is the same as that between E_λ and E_i and the values of the scan rate v forward and v reverse are always written with positive numbers. Oxidation usually takes place during the forward part of the CV, if scanned from a negative to a positive potential. The reverse part of the CV will then represent reduction, with the potential running from a positive to a negative potential. However, if the potential is scanned from a positive to a negative value, then reduction would occur during the forward part of the CV scan and oxidation during the reverse CV scan. Important parameters are usually obtained from cyclic voltammograms for analysis of reversible reaction properties and properties of an electroactive sample. These parameters include anodic and cathodic peak potentials, denoted as E_{pa} and E_{pc}, respectively as well as anodic and cathodic peak currents denoted as I_{pa} and I_{pc}, respectively. A typical cyclic voltammogram illustrating these parameters is shown in Table 2.2.

In voltammetry the magnitude of the current is proportional to the concentration of the analyte. Thus the equality in size between I_p (forward) and I_p (reverse) implies a quantitative retrieval of electromodified material, which follows from Faraday's laws (Zanello, 2003). In cyclic voltammetry, the position of both the cathodic and anodic peaks gives us thermodynamic information of the redox couple used. The anodic and cathodic peak

potentials also enable the calculation of the formal electrode potential, $E^{o'}$, as shown in Table 2.2.

The formal electrode potential (normally called the formal potential or the formal redox potential) is in concept similar to the standard electrode potential, E^{θ} (Zanello, 2003). Some important information about the sample under investigation can be obtained from the peak parameters. This includes whether the electrochemical process displayed by the sample is reversible, irreversible or quasi-reversible. It also gives insight into how fast the electron transfer process is, relative to other processes such as diffusion. For example, if the electron transfer is fast relative to the diffusion of electroactive species from the bulk solution to the surface of the electrode, the reaction is said to be electrochemically reversible and the peak separation is denoted by (ΔE_p) as shown in Table 2.2, where ΔE_p is the peak separation (V), E_{pa} is the anodic peak potential (V), E_{pc} is the cathodic peak potential (V), n is the number of electrons transferred, F is the Faraday constant (96,485 C mol^{-1}), R is the gas constant (8.314 J mol^{-1} K^{-1}) and T is the absolute temperature (K).

The peak separation can be used to determine the number of electrons transferred, and as a criterion for Nernstian behaviour (Joseph, 2000). This means that for reversible one-electron processes, the peak-to-peak separation assumes different values as a function of the temperature (Zanello, 2003). When the value of ΔE_p is measured, a departure of 10-20 mV from the theoretical value, especially at high scan rates, does not compromise the criterion for reversibility. This is due to the fact that the eventual presence of solution resistance, if not adequately compensated by the electrochemical instrumentation, tends to shift the forward/reverse peaks system, thereby increasing the relative value of ΔE_p (Zanello, 2003). The chemical meaning of an electrochemical reversible process suggests that no important structural reorganisation accompanies the redox step. This will also be the case for an electrode process in which the rate of electron transfer is higher than the rate of mass transport.

a) The Randles-Sevčik equation

According to the Randles-Sevčik equation (equation 5) below, the magnitude of the peak current, I_p, in a cyclic voltammogram is a function of the temperature (T), bulk concentration (C_0), electrode area (A), the number of electrons transferred (n), the diffusion coefficient (D), and the speed at which the potential is scanned (v), (Monk, 2001):

$$I_p = 0.4463nFA\left(\frac{nF}{RT}\right)^{1/2} D^{1/2}v^{1/2}C_0 \quad \text{.....Equation 4}$$

At 25 °C the above equation reduces to (Allen and Larry, 2001; Monk, 2001)

$$I_p = 2.686x10^5 n^{3/2}A^{1/2}D^{1/2}v^{1/2}C_0 \quad \text{.....Equation 5}$$

Where A is the electrode area (cm^2) and F, R, and T are as explained in section 2.11.1. Several voltammograms performed at different scan rates can lead to the preparation of several linear plots whose slopes could give further information about the redox properties of the sample in question. For instance, when the peak current is plotted against the square root of the scan rate, the slope of the linear plot can be used to estimate the diffusion coefficient according to the Randles-Sevčik equation.

The Randles-Sevčik equation is obeyed if a plot of peak current (I_p) against analyte concentration (C_0) yields a straight line. It also means that if the electrolyte composition is constant in terms of temperature, solvent, swamping electrolyte, then the Randles-Sevčik equation can be used to the determine the concentration of analyte by the construction of a suitable calibration curve (Allen and Larry, 2001). Furthermore, in the Randles-Sevčik plot, a straight line should be obtained that passes through the origin, the slope of the linear plot can be used to determine the concentration of the analyte (C_0) if the diffusion coefficient D is known precisely. A Randles-Sevčik plot is the best way to determine an experimental value of the diffusion coefficient, D, if it is not available in the literature, in the case of a reversible reaction (Monk, 2001).

From the Randles-Sevčik equation, it is also possible to calculate the other variables listed in equations 4 and 5. If the peak current (I_p) at a certain scan rate (v) is measured, and the area of the electrode (A), the diffusion coefficient (D) and the concentration (C) of the species under study are known, one is able to calculate the number of electrons (n) involved in the redox change. Similarly, if the number of electrons (n) is known, one can calculate the diffusion coefficient (D) of the species, and any of the other variables. When plotted, the log of peak current versus the log of scan rate gives a linear plot whose slope distinguishes between diffusion controlled peaks, adsorption controlled peaks or even a mixture of the two. When a slope of 0.5 is obtained, we have a diffusion controlled peak and a slope of 1 is for an adsorption peak. Moreover, when an intermediate value of the slope (0.5-1) is obtained, the suggested mechanism is mixed (diffusion-adsorption) (David and Gosser, 1993). For totally irreversible systems, the individual peaks are reduced in size and widely separated as

shown in Table 2.2 (Curve A). Further differences in the electrochemical processes are discussed in Table 2.2 below where each system is discussed separately.

Table 2.2: Summary of reversible and irreversible electrochemical processes

Reversible systems	Irreversible systems (A)
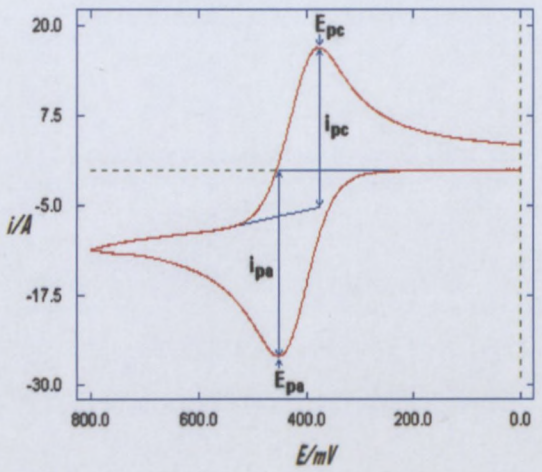	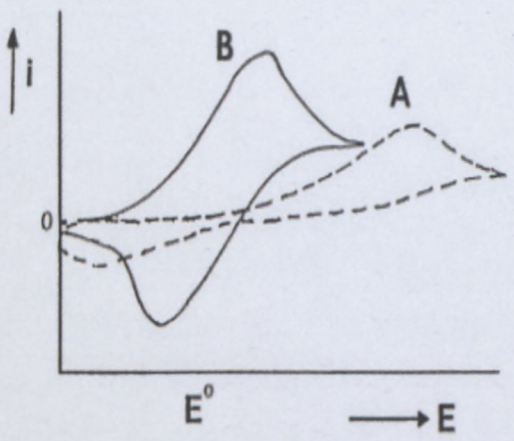
Equal opposite peaks	One peak
$I_{pc}/I_{pa} = 1$, or $I_{pa}/_{pc} = 1$	I_{pa} or I_{pc} is proportional to $v^{1/2}$
$E^0 = \frac{E_{pa} + E_{pc}}{2}$	$\lvert E_{pa} - E_{pc} \rvert = \frac{48mV}{\alpha}$
E_{pa} and E_{pc} are independent of scan rate, v	E_p shifts $-\frac{30}{\alpha n}$ for each decade increase in v
I_p is proportional to $v^{1/2}$	I_p shifts with the scan rate
$\Delta E_p = \lvert E_{pa} - E_{pc} \rvert = 2.30\frac{RT}{nF}$ $\lvert E_{pa} - E_{pc} \rvert = \frac{59mV}{n}$ if 1 electron process $\lvert E_{pa} - E_{pc} \rvert = 30mV$ if 2 electron process	

The dependence of peak potential with scan rate for an irreversible process is expressed in the following equation (Joseph, 2000):

$$E_p = E^{o'} - \frac{RT}{\alpha nF}\left[0.78 - \ln\left(\frac{k^0}{D^{1/2}}\right) + \ln\left(\frac{\alpha nFv}{RT}\right)^{1/2}\right] \quad \text{.....Equation 6}$$

Where k^0 is heterogeneous rate constant and α is the transfer coefficient. Thus, E_p occurs at higher potentials than $E^{0'}$, when the over-potential depends on k^0 and α. In a case where E_p is independent of k^0, the shift of the peak potential could be compensated by an appropriate change of the scan rate. Therefore, when αn decreases, the voltammogram could become more drawn out. Equation 6 also allows for the calculation of the heterogeneous rate constant, k^0, if the values of $E^{\circ'}$ and D are known. The peak current for an irreversible process is given by:

$$I_p = \left(2.99x10^5\right) n\left(\alpha n\right)^{1/2} AC_0 D^{1/2} v^{1/2} \quad \text{.....Equation 7}$$

For the irreversible process, the peak current (I_p) is proportional to the bulk concentration (C_0) but can be lower in value depending on the value of the transfer coefficient (α). Assuming that α = 0.5, the ratio of reversible-to-irreversible peak current will be 1.27. The chemical meaning of an irreversible electrochemical process implies that a large activation barrier to the electron transfer takes place causing breakage of the original molecular frame with the formation of new species (Zanello, 2003).

2.11.2 Square wave voltammetry (SWV)

Square wave voltammetry is a type of pulse voltammetry that offers the advantage of speed and high sensitivity. An entire voltammogram is obtained in a few seconds or less. In addition, square wave voltammetry (SWV) has proved to be a suitable method to investigate redox reactions with overlapping waves. The excitation signal in SWV consists of a symmetrical square wave pulse of amplitude superimposed on staircase wave form of step height ΔE. The forward pulse coincides with the staircase step. A typical square wave voltammogram is shown in Figure 2.4 below.

The net current (I_{net}) is obtained by taking the difference between the forward and the reverse currents (I_{fwd}-I_{rev}) and is centred on the redox potential. In SWV, the peak height is directly proportional to the concentration of the electroactive species. Excellent sensitivity is achieved from the fact that the net current is larger than either the forward or the reverse components, since it is the difference between them and direct detection limit as low as 10^{-8} M are possible.

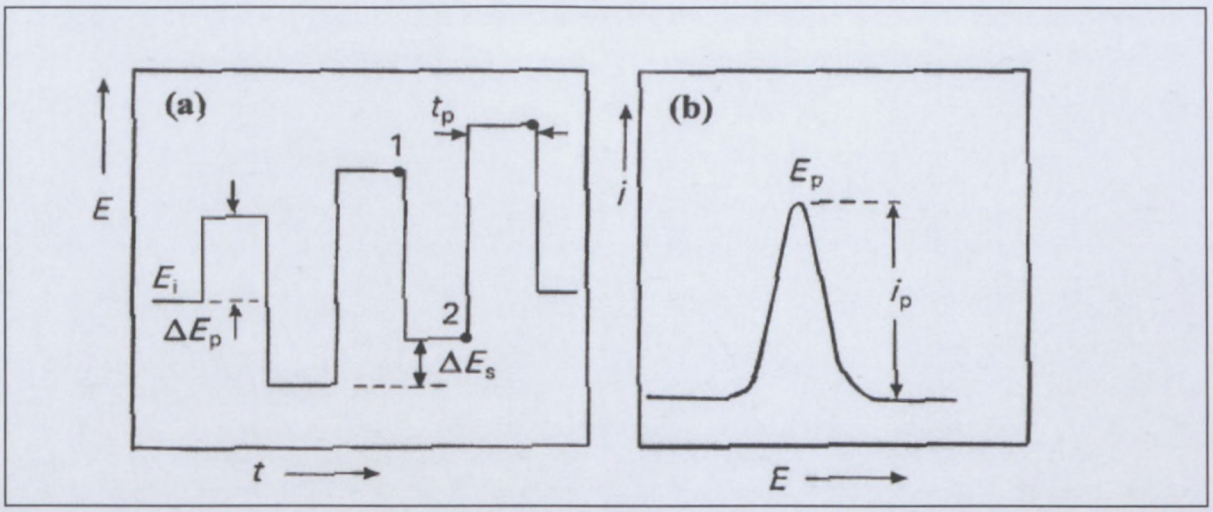

Figure 2.4: Excitation waveform of square wave voltammetry (Curve a) and response obtained by square wave voltammetry (Curve b).

Square wave voltammetry presents some advantages over cyclic voltammetry. These include excellent sensitivity and rejection of background currents. The scanning speed in SWV is also high and, coupled with computer control and signal averaging experiments, can be performed repetitively with increases in the signal to noise ratio. SWV is also applied in the study of electrode kinetics with regard to preceding, following or catalytic homogeneous chemical reactions and determination of some species at trace levels.

2.12 Conclusion

In conclusion, this chapter presented a review of relevant literature related to electrochemical analysis. The chapter initially briefly introduces the background knowledge of PCBs, basic concepts of electrochemical analysis of PCBs and different methods used in analysis and remediation followed by citing relevant literature related to PCBs. Furthermore, few important key concepts regarding conducting polymers and their composites which will be used to synthesize PANIs for adsorption studies were also introduced. The review showed that the electrochemical analysis of PCBs involves the electrochemical reduction of chlorine atoms attached to the biphenyl ring which occurs via stepwise or concerted mechanism. The conducting polymer of interest was polyaniline and its composites due to their environmental stability, ease of synthesis and porosity of structures necessary for enhancement of their adsorption properties.

2.13 References

Abburi, K. 2003. Adsorption of phenol and *p*-chlorophenol from their single and bisolute aqueous solutions on Amberlite XAD-16 resin, *J. Hazard. Mater.*, B105: 143-156.

Abramowitz, D.A. 1990. Aerobic and anaerobic biodegradation of PCBs: a review. *Crit. Rev. Biotechnol.,* 10: 241-251.

Adenipekun, C.O. and Lawal, R. 2012. Uses of mushrooms in bioremediation: A review. *Biotechnology and Molecular Biology Review,* 7(3): 62-68.

Agarwal, S., Al-Abed, S.R. and Dionysiou, D.D. 2007. Enhanced corrosion based Pd/Mg bimetallic systems for dechlorination of PCBs. *Environ. Sci. Technol.*, 41: 3722-3727.

Agency for Toxic Substances and Disease Registry. 2000. Toxicological Profile for Polychlorinated Biphenyls (PCBs). Agency for Toxic Substances and Disease Registry (ATSDR) Web page: http://www.atsdr.cdc.gov/toxprofiles/tp17.html [20 April 2012].

Ai, L., Jiang, J. and Zhang, R. 2010. Uniform polyaniline microspheres: A novel adsorbent for dye removal from aqueous solution. *Synth. Met.,* 160: 762-767.

Allen, J.B. and Larry, R.F. 2001. *Electrochemical methods: fundamentals and applications.* 2nd ed. New York, NY 10158-0012, USA: John Wiley & Sons, Inc.

Ansari, R. and Mosayebzadeh, Z. 2010. Removal of Eosin Y, an anionic dye, from aqueous solutions using conducting electroactive polymers. *Iran. Polym. J.*, 19(7): 541-551.

Araujo, J.R., Waldman, W.R. and Paoli, M.A.D. 2008. Thermal properties of high density polyethylene composites with natural fibres: coupling agent effect. *Polym. Degrad. Stab.*, 93: 1770-1775.

Arbon, R.E., Mincher, B.J. and Knighton, W.B. 1994. Gamma ray destruction of individual PCB congeners in neutral 2-propanol. *Environ. Sci. Technol.,* 28(12): 2191-2196.

Arbon, R.E., Mincher, B.J. and Knighton, W.B. 1996. Gamma ray destruction of PCBs in isooctane and transformer oil. *Environ. Sci. Technol.,* 30(6): 1866-1871.

Arctic Monitoring and Assessment Program. 1998. Assessment Report: Arctic Pollution Issues. Arctic Monitoring and Assessment Program (AMAP), Oslo, Norway. 12:859. ISBN 82-7655-061-4.

Augus, I.K. and John, L.H. (eds). 2007. *Nanocharacterisation.* The Royal Society of Chemistry: Thomas Graham House, Science Park, Milton Road, Cambridge CB4 0WF, UK.

Australian and New Zealand Environment and Conservation Council. 1997. *Identifying PCB-Containing Capacitors.* (ANZECC): 4-5. ISBN 0-642-54507-3.

Ayad, M.M. and Abu El-Nasr, A. 2010. Adsorption of cationic dye (Methylene Blue) from water using polyaniline Nanotubes Base. *J. Phys. Chem.,* C114: 14377-14383.

Ballschmiter, K., Bacher, R., Mennel, A., Fischer, R., Riehle, U. and Swerev, M. 1992. The determination of chlorinated biphenyls, chlorinated dibenzodioxins, and chlorinated dibenzofurans by GC-MS. *J. High Resolut. Chromatogr.*, 15: 260-270.

Ballschmiter, K. and Zell, M. 1980. Analysis of polychlorinated biphenyls (PCB) by glass capillary gas chromatography. Composition of technical Aroclor- and Clophen-PCB mixtures. *Fresenius Zeitung der Analytische Chemie,* 302: 20-31.

Bard, A.J. and Faulkner, L.R. 2001. *Electrochemical Methods, Fundamentals and Applications.* 2nd ed. New York: John Wiley & Sons Inc.

Baukal, C.E, Schafer, L.L. and Papadelis, E.P. 1994. PCB Clean up Using an Oxygen/Fuel-Fired Mobile incinerator. *Environ. Progress*, 13(3): 188-191.

Baya, M.P., Panayotis, P.A. and Davankov, V.A. 2000. Evaluation of a hypercrosslinked polystyrene, MN-200, as a sorbent for the preconcentration of volatile organic compounds in air. *J. Assoc. Off. Anal., Chem. Int.*, 83: 579-583.

BCC Research, http://www.bccresearch.com/report/polymer-absorbents-adsorbents-pls046a.html [10 June 2012].

Berdowski, J.J.M., Baas, J., Bloos, J.P.J., Visschedijk, A.J.H. and Zandveld, P.Y.J. 1997. The European Atmospheric Emission Inventory for Heavy Metals and Persistent Organic Pollutants. Umweltforschungsplan des Bundesministers fur Umwelt, Naturschutz und Reaktorsicherheit. Luftreinhaltung. Forschungbericht 104 02 672/03. TNO, Apeldoorn, The Netherlands.

Bhadra, S., Khastgir, D., Singha, N.K. and Lee, J.H. 2009. Progress in preparation, processing and applications of polyaniline. *Prog. Polym. Sci.,* 34: 783-810.

Bicak, N. and Karagoz, B. 2006. Polymerization of aniline by copper-catalyzed air oxidation. *J. Polym. Sci. A: Polym. Chem.,* 44: 6025-6031.

Boate, A., Deleersnyder, G., Howarth, J., Mirabelli, A. and Peck, L. 2004. Chemistry of PCBs. http://wvlc.uwaterloo.ca/biology447/modules/intro/assignments/Introduction2a.html [3 September 2012].

Bohm, S., Olthuis, W. and Bergveld, P. 1999. A plastic micropump constructed with conventional techniques and materials. *Sens. Actuators, A.*, 77: 223-228.

Boopathy, R. 2000. Factors Limiting Bioremediation Technologies. *Bioresource Technol.,* 74(1): 63-67.

Breivik, K., Sweetman, A., Pacyna, J.M., Jones, K. 2002a. Towards a Global Historical Emission Inventory for Selected PCB Congeners – a Mass Balance Approach. 1. Global Production and Consumption. *Sci. Total Environ.*, 290: 181-198.

Bremle, G. and Larsson, P. 1998. PCB in the air during landfilling of contaminated lake sediment. *Atmos. Environ.,* 32(6): 1011-1019.

Brinkman, D.W., Dickson, J.R. and Wilkinson, D. 1995. Full Scale Hydrotreatment of Poly-Chlorinated Biphenyls in the Presence of Used Lubricating Oils. *Environ. Sci. Technol.*, 29: 87-91.

Brown, G.C. 1996. Solvated electron destruction of PCBs, *14th Annu. Environ. Manage. Technol. Conf. Int.,* 497-502.

Buchmann, A., Kunz, W., Wolf, C.R., Oesch, F. and Robertson, L.W. 1986. Polychlorinated biphenyls, classified as either phenobarbital-or 3-methylcholantrene-type inducers of

cytochrome *P*-450, are both hepatic tumor promoters in diethylnitrosamine-initiated rats. *Cancer lett.*, 32: 243-253.

Buehler, S.S., Basu, I. and Hites, R.A. 2002. Gas-phase polychlorinated biphenyl and hexachlorocyclohexane concentrations near the Great Lakes: a historical perspective. *Environ. Sci. Technol.*, 36: 5051-5056.

Cataldo, F. and Maltese, P. 2002. Synthesis of alkyl and N-alkyl-substituted polyanilines: A study on their spectral properties and thermal stability. *Eur. Polym. J.*, 38: 1791-1803.

Centi, S., Rozum, B., Laschi, S., Palchetti, I. and Mascini, M. 2006. Disposable Electrochemical Magnetic Beads-Based Immunosensors for Monitoring Polychlorinated Biphenyl (PCBs) Pollutants. *Chem. Anal.*, (Warsaw), 51: 963-975.

Chauhan, K.R., Kodavanti, P.R. and McKinney, J.D. 2000. Assessing the role of ortho-substitution on polychlorinated biphenyl binding to transthyretin, a thyroxine transport protein. *Toxicol. Appl. Pharmacol.*, 162(1): 10-21.

ChemIDplus. 2009. *ChemIDplus Advanced.* National Library of Medicine. http://chem.sis.nlm.nih.gov/chemidplus and select Registry Number and search on CAS number. [25 August 2012].

Chen, K.L., Mylon, S.E. and Elimelech, M. 2007. Enhanced aggregation of alginate-coated iron oxide (hematite) nanoparticles in the presence of calcium, strontium, and barium cations, *Langmuir*, 23: 5920-5928.

Cherstiouk, O.V., Simonov, P.A. and Savinova, E.R. 2003. Model approach to evaluate particle size effects in electrocatalysis: preparation and properties of Pt nanoparticles supported on GC and HOPG. *Electrochim. Acta*, 48(25-26): 3851-3860.

Chu, W., Chan, K.H., Kwan, C.Y. and Jafvert, C.T. 2005. Acceleration and quenching of the photolysis of PCB in the presence of surfactant and humic materials. *Environ. Sci. Technol.*, 39(23): 9211-9216.

Chuang, F., Larson, R.A. and Wessman, M.S. 1995. Zero-valent iron-promoted dechlorination of polychlorinated biphenyls. *Environ. Sci. Technol.*, 29(9): 2460-2463.

Davankov, V.A. and Tsyurupa, M.P. 1990. Structure properties of hypercrosslinked polystyrenes: The first representative of a new class of polymer networks. *React. Polym.*, 13: 27-42.

David, K. and Gosser, J. 1993. Cyclic voltammetry: Simulation and Analysis of Reaction Mechanisms, 220 East 23rd Street New York, NY 10010: VCH Publishers, Inc.

De Filippis, P., Chianese, A. and Pochetti, F. 1997. Removal of PCBs from mineral oils. *Chemosphere*, 35: 1659-1667.

Del Carlo, M., Lionti, I., Taccini, M., Cagnini, A. and Mascini, M. 1997. Disposable screen-printed electrodes for the immunochemical detection of polychlorinated biphenyls. *Analyt. Chim. Acta*, 342: 189-197.

Dickhut, R.M. and Gustafson, K.E. 1995. Atmospheric washout of polycyclic aromatic hydrocarbons in the Southern Chesapeake Bay region: *Environ. Sci. Technol.*, 29(6): 1518-1525.

Dimitriev, O.P. 2004. Doping of polyaniline by transition metal salts: effect of metal cation on the film morphology. *Synth. Met.,* 142: 299-303.

Dufaure, C., Thamrin, U. and Mouloungui, Z. 1999. Comparison of the thermal behaviour of some fatty esters and related ethers by TGA-DTA analysis. *Thermochim. Acta,* 338: 77-83.

Duffy, J.E., Carlson, E., Li, Y., Prophete, C. and Zelikoff, J.T. 2002. Impact of polychlorinated biphenyls (PCBs) on the immune function of fish: age as a variable in determining adverse outcome. *Mar. Environ. Res.*, 54(3-5): 559-563.

Ehrenstein, G.W., Riedel, G. and Trawiel, P. 2003. Praxis der Thermischen Analyse von Kunststoffen, second ed., Carl Hanser Verlag, München.

Eisenreich, S.J., Baker, J.E. and Franz, T. 1992. Atmospheric deposition of hydrophobic organic contaminants to the Laurentian Great Lakes. In: Schnoor JL, ed. Fate of pesticides and chemicals in the environment. New York, NY: John Wiley & Sons, Inc.: 51-78.

Erickson, M.D. 1997. Analytical Chemistry of PCBs. 2nd ed. Boca Raton, FL: CRC Press/Lewis Publishers.

Erickson, M.D. 2001. Introduction: PCB properties, uses, occurrence, and regulatory history. In: PCBs: *Recent Advances in Environmental Toxicology and Health Effects.* Robertson, L.W., Hansen, L.G. (eds). Lexington, KY: The University Press of Kentucky, xi–xxx.

Fan, M., Boonfueng, T., Xu, Y., Axe, L. and Tyson, T.A. 2005. Modeling Pb sorption to microporous amorphous oxides as discrete particles and coatings. *J. Colloid Interface Sci.*, 281: 39-48.

Fava, F., Gentilucci, S. and Zanaroli, G. 2003. Anaerobic biodegradation of weathered polychlorinated biphenyls (PCBs) in contaminated sediments of Porto Marghera (Venice, Lagoon, Italy). *Chemosphere*, 53: 101-109.

Ferrario, J., Byrne, C. and Dupuy, A.E., Jr. 1997. Background contamination by coplanar polychlorinated biphenyls (PCBs) in trace level high-resolution gas chromatography/high-resolution mass spectrometry (HRGC/HRMS) analytical procedures. *Chemosphere*, 34: 2451-2465.

Fillmann, G., Galloway, T.S., Sanger, R.C., Depledge, M.H. and Readman, J.W. 2002. Relative performance of immunochemical (enzyme-linked immunosorbent assay) and gas chromatography-electron-capture detection techniques to quantify polychlorinated biphenyls in mussel tissues. *Analyt. Chim. Acta,* 461(10): 75-84.

Finch, S. 1990. Alternative methods of PCB analysis, [17 January 2012] http://www.dexsil.com/uploads/docs/dtr_10_01.pdf

Frame, G.M., Cochran, J.W., and Boewadt, S.S. 1996. Complete PCB congener distributions for 17 Aroclor mixtures determined by 3 HRGC systems optimized for comprehensive, quantitative, congener-specific analysis. *J. High Res. Chromatogr.,* 19: 657-668.

Furukawa, K., Suenaga, H. and Goto, M. 2004. Biphenyl dioxygenases: Functional versatilities and directed evolution. *J. Bacteriol.*, 186: 5189-5196.

Furukawa, Y., Ueda, F., Ohydo, Y., Harada, I., Nakajima, T. and Kawagoe, T. 1988. Vibrational spectra and structure of polyaniline. *Macromolecules*, 21: 1297-1305.

Gan, D.R. and Berthouex, P.M. 1994. Disappearance and crop uptake of PCBs from sludge-amended farmland. *Water Environ. Res.*, 66(1): 54-69.

Gayatri, S.L. and Ahmaruzzaman, Md. 2010. Adsorption technique for the removal of phenolic compounds from wastewater using low-cost natural adsorbents. *J. Assam Sci. Soc.*, 5(2): 156-166.

Gibson, D.T., Cruden, D.L., Haddock, J.D., Zylstra, G.J. and Brand, J.M. 1993. Oxidation of polychlorinated biphenyls by *Pseudomonas* sp. Strain LB400 and *Pseudomonas pseudoalcaligenes* KF707. *J. Bacteriology*, 175: 4561.4564.

Gopal, K., Tripathy, S.S., Bersillon, J.L. and Dubey, S.P. 2007. Chlorination by-products, their toxicodynamics and removal from drinking water, *J. Hazard. Mater.*, 140: 1-6.

Guitart, R., Puig, P. and Gómez-Catalán, J. 1993. Requirement for a standardized nomenclature criterium for PCBs: computer assisted assignment of correct congener denomination and number. *Chemosphere*, 27:1451-1459.

Gunkel, G., Mast, P.G. and Nolte, C. 1995. Pollution of aquatic ecosystems by polychlorinated biphenyls (PCB). *Limnologica,* 25(4): 321-331.

Guo, X.J. and Chen, F.H. 2005. Removal of arsenic by bead cellulose loaded with iron oxyhydroxide from groundwater, *Environ. Sci. Technol.*, 39: 6808-6818.

Hansen, B.O., Kwan, P., Benjamin, M.M., Li, C.W. and Korshin, G.V. 2001. Use of iron oxide-coated sand to remove strontium from simulated hanford tank wastes. *Environ. Sci. Technol.*, 35: 4905-4909.

Hansen, L.G. 1999. The ortho side of PCBs: Occurrence and disposition. Boston, MA: Kluwer Academic.

Hansen, L.G., Green, D., Cochran, J., Vermette., S. and Bush, B. 1997. Chlorobiphenyl (PCB) composition of extracts of subsurface soil, superficial dust and air from a contaminated landfill. *Fresenius J. Anal. Chem.,* 357: 442-448.

Hawari, J., Demeter, A. and Samson, R. 1992. Sensitized photolysis of polychlorobiphenyls in alkaline 2-propanol: dechlorination of Aroclor 1254 in soil samples by solar radiation. *Environ. Sci. Technol.,* 26(10): 2022-2027.

Hawari, J.J. 1992. Regioselectivity of Dechlorination: Reductive Dechlorination of Polychlorobiphenyls by Polymethylhydrosiloxane-Alkali Metal. *Organomet. Chem.,* 437: 91-98.

Hazardous Substances Data Bank, (HSDB). 2009. National Library of Medicine. http://toxnet.nlm.nih.gov/cgi-bin/sis/htmlgen?HSDB and search on CAS number. [25 August 2012].

Herrick, R.F., McClean, M.D., Meeker, J.D., Baxter, L.K. and Weymouth, G.A. 2004. An unrecognized source of PCB contamination in schools and other buildings. *Environ. Health Perspect.,* 112: 1051-1053.

Hofelt, C. and Shea, D. 1997. Accumulation of organochlorine pesticides and PCBs by semipermeable membrane devices and *Mytilus edulisin* New Bedford harbour. *Environ. Sci. Technol.,* 31: 154-159.

Hong, C.S., Wang, Y. and Bush, B. 1998. Kinetics and products of the TiO_2 photocatalytic degradation of 2-chlorobiphenyl in water. *Chemosphere,* 36(7): 1653-1667.

Huang, Q. and Rusling, J.F. 1995. Formal Reduction Potentials and Redox Chemistry of Polyhalogenated Biphenyls in a bicontinuos microemulsion. *Environ. Sci. Technol.,* 29(1): 98-103.

Hutzinger, O. and Verrkamp, W. 1981. *Microbial Degradation of Xenobiotics and Recalcitrant Compounds.* New York: Academic Press.

In het Panhuis, M., Sainz, R., Innis, P.C., Kane-Maguire, L.A.P., Benito, A.M., Martinez, M.T., Moulton, S.E., Wallace, G.G. and Maser, W.K. 2005. *J. Phys. Chem.,* B109: 22725-22729.

International Agency for Research on Cancer. 1978. IARC Monographs on the Evaluation of the Carcinogenic Risk of Chemicals to Humans. Some Aromatic Amines and related Nitro Compounds-Hair Dyes, Colouring Agents and Miscellaneous Industrial Chemicals, Lyon, IARC Press. 16: 287-291.

International Register of Potentially Toxic Chemicals, (IRPTC). 1985. Zinc + compounds. N.F. Izmerov (ed.). Centre of International Projects, GKNT, Moscow.

Inzelt, G. 2008. Conducting Polymers. A New Era in Electrochemistry. Springer-Verlag Berlin Heidelberg. 169-265.

Iranzo, M., Sainz-Padro, I., Boluda, R., Sanchez, J. and Mormeneo, S. 2001. The Use of Microorganisms in Environmental Engineering. *Ann. Microbiol.,* 51: 135-143.

Iwata, H., Tanabe, S., Sakai, N., Nishimura, A. and Tatsukawa, R. 1994. Geographical distribution of persistent organochlorines in air, water and sediments from Asia and Oceania, and their implications for global redistribution from lower latitudes. *Environ. Pollut.,* 85: 15-33.

Jang, J.H. and Dempsey, B.A. 2008. Coadsorption of arsenic (III) and arsenic (V) onto hydrous ferric oxide: effects on abiotic oxidation of arsenic (III), extraction efficiency, and model accuracy, *Environ. Sci. Technol.,* 42: 2893-2898.

Jang, M., Chen, W.F. and Cannon, F.S. 2008. Preloading hydrous ferric oxide into granular activated carbon for arsenic removal, *Environ. Sci. Technol.,* 42: 3369-3374.

Jang, M., Min, S.H., Park, J.K. and Tlachac, E.J. 2007. Hydrous ferric oxide incorporated diatomite for remediation of arsenic contaminated groundwater, *Environ. Sci. Technol.*, 41: 3322-3328.

Jang, Y., Zhao, C., Cui, D., Hou, J., Wan, M. and Xu, M. 1995. Polyaniline/polypropylene film composites with high electric conductivity and good mechanical properties. *J. Appl. Polym. Sci.*, 56(7): 831-836.

Jing, X., Wang, Y., Wu, D., She, L. and Guo, Y. 2006. Polyaniline nanofibers prepared with ultrasonic irradiation. *J. Polym. Sci. A: Polym. Chem.,* 44: 1014-1019.

Jones, K.C. Sanders, G., Wild, S.R., Burnett, V. and Johnston, A.E. 1992. Evidence for a decline of PCBs and PAHs in rural vegetation and air in the United Kingdom. *Nature*, 356: 137-140.

Joseph, W. 2000. *Analytical Electrochemistry.* 2nd rev. ed. New York, NY 10158-0012, USA: John Wiley & Sons, Inc.

Karthikeyan, M., Satheeshkumar, K.K. and Elango, K.P. 2009. Removal of fluoride ions from aqueous solution by conducting polypyrrole. *J. Hazard. Mater.,* 167: 300-305.

Kastanek, F., Kastanek, P. and Demnerova, K. 2004. Decontamination of wastewater contaminated by polychlorinated biphenyls (PCBs). *Water Sci.Technol.*, 50(2): 131-138.

Kester, M.H.A., Bulduk, S., Tibboel, D., Meinl, W., Glatt, H., Falany, C.N., Coughtrie, M., Bergman A., Safe, S.H., Kuiper, G., Schuur, A.G., Brouwer, A. and Visser, T.J. 2000. Potent inhibition of estrogen sulfotransferase by hydroxylated PCB metabolites. A novel pathway explaining the estrogenic activity of PCBs. *Endocrinology*, 141: 1897-1900.

Kim, M., Kim, S., Yun, S., Lee, M., Cho, B., Park, J., Son, S. and Kim, O. 2004. Comparison of seven indicator PCBs and three coplanar PCBs in beef, pork and chicken fat. *Chemosphere*, 54(10):1533-1538.

Kotani, A., Kusu, F. and Takamura, K. 2002. New electrochemical detection method in high-performance liquid chromatography for determining free fatty acids. *Analyt. Chim. Acta,* 465: 199-206.

Kulkarni, P.S., Crespo, J.G. and Afonso. C.A.M. 2008. Dioxins sources and current remediation technologies-A review. *Environ. Int.*, 34: 139-153.

Kumar, P.A., Chakraborty, S. and Ray, M. 2008. Removal and recovery of chromium from wastewater using short chain polyaniline synthesized on jute fiber. *Chem. Eng. J.*, 141(1-3): 130-140.

Kunz, S., Schwarz, M., Schilling, B., Papke, O., Lehmler, H.J., Robertson, L.W., Schrenk, D. and Schmitz, H.J. 2006. Tumor promoting potency of PCBs 28 and 101 in rat liver. *Toxicol. Lett.,* 164: 133-143.

Larsson, P. 1985. Contaminated sediments of lakes and oceans act as sources of chlorinated hydrocarbons for release to water and atmosphere. *Nature*, 317: 347-349.

Lee, J.W., Jung, H.J., Kwak, D.H. and Chung, P.G. 2005. Adsorption of dichloromethane from water onto a hydrophobic polymer resin XAD-1600, *Water Res.*, 39: 617-629.

Li, X., Wang, G., Li, X. and Lu, D. 2004. Surface properties of Polyaniline/nano-TiO_2 composites. *Appl. Surf. Sci.,* 229: 395-401.

Li, X.G., Liu, R., Huang and M.R. 2005. Facile Synthesis and Highly Reactive Silver Ion Adsorption of Novel Microparticles of Sulfodiphenylamine and Diaminonaphthalene Copolymers. *Chem. Mater.,* 17(22): 5411-5419.

Liebl, B., Schettgen, T., Kerscher, G., Broding, H.C., Otto, A., Angerer, J. and Drexler, H. 2004. Evidence for increased internal exposure to lower chlorinated polychlorinated biphenyls (PCB) in pupils attending a contaminated school. *Int. J. Hyg. Environ. Health,* 207: 315-324.

Lin, J.M. and Que Hee, S.S. 1987. Change in chromatogram patterns after volatilization of some Aroclors, and the associated quantitation problems. *Am. Ind. Hyg. Assoc. J.,* 48: 599-607.

Lin, Y.Y., Liu, G., Wai, C.M. and Lin, Y. 2008. Bioelectrochemical immunoassay of polychlorinated biphenyl. *Anal. Chim. Acta*, 612(1): 23-28.

Liu, P., Long, C., Li, Q.F., Qian, H.M., Li, A.M. and Zhang, Q.X. 2009. Adsorption of trichloroethylene and benzene vapors onto hypercrosslinked polymeric resin. *J. Hazard. Mater.*, 166: 46-51.

Liu, W., Kumar, J., Tripathy, S., Sanecal, K. J. and Samuelson, L. 1999. Enzymatically synthesized conducting polyaniline. *J. Am. Chem. Soc.*, 121: 71-78.

Long, C., Li, Q.F., Li, Y., Liu, Y., Li, A.M. and Zhang, Q.X. 2010. Adsorption characteristics of benzene-chlorobenzene vapor on hyper crosslinked polystyrene adsorbent and a pilot-scale application study. *Chem. Eng. J.,* 160: 723-728.

Long, C., Liu, P., Li, Y., Li, A. and Zhang, Q. 2011. Characterization of Hydrophobic Hyper crosslinked Polymer as an Adsorbent for Removal of Chlorinated Volatile Organic Compounds. *Environ. Sci. Technol.,* 45: 4506-4512.

Longnecker, M.P., Wolff, M.S., Gladen, B.C., Brock, J.W., Grandjean, P. and Jacobson, J.L. 2003. Comparison of polychlorinated biphenyl levels across studies of human neurodevelopment. *Environ. Health Perspect.*, 111: 65-70.

Lu, Q.F., Huang, M.R. and Li, X.G. 2007. Synthesis and heavy-metal-ion sorption of pure sulfophenylenediamine copolymer nanoparticles with intrinsic conductivity and stability. *Chem. Eur. J.,* 13(21): 6009-6018.

Mackay, D. 1989. Modeling the long-term behaviour of an organic contaminant in a large lake: Application to PCBs in Lake Ontario. *J. Great Lakes Res.,* 15: 283-297.

Mahan, M. 1998. Are PCBs still a problem in the great lakes? Retrieved from http://www.cevl.msu.edu/~long/pcb.html [10 July 2012].

Mahanta, D., Madras, D., Radhakrishnan, S. and Patil, S. 2008. Adsorption of Sulfonated Dyes by Polyaniline Emeraldine Salt and Its Kinetics. *J. Phys. Chem.,* B112: 10153-10157.

Manlon, J.A., Mulder, P. and Louw, R. 1985. Gas-phase hydrogenolysis of polychlorobiphenyls. *Environ. Sci. Technol.,* 19(3): 280-282.

Mansour, M.S., Ossman, M.E. and Farag, H.A. 2011. Removal of Cd (II) ion from waste water by adsorption onto polyaniline coated on sawdust. *Desalination*, 272: 301-305.

Matsunaga, A. and Yasuhara, A. 2005. Dechlorination of PCBs by electrochemical reduction with aromatic radical anion as mediator. *Chemosphere*, 58: 897-904.

Meyer, J.E.P.A.R.T. FTIR Spectroscopy. 1994-2009 Available from: http://www.irgas.com/ftir_spectroscopy.html [13 May 2012].

Mirceski, V., Komorsky-Lovric, S. and Lovric, M. 2007. Square Wave Voltammetry Theory and Application; Scholz, F., ed.; Springer-Verlag Pub.: Berlin.

Monk, P.M.S. 2001. *Fundamentals of Electroanalytical Chemistry*, ed. C. David J. Ando, Dartford, Kent, UK, Southern Gate, Chichester, West Sussex PO19 SSQ, England: John Wiley & Sons Ltd. 158-159.

Mori, T. and Kondo, R. 2002. Oxidation of chlorinated dibenzo-p-dioxin and dibenzofuran by white-rot fungus, Phlebia lindtneri. *FEMS Microbiol Lett.,* 216: 223-227.

Muir, D. and Sverko, E. 2006. Analytical methods for PCBs and organochlorine pesticides in environmental monitoring and surveillance: a critical appraisal. *Anal. Bioanal. Chem.*, 386:769-789.

Murphy, T., Formanski, L.J., Brownawell, B.B. and Meyer, J.A. 1985. PCB emissions to the atmosphere in the Great Lakes region. Municipal landfills and incinerators. *Environ. Sci. Technol.*, 19: 942-946.

Muthukrishnan, A., Boyarskiy, V.P., Sangaranarayanan, M.V. and Boyarskaya, I.A. 2012. Mechanism and Regioselectivity of the Electrochemical Reduction in Polychlorobiphenyls (PCBs): Kinetic Analysis for the Successive Reduction of Chlorines from Dichlorobiphenyls. *J. Phys. Chem. C*116: 655-664.

Nelson, E.D., McConnell, L.L. and Baker, J.E. 1998. Diffusive exchange of gaseous polycyclic aromatic hydrocarbons and polychlorinated biphenyls across the air-water interface of Chesapeake Bay. *Environ. Sci. Technol.*, 32: 912-919.

Oesterle, D. and Deml, E. 1981. Promoting effect of various PCBs and DDT on enzyme altered islands in rat liver. *Arch. Pharmacol. Supple.,* 316: 16.

Oku, A., Yasufuku, K. and Kataoka, H. 1978. A complete dechlorination of polychlorinated biphenyl by sodium naphthalene. *Chem. Ind.,* 4: 841-842.

Okumu, F.O. and Matoetoe, M.C. 2012. Mechanism and kinetics for adsorption of indigo with polyaniline. Paper presented at the Environmin 2012 Conference: Environmental Health Aspects of Mining, Refining and Related Industries, Forever Resorts, Middleburg, 11-15 March 2012.

Oliver, B.G. and Niimi, A.J. 1988. Trophodynamic Analysis of Polychlorinated Biphenyl Congeners and Other Chlorinated Hydrocarbons in the Lake Ontario Ecosystem. *Environ. Sci. Technol.*, 22: 388-397.

Oniyama, E. and Wahlbeck, P.G. 1995. Application of transpiration theory to TGA data: calcium carbonate and zinc chloride. *Thermochim. Acta*, 250: 41-53.

Otero, M., Zabkova, M., A.E. and Rodrigues, A.E. 2005.Comparative study of the adsorption of phenol and salicylic acid from aqueous solution onto nonionic polymeric resins, *Sep. Purif. Technol.*, 45: 86-95.

Pan, B.C., Chen, J.L., Zhang, Q.X. and Wang, Y. 1999. Treatment and resource reuse of industrial wastewater from production process of phenyl acetic acid, Chin. *J. React. Polym.*, 8: 82-89.

Pan, B.C., Zhang, Q.X., Meng, F.W., Li, X.T., Zhang, X., Zheng, J.Z., Zhang, W.M., Pan, B.J. and Chen, J.L. 2005. Sorption enhancement of aromatic sulfonates onto an aminated hyper-cross-linked polymer, *Environ. Sci. Technol.,* 39: 3308-3313.

Pan, B. Pan, B. Zhang, W., Lv, L., Zhang, Q. and Zheng, S. 2009. Development of polymeric and polymer-based hybrid adsorbents for pollutants removal from waters. *Chem. Eng. J.*, 151: 19-29.

Pearson, R.F. 1996. Concentrations, accumulations, and inventories of hydrophobic organochlorine compounds in sediments of the Great Lakes and in the benthic nepheloid layer of Lake Michigan. Department of Environmental Health, University of Minnesota, Minneapolis, MN.

Pham, T.T. and Proulx, S. 1997. PCBs and PAHs in the Montreal urban community (Quebec, Canada) wastewater treatment plant and in the effluent plume in the St. Lawrence River. *Water Res.,* 31(8): 1887-1896.

Rajashwar, K. and Ibanez, J.G. 1997. Fundamentals and applications in pollution abatement, *Environmental Chemistry*: San Diego, California: Academic Press: 21 and 88.

Reddy, K.R., Lee, K.P. and Gopalan, A.I. 2008. Self-assembly approach for the synthesis of electro-magnetic functionalized Fe_3O_4/polyaniline nanocomposites: Effect of dopant on the properties. *Colloids Surf.,* A320(1-3): 49-56.

Reddy, K.R., Sin, B.C., Yoo, C.H., Sohn, D. and Lee, Y. 2009. Coating of multiwalled carbon nanotubes with polymer nanospheres through microemulsion polymerization. *J. Colloid Interface Sci.,* 340(2): 160-165.

Reichert, A. and Korte, H. 2009. Methoden zur Bestimung der Masseanteile in Verbundwerkstoffenaus thermoplastischen Polymeren und Lignocellulosen, Holztechnologie 50: 38-43.

Rehmann, L. and Daugulis, A.J. 2008. Biodegradation of PCBs in two-phase partitioning bioreactors following solid extraction from soil. *Biotechnol. Bioeng.,* 99(5):1273-1280.

Renneckar, S., Zink-Sharp, A.G., Ward, T.C. and Glasser, W.G. 2004. Compositional analysis of thermoplastic wood composites by TGA. *J. Appl. Polym. Sci.,* 93: 1484-1492.

Ross, R.A. and Lemay, R. 1987. Efficiencies of aluminium, magnesium, and their oxides in the destruction of vapour-phase polychlorinated biphenyls. *Environ. Sci. Technol.*, 21: 1115-1118.

Roth, J.A., Dakoji, S.R., Hughes, R.C. and Carmody, R.E. 1994. Hydrogenolysis of polychlorinated biphenyls by sodium borohydride with homogeneous and heterogeneous nickel catalysts. *Environ. Sci. Technol.*, 28: 80-87.

Ryslava, E., Krejcik, Z., Macek, T., Novakova, H., Denmerova, K., and Mackova, M. 2003. Study of PCB Degradation in Real Contaminated Soil. *Fres. Environ. Bull.*, 12: 296-301.

Sabata, S., Friesova, A., Rericha, R. and Hetflejs, J. 1993. Limits to the use of KOH/PEG method for destruction of PCB liquids of Czechoslovak production. *Chemosphere,* 27: 1201-1210.

Safe, S., Bandiera, S., Sawyer, T., Robertson, L., Safe, L., Parkinson, A., Thomas, P.E., Ryan, D.E., Reik, L.M. and Levin, W. 1985. PCBs: structure-function relationships and mechanism of action. *Environ. Health Perspect.,* 60: 47-56.

Safe, S. and Hutzinger, Otto. 1984. Polychlorinated biphenyls (PCBs) and polybrominated biphenyls (PBBs): Biochemistry, toxicology, and mechanism of action. *CRC Crit. Rev. Toxicol.*, 13: 319-395.

Sako, T., Sato, M., Sugeta, T., Otake, K. and Okano, M. 2000. Method of decomposing polychlorobiphenyls. U.S. Patent, (Sep-26), Number 6124519.

Sandal. S., Yilmaz, B. and Carpenter, D.O. 2008. Genotoxic effects of PCB 52 and PCB 77 on cultured human peripheral lymphocytes. *Mutat. Res.*, 654: 88-92.

Sargent, L. Dragan, Y.P. and Erikson, C. 1991. Study of the separate and combined effects of the non-planar 2, 5, 2', 5'- and the planar 3, 4, 3', 4'-tetrachlorobiphenyl in liver and lymphocytes *in vivo. Carcinogenesis,* 12: 793-800.

Sediak, D.L. and Andren, A.W. 1991. Aqueous-Phase Oxidation of Polychlorinated Biphenyls by Hydroxyl Radicals. *Environ. Sci. Technol.*, 25: 1419-1427.

Seo, D.K., Park, S.S., Hwang, J. and Tae-U Yu. 2010. Study of the pyrolysis of biomass using thermo-gravimetric analysis (TGA) and concentration measurements of the evolved species. *J. Anal. Appl. Pyrolysis*, 89: 66-73.

Sharypov, V.I., Marin, N., Beregovtsova, N.G., Baryshnikov, S.V., Kuznetsov, B.N., Cebolla, V.L. and Weber, J.V. 2002. Co-pyrolysis of wood biomass and synthetic polymer mixtures. Part I: influence of experimental conditions on the evolution of solids, liquids and gases. *J. Anal. Appl. Pyrolysis,* 64: 15-28.

Shear, N.M., Schmidt, C.W., Huntley, S.L. 1996. Evaluation of the factors relating combined sewer overflows with sediment contamination of the lower Passaic River. *Mar. Pollut. Bull.,* 32(3): 288-304.

SiliconFarEast.com. FTIR Spectroscopy. 2001-2005: Available from: http://www.siliconfareast.com/FTIR.html [13 May 2012].

Silkworth, J.B., Antrim, L. and Kaminsky, L.S. 1984. Correlations between polychlorinated biphenyl immunotoxicity, the aromatic hydrocarbon locus, and liver microsomal enzyme induction in C57BL/6 and DBA/2 mice. *Toxicol. Appl. Pharmacol.,* 75(1): 156-165.

Simon, T., Britt, J.K. and James, R.C. 2007. Development of a neurotoxic equivalence scheme of relative potency for assessing the risk of PCB mixtures. *Regul. Toxicol. Pharm.,* 48(2): 148-170.

Simpson, E.J., Koros, W.J. and Schechter, R.S. 1996. An emerging class of volatile organic compound sorbents: friedel-crafts modified polystyrenes. 2. Performance comparison with commercially-available sorbents and isotherm analysis. *Ind. Eng. Chem. Res.,* 35: 4635-4645.

Singer, D., Smith, W.A., Jury, W.A., Hathuc, K. and Crowley, D.E. 2003. Impact of the plant rhizosphere and augmentation on remediation of polychlorinated biphenyls contaminated soil AC. *Environ. Toxicol. Chem.*, 1998-2004.

Sklarew, D.S. and Girvin, D.C. 1987. Attenuation of polychlorinated biphenyls in soils. *Rev. Environ. Contam. Toxicol.,* 98:1-41.

Skoog, E.A. 2007. *Principles of Instrumental analysis.*6th ed. Singapore: Thomson Brooks/Cole: 169-173.

Skotheim, T.A. 1986. *Handbook of Conducting Polymers.* New York: Marcel Dekker: Chapter 15.

Smith, K.E., Schwab, A.P. and Banks, M.K. 2007. Phytoremediation of Polychlorinated Biphenyl (PCB)-Contaminated Sediment A Greenhouse Feasibility Study – *J. Environ. Qual.,* 36(1): 239-244.

Sotelo, J.L., Ovejero, G., Delgado, J.A. and Martinez, I. 2002. Comparison of adsorption equilibrium and kinetics of four chlorinated organic from water onto GAC. *Water Res.*, 36: 599-608.

Suzuki, H. 1997. Process for decomposition of PCBs by sodium dispersion. *Environ. Manag.,* 33: 889-894.

Swackhamer, D.L. and Armstrong, D.E. 1986. Estimation of the atmospheric and nonatmospheric contributions and losses of polychlorinated biphenyls for Lake Michigan on the basis of sediment records of remote lakes. *Environ. Sci. Technol.,* 20: 879-883.

Syracuse Research Corporation, (SRC). 2009. *Interactive PhysProp Database Demo.* http://www.syrres.com/what-we-do/databaseforms.aspx?id=386 and search on CAS number. [12 August 2012].

Tang, L., Wu, T. and Kan, J. 2009. Synthesis and properties of polyaniline–cobalt coordination polymer. *Synth. Met.,* 159(15-16): 1644-1648.

Tiedje, J.M., Quensen, J.F. III, Chee-Sanford, J., Schimel, J.P. and Boyd, S.A. 1993. Microbial reductive dechlorination of PCBs, *Biodegradation*, 4: 231-240.

Timberlake, D.L. and Garbaciak, S. 1995. Bench-Scale Testing of Selected Remediation Alternatives for Contaminated Sediments. *J. Air Waste Manage. Assoc.,* 45(1): 52-56.

Trivedi, D.C. 1999. Influence of counter ion on polyaniline and polypyrrole, *Bull. Mater. Sci.*, 22(3): 447-455.

Trivedi, P., Axe, L. and Tyson, T.A. 2001. XAS studies of Ni and Zn sorbed to hydrous manganese oxide, *Environ. Sci. Technol.*, 35: 4515-4521.

Tsyurupa, M.P. and Davankov, V.A. 2006. Porous structure of hypercrosslinked polystyrene: State-of-the-art mini-review. *React. Funct. Polym.,* 66: 768-779.

U.S. Environmental Protection Agency. 2003. PCB ID-Table of PCB Congeners and Other Species. Washington, DC: Environmental Protection Agency.

Unde, S., Ganu, J. and Radhakrishnan, S. 1996. Conducting polymer-based chemical sensor: Characteristics and evaluation of polyaniline composite films. *Adv. Mater. Opt. Electron.,* 6(3): 151-157.

United Nations Environmental Programme. 1999. Guidelines for the identification of PCBs and materials containing PCBs, first issue, August 1999, prepared by UNEP Chemicals.

United Nations Environment Programme Chemicals. 2005. Ridding the World of POPs: A Guide to the Stockholm Convention on Persistent Organic Pollutants, United Nations Environment Programme Chemicals, Geneva, Switzerland: UNEP.

United Nations Environment Programme. 1997. Proceedings of the Subregional Awareness Raising Workshop on Persistent Organic Pollutants (POPs), Bangkok, Thailand. United Nations Environment Programme. November 25-28th, 1997.

Waid, J.S. 1986b. PCBs and the environment. Vol. II. CRC Press, Inc., Boca Raton, Fla.

Wallace, J.C., Basu, I. and Hites, R.A. 1996. Sampling and analysis artifacts caused by elevated indoor air polychlorinated biphenyl concentrations. *Environ. Sci. Technol.,* 30(9): 2730-2734.

Wang, J., Deng, B., Chen, H., Wang, X. and Zheng, J. 2009. Removal of aqueous Hg (II) by polyaniline: sorption characteristics and mechanisms. *J. Environ. Sci. Technol.,* 43(14): 5223-5228.

Wang, M.L., Meng, G.W., Huang, Q., Li, M.T., Li, Z.B. and Tang, C.L. 2011. *Analyst*, 136: 278.

Wang, S.L., Chang, Y.C., Chao, H.R., Li, C.M., Li, L.A., Lin, L.Y. and Päpke, O. 2006. Body burdens of polychlorinated dibenzo-p-dioxins, dibenzofurans, and biphenyls and their relations to estrogen metabolism in pregnant women. *Environ. Health Perspect.*, 114(5): 740-745.

Wania, F. and Mackay, D. 1996. Tracking the distribution of persistent organic pollutants. *Environ. Sci. Technol.*, 30(9): 390A-396A.

Waryo, T.T., Songa, E.A., Matoetoe, M.C., Ngece, R.F., Ndangili, P.M., AlAhmed, A., Jahed, N.M., Baker, P.G.L. and Iwuoha, E.I. 2009. Functionalisation of polyaniline nanomaterials for amperometric biosensing, *Nanostructured Materials for Electrochemical Biosensors*, New York: Nova Science Publishers.

Webster, R.D. 2004. *In situ* electrochemical-NMR spectroscopy. Reduction of aromatic halides. *Anal. Chem.*, 76(6): 1603-1610.

Wesolwski, M. 1995. Thermogravimetric and principal component analyses in quality assessment of lubricating oils. *J. Therm. Anal.*, 43: 291-297.

Wiegel, J. and Wu, Q.Z. 2000. Microbial reductive dehalogenation of polychlorinated biphenyls. *FEMS Microbiol. Ecol.*, 32: 1-15.

Willman, E.J., Manchester-Neesvig, J.B., Agrell, C. and Armstrong, D.E. 1999. Influence of ortho-substitution homolog group on polychlorobiphenyl bioaccumulation factors and fugacity ratios in plankton and zebra mussels (*Dreissena polymorpha*). *Environ. Toxic. Chem.*, 18: 1380-1389.

Windt, M., Meier, D. and Lehnen, R. 2011. Quantification of polypropylene (PP) in wood plastic composites (WPCs) by analytical pyrolysis (Py) and differential scanning calorimetry (DSC), Holzforschung, 65: 199-207.

Winneke, G., Bucholski, A., Heinzow, B., Kramer, U., Schmidt, E., Walkowiak, J., Wiener, J.A. and Steingruber, H.J. 1998. Developmental neurotoxicity of polychlorinated biphenyls (PCBs): cognitive and psychomotor functions in 7-month old children. *Toxicol. Lett.*, 102-103: 423-428.

Woodhouse, A.J. and Cooke, G.M. 2004. Suppression of aromatase activity in vitro by PCBs 28 and 105 and Aroclor 1221. *Toxicol. Lett.*, 152: 91-100.

World Health Organization. 2003. *Health Risks of Persistent Organic Pollutants from Lon-range Transboundary Air Pollution*, The Regional Office for Europe of the World Health Organization, Copenhagen, Denmark: WHO.

Wu, Q., Sowers, K.R. and May, H.D. 1998. Microbial Reductive Dechlorination of Aroclor 1260 in Anaerobic Slurries of Estuarine Sediments. *Appl. Environ. Microbiol.*, 1052-1058.

Xu, G., Wang, W., Qu, X., Yin, Y., Chu, L., Wu, H., Fang, J., Bao, Y. and Liang, L. 2009. Electrochemical properties of polyaniline in *p*-toluene sulfonic acid solution. *Eur. Polym. J.*, 45: 2701-2707.

Yang, L. 2008. *Materials Characterization:* Introduction to Microscopic and Spectroscopic Methods. Singapore: John Wiley & Sons (Asia) Pty Ltd.

Ye, D., Quensen, J.F., Tiedje, J.M. and Boyd, S.A. 1995. Evidence for para dechlorination of polychlorobiphenyls by methanogenic bacteria. *Appl. Environ. Microbiol.*, 61: 2166-2171.

Yue, J. and Epstein, A.J. 1990. Synthesis of self-doped conducting polyaniline. *J. Am. Chem. Soc.*, 112(7): 2800-2801.

Zanello, P. 2003. *Inorganic Electrochemistry.* Theory, Practice and Application, Cambridge CB4 OWF, UK: The Royal Society of Chemistry.

Zhang, P.C., Scrudato, R.J., Pagano, J.J. and Roberts, R.N. 1993. Photodecomposition of PCBs in aqueous systems using TiO_2 as catalyst. *Chemosphere*, 26: 1213-1223.

Zhang, S. and Rusling, J.F. 1995. Dechlorination of polychlorinated biphenyls on soils and clay by electrolysis in a bicontinuous microemulsion. *Environ. Sci. Technol.,* 29: 1195-1199.

Zheng, K., Pan, B.C., Zhang, Q.J., Zhang, W.M., Pan, B.J., Han, Y.H., Zhang, Q.R., Du, W., Xu, Z.W. and Zhang, Q.X. 2007. Enhanced adsorption of *p*-nitroaniline from water by a carboxylated polymeric adsorbent, *Sep. Purif. Technol.*, 57: 250-256.

CHAPTER THREE
ELECTROCHEMICAL ANALYSIS OF PCBs

3.1 Introduction

This chapter focuses on the electroanalytical aspect of polychlorinated biphenyls (PCBs) since PCBs have been found to have formal reduction potentials (Huang and Rusling, 1995). This insight allows possible monitoring of their electrochemical behaviour through various electroanalytical studies. In this respect, the electroactive species in the PCBs is exploited through the development of an electroanalytical technique and much attention paid on their redox activity. Analytical methods for the analysis of polychlorinated biphenyls (PCBs) are widely available and are the result of a vast amount of environmental analytical method development and research on persistent organic pollutants (POPs) over the past 30-40 years.

The development of electrochemical methods for the measurement of PCBs continues to be the subject of several research and development efforts. A number of methods have been proposed or developed for the determination of PCBs. These include gas chromatography with electron capture detector, mass selective detectors, and mass spectrometers (Erickson, 1992). Although these methods are accurate and reliable, they are often tedious and too expensive for large-scale screening purposes, and they utilize large volumes of expensive and toxic solvents. Some less expensive but more widely available field screening techniques for PCBs and other priority pollutants are provided through a number of colorimetric kits, enzyme immunoassays (EIAs), and biosensors (Rogers and William, 1995). Among these field analytical techniques, electrochemical analyses are especially suitable for rapid, continuous, and *in-situ* on-site analysis of environmental pollutants.

Recently the electroanalytical methods have been the preferred choice over other methods as they are simple and have rapid procedures with a potential for a wide range of applications (Kotani *et al.,* 2002). Electrochemical analysis involves the use of electroanalytical methods to measure the potential (volts) and/or current (amps) in an electrochemical cell containing the analyte (Skoog *et al.,* 1988; Bard and Faulkner, 2001) of interest. Electrochemical methods of analysis are the aggregate of methods of qualitative and quantitative analysis based on electrochemical phenomena occurring within a medium or at the phase boundary and related to changes in the structure, chemical composition, or concentration of the compound being analyzed. These methods can be categorized according to which aspects of the cell are controlled and which are measured. The three

main categories are potentiometry (the difference in electrode potentials is measured), coulometry (the cell's current is measured over time), and voltammetry (the cell's current is measured while actively altering the cell's potential). In this study, attention is paid to voltammetric methods.

The use of voltammetric techniques is very attractive for the development of *in situ* analytical tools (Del Carlo *et al.,* 1997) and this has widened their application in electrochemical analysis. For direct electrochemical determination of PCBs it is necessary to use a nonaqueous, polar aprotic medium, in particular *N,N*-dimethylformamide (DMF), dimethylsulfoxide (DMSO) and acetonitrile (ACN), although, from an analytical point of view, 3±5vol. % of water is not excluded as well as the presence of tetraalkylammonium salts as supporting electrolyte, to reach highly negative potentials necessary for the reduction of low substituted derivatives (Rusling *et al.,* 1985).

The rest of this chapter presents the results of analysis of the PCB congeners employing the two voltammetric techniques; cyclic voltammetry (CV) and square wave voltammetry (SWV) with in depth discussions. These techniques were used to develop and validate a method of analysis of the selected PCB congeners (PCB 28, PCB 52 and PCB 101). Bare glassy carbon electrode (GCE) was used to provide an environment for the electrochemical reduction and has been exploited for the detection of PCBs. PCB congener analytes were placed into a three-electrode electrochemical cell containing a fixed concentration of supporting electrolyte and their electrochemistry investigated. The electrodes were connected to a computer-controlled electrochemical analyzer and the determination of the reduction of polychlorinated biphenyls achieved directly. In both CV and SWV studies, the current response was measured by investigating its glassy carbon activity towards the reduction of the PCBs.

3.2 Experimental method

3.2.1 Instrumentation

Cyclic and square wave voltammetry electrochemical experiments were carried out using a BAS 100W electrochemical analyzer from Bioanalytical systems inc. (West Lafayette, IN) with conventional three electrode system consisting of glassy carbon electrode (GCE) as the working electrode (A = 0.071 cm^2), a platinum wire (3 mm diameter) from Sigma Aldrich and Ag/AgCl (3 M NaCl) electrodes from BAS were used as auxiliary and reference electrodes respectively.

All experimental solutions were purged with high purity argon gas and blanketed with argon atmosphere during measurements. The experiments were carried out at room temperature (25 °C). Alumina micropowder and polishing pads were obtained from Buehler, IL, USA and were used for polishing of the GCE. All potentials were quoted with respect to Ag/AgCl.

3.2.2 Reagents and materials

The reagents used in this study included: acetonitrile (HPLC grade), phosphate buffer (PBS) at pH 7.4. Analytical grade argon (Afrox, South Africa) was used to degas the system. Tetrabutylammonium perchlorate, (TBAP; Sigma Aldrich, electrochemical grade) was used without further purification. PCB standards (PCB 28, 52 and 101 analytical standards) purchased from Dr. Ehrenstofer (Germany). The working solutions of PCB 28, PCB 52 and PCB 101 were freshly diluted from their stocks.

3.2.3 Electrode preparation

The working electrode a glassy carbon electrode (GCE) was polished consecutively with aqueous slurries of 1.0, 0.3, and 0.05 μm alumina (Al_2O_3) powders on a microcloth pad (Bühler). The GCE was rinsed with distilled water after cleaning them with Al_2O_3 powder of different micrometer sizes then gently rinsed with deionised water. Thereafter the electrode was ultrasonicated for 5 min in ethanol followed by water in order to remove residual polishing material. After rinsing once more with water, the electrode surface was ready for use. The reference electrode, Ag/AgCl (3 M NaCl) was rinsed with distilled water and ready to use. The counter electrode, platinum (Pt) wires surface was cleaned by burning in a flame for several minutes.

3.2.4 Suitability of solvent used as supporting electrolyte

Polychlorinated biphenyls are generally insoluble in water hence a suitable organic solvent is necessary to completely dissolve them. The choice of solvents used was determined by several factors, including conductance, solubility of electrolyte and electroactive substance and the reactivity with electrolytic products. In Fry and Britton's handy review of solvents and electrolytes (Fry and Britton, 1984) acetonitrile, ethanol, methanol, and methylene chloride are recommended as good oxidative (anodic) electrochemical solvents, while DMF and DMSO are suggested for reductive (cathodic) electrochemistry. However, in this study, acetonitrile (CH_3CN) was chosen as a good reductive (cathodic) electrochemical solvent since it is widely used in HPLC analysis which is the accepted methods of analysis of PCBs and it was found to dissolve most of the PCBs and has been reported to have a relatively

high dielectric constant, has the ability to dissolve electrolytes, is relatively non-toxic and portrays good electrochemical properties. Since, acetonitrile is a non-aqueous electrolyte, a suitable supporting electrolyte was necessary to further enhance conductivity, minimize double-layer and migration currents. Tetrabutylammonium perchlorate (TBAP) was chosen as the supporting electrolyte based on its solubility in acetonitrile and its inertness towards the electroactive species (PCBs). However, since most PCBs are found in wastewater a phosphate buffer of pH 7.4 was introduced to provide a suitable medium to improve solubility of the PCB analytes.

In this work, phosphate buffer was introduced in to the acetonitrile by preparing a solution of acetonitrile and phosphate buffer (PBS) in the ratio 80:20 v/v (acetonitrile: phosphate buffer respectively). The mixture of acetonitrile and phosphate buffer was used as the solvent in all voltammetric applications. Before each experiment the total volume of the supporting electrolyte was kept constant at 5 mL. Before applying potential, the solution was degassed by bubbling argon gas through for 15 mins and then maintained oxygen free by keeping a blanket of argon above the solution.

3.3 Preparation of PCB analyte

Stock solutions were prepared in acetonitrile/methanol to make 3.88×10^{-3} M for PCB 28 and 3.06×10^{-3} M PCB 101. For the PCB 52, the 3.42×10^{-5} M stock solution was purchased prepared in Isooctane. All the stock solutions were kept in a refrigerator. For further analysis, fresh amounts of 5 µL of the stock solution of each analyte were added before each experiment to give different concentrations from the standard stock solution in 0.1 M TBAP/ACN/PBS 80:20 v/v solution. The electrochemical properties of PCB 28, PCB 52 and PCB 101 were examined at the glassy carbon electrode surface in 0.1 M TBAP/ACN/PBS 80:20 v/v solution using both cyclic and square wave voltammetry at optimised potential window.

3.4 Electrochemical property of PCBs at GC electrode surface

As the main objective of the study was to develop an electrochemical method of analysis for selected polychlorinated biphenyls congeners, the electrochemical behaviour of the PCBs was investigated. The electrochemical processes observed at the glassy carbon electrode were only of the reduction processes showing cathodic peaks as noted (Figure 3.1 and 3.2). This behaviour of the selected PCB congeners is typical of irreversible reduction process and proved that the PCB congeners' were electroactive and exhibited irreversible electrochemistry.

The response of the GC electrode in PCB analysis was studied between -2500 and 500 mV (vs. Ag/AgCl) where no redox peak occurred for the PCBs studied in the blank supporting electrolyte as shown in Figure 3.1 and 3.2. On addition of PCB to the supporting electrolyte, an irreversible reduction peak was observed at the glassy carbon electrode. The fact that no oxidation peaks of PCB were observed at the GCE is in agreement with the related studies elsewhere (Muthukrishnan *et al.*, 2012).

The blank voltammograms corresponds to addition of blank solutions prepared the same way as the standard solutions (Figure 3.1). No significant change in current was observed when blank solutions were added. This shows that the increase in current was entirely due to the PCB congeners. After measurement of the blank responses, a given known concentration of PCBs standards were injected successively into 0.1 M TBAP/ACN/PBS 80:20 v/v solution and their peak currents recorded as response.

The peak 1 and peak 2 in each voltammogram corresponds to the first and second reductions respectivey in each PCB analyte used. These reductions are due to the electron transfer leading to C-Cl cleavage in the biphenyl molecule as discussed in section 3.4.1.

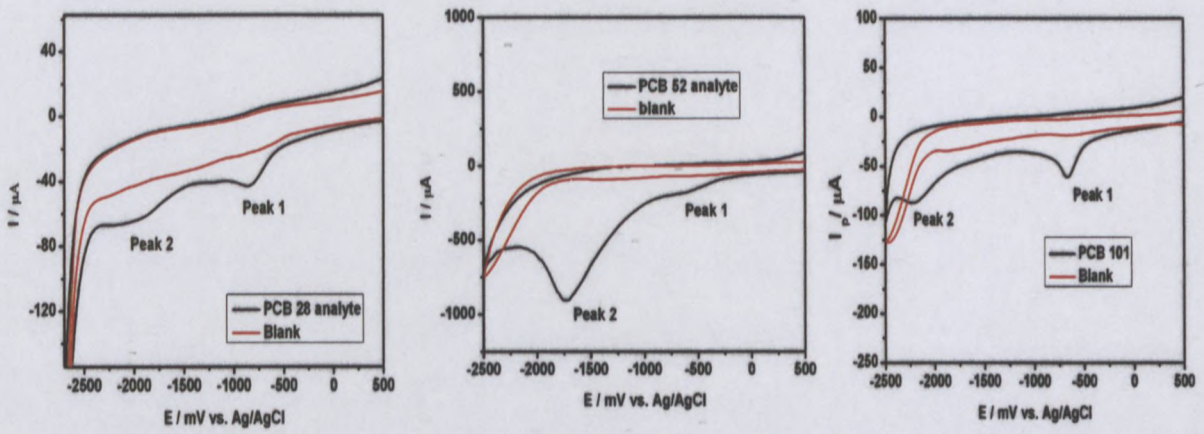

Figure 3.1: Cyclic voltammetry of blank and PCB analytes in 0.1 M TBAP/ACN/PBS 80:20 v/v solution at 20 mV/s.

The CV characterization further displayed the reduction of the PCB congeners as dependent on the scan rates (discussed in section 3.4.2). The results in Figure 3.2 were based on the square wave voltammetric responses to PCB 28, PCB 52 and PCB 101 dissolved in the 0.1 M TBAP/ACN/PBS 80:20 v/v solution.

The results in this study can be elucidated with a mechanism of the PCB reduction represented by Scheme 3.1. The decomposition of each C-Cl bond in polychlorinated biphenyls congeners in this study were suggested to have followed one of the two different mechanisms namely; (i) stepwise and (ii) concerted (Muthukrishnan *et al.*, 2012) (Scheme 3.1).

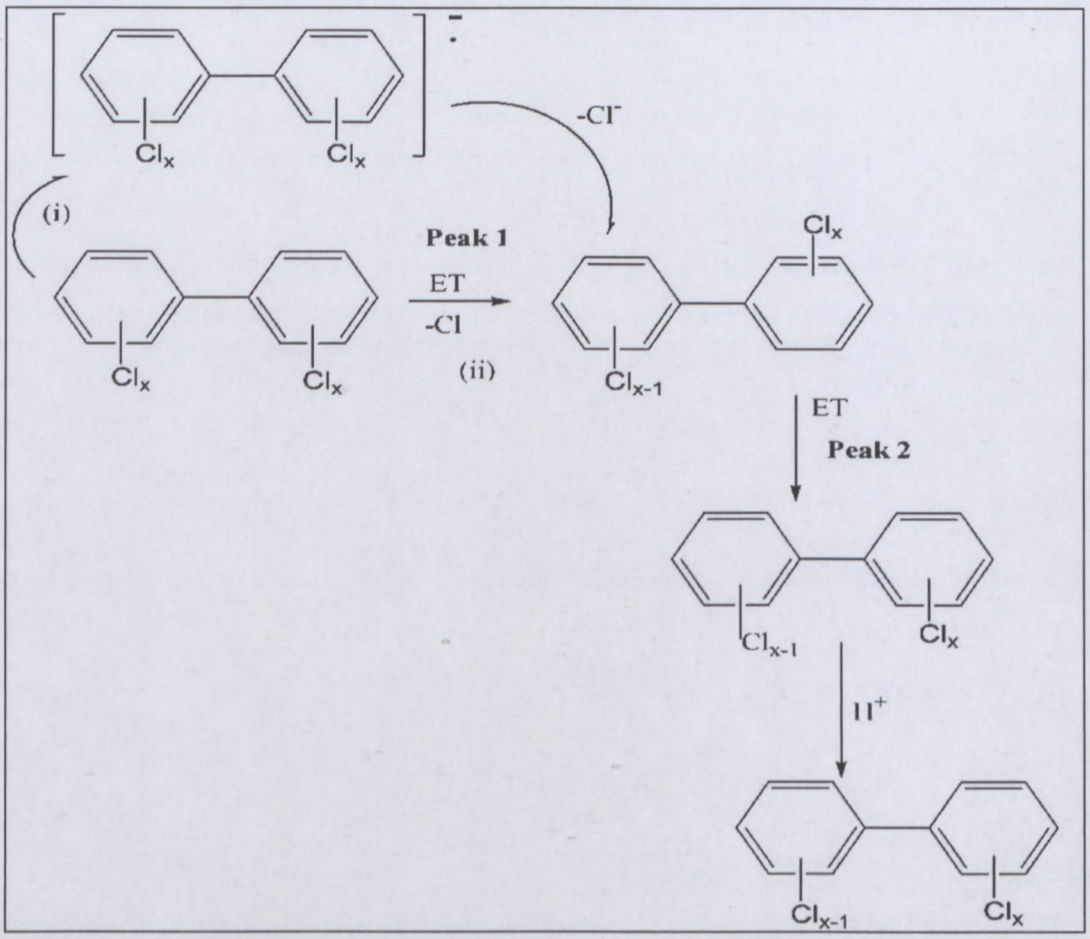

Scheme 3.1: Mechanism of electrochemical reduction of polychlorinated biphenyls.

In Scheme 3.1, ET refers to the electron transfer and steps (i) and (ii) indicate the mechanism steps dependent on the transfer coefficients deduced. The first electron transfer was attributed to step 1 and explains the first reduction peak in each PCB reduction through C-Cl cleavage to give a less chlorinated species in solution while the corresponding 2nd electron transfer yields a much less chlorinated molecule which was associated with the peak 2 in each of the PCB analytes. All three chlorinated biphenyls employed for the analysis exhibited two irreversible peaks corresponding to the dissociation of the two carbon chlorine bonds. Distinguishing between stepwise and concerted mechanism lies in deducing the transfer coefficient values (Nicholson, 1964; Muthukrishnan *et al.*, 2012).

Since all the PCBs were reduced irreversibly in 0.1 M TBAP/ACN/PBS 80:20 v/v solution, the electrochemical transfer coefficient, α in the reduction process was deduced using equation 1 (Bard and Faulkner, 2001) to explain the mechanism involved.

$$\left|E_p - E_{p/2}\right| = \frac{48mV}{\alpha} \quad \text{.....Equation 1}$$

at 25 °C

Where, E_p and $E_{p/2}$ denote the peak potential (V) and half peak potential (V) respectively. The transfer coefficients α, deduced determined the reaction mechanism steps taken. Normally, for values of α > 0.5, stepwise mechanism is inferred and α □ 0.5 concerted mechanism is preferred (Muthukrishnan *et al.,* 2012). The magnitude of the transfer coefficient plays a central role in inferring the reaction mechanism (Antonello and Maran, 1999). The fast electron transfer processes lead to α > 0.5 while α < 0.5 imply the electron transfer step to be rate determining.

In this study, the estimated transfer coefficients at v = 20 mV/s for PCB 52 for the first and second peaks at the peak potential respectively were obtained as 0.30 and 0.35 based on equation 1, this suggested the occurrence of the concerted mechanism for each C-Cl bond cleavage during reduction where both bonds cleave without any intrinsic barrier, thus implying a concerted mechanism (Muthukrishnan *et al.,* 2012). Similarly, PCB 28 had a transfer coefficient of 0.30 for reduction peak 2 at v = 20 mV/s.

The corresponding transfer coefficients of PCB 101 for the first and second peaks respectively were 0.31 and 0.33, suggesting a concerted mechanism of reduction for each C-Cl bond cleavage in 2, 2', 4, 5, 5'-pentachlorobiphenyl. These values were similar to those found in studies involving chloro- and bromobenzenes reduction (Andrieux *et al.,* 1979; Huang and Rusling, 1995). Studies having similar mechanism were also noted by Muthukrishnan *et al.,* 2012, in the reduction of 2, 3-dichlorobiphenyl in 0.1 M TBAP/ACN solution. The mechanism of PCB reduction has been determined through analysis using convolution potential sweep voltammetry (CPSV) recently carried out (Muthukrishnan *et al.,* 2010) where the electrochemical reduction of polychlorinated biphenyls was reported to involve the dissociation of the C-Cl bonds.

3.4.1 Effect of scan rate

The effect of potential scan rate was investigated here with the increase in the scan rates observed to cause an increase in the peak current. Figure 3.3 shows the SWV of PCB 28, PCB 52 and PCB 101 respectively at different scan rates. Upon increasing the scan rates,

the magnitude of the peak current increased and the peak potentials shifted to more negative potentials. The reduction potential shifts to more negative values as was observed in this work when the scan rate was progressively increased from 20 mV/s to 100 mV/s in PCB 28 (reduction potential shifts progressively as -1907 to -2200 mV), similarly for PCB 52, as the scan rates increased from 10 mV/s to 500 mV/s reduction peaks got wider and overlapped with shifts in the peak potentials (reduction potential shifts progressively as -739, to -833 mV) and for PCB 101, increase in scan rates from 10 mV/s to 400 mV/s resulted in (reduction potential shifts progressively as -610, to -725 mV). Although high scan rates were used, scan rates of 20 mV/s (PCB 28), 30 mV/s (PCB 52) and 20 mV/s (PCB 101) were chosen for further voltammetric studies in each case. The potentials were quoted versus Ag/AgCl reference electrode used in the experimental set-up.

For CV, the peak current (I_p) for an irreversible reaction under diffusion control is given by;

$$I_p = \left(2.99x10^5\right) n\left(\alpha n_a\right)^{1/2} A C_0 D^{1/2} v^{1/2} \quad \text{.....Equation 2}$$

Where all parameters except for scan rate are constant. Thus, the relationship between the peak current and scan rate denotes that the electrochemical process is limited by the rate of diffusion of PCB from the solution to the electrode surface. Peak currents of PCB 28, PCB 52 and PCB 101 (Figure 3.3) showed a linear relationship with the square root of the scan rate. This confirmed that the peak currents were diffusion-controlled (Mathebe *et al.*, 2004).

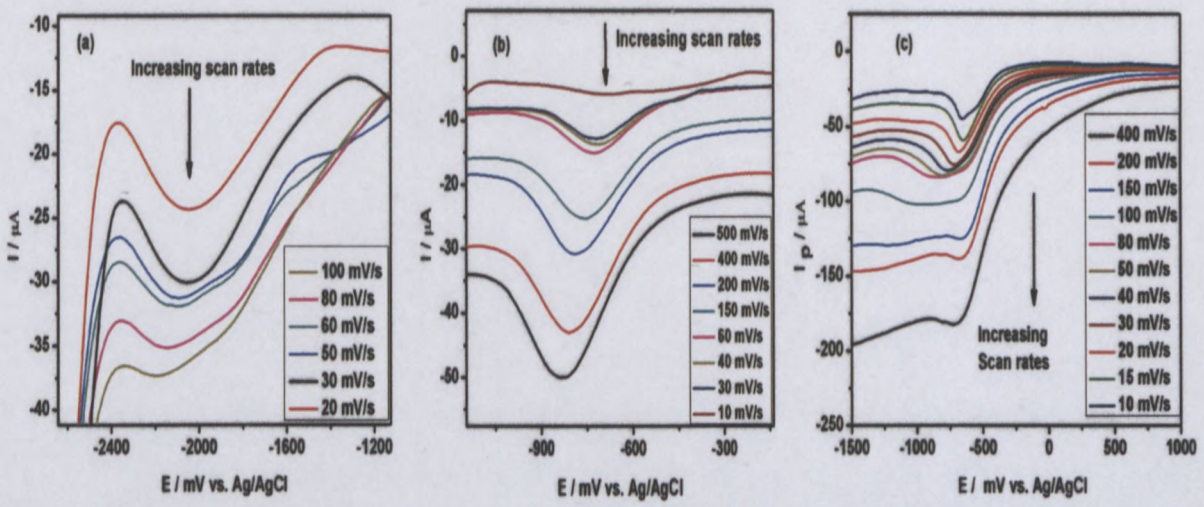

Figure 3.2: Square wave voltammetry of (a) Peak 2 for PCB 28 at concentration 2.5 x 10^{-5} M, (b) Peak 1 for PCB 52 at concentration 1.7 x 10^{-7} M (c) Peak 1 for PCB 101 at concentration 3.1 x 10^{-6} M at different scan rates in glassy carbon electrode in 0.1 M TBAP/ACN/PBS 80:20 v/v solution.

Based on the preferrance of the best signals in CV, the relationship of current with scan rate was monitored for the peaks that gave better results. Peak 1 was analysed for PCB 52 and 101 while peak 2 was analysed for the case of PCB 28 as shown below.

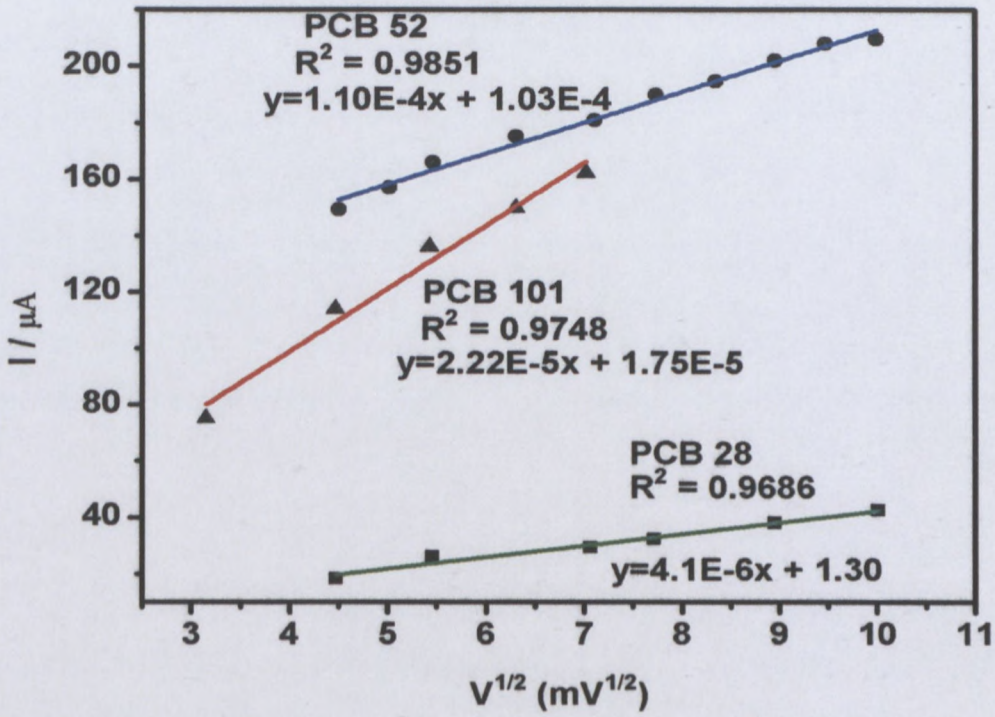

Figure 3.3: Dependence of current (I_p) on the square root of scan rate ($v^{1/2}$) (Randles plot) for peak 1 of PCB 52, PCB 101 and peak 2 for PCB 28 in 0.1 M TBAP/ACN/PBS 80:20 v/v solution.

In Figure 3.4, the results showed that in each PCB analyte reduction, peak currents were diffusion controlled and the electron charge transport coefficient (D_0) of the PCBs was deduced as 1.4 x 10^{-6} cm^2/s, (PCB 28), 4.6 x 10^{-6} cm^2/s (PCB 52) and 5.3 x 10^{-4} cm^2/s (PCB 101) from slopes of I_p vs. $v^{1/2}$ plots using equation 2. These values were close to those of other non-polar organic compounds reported in similar studies (Iwunze *et al.*, 1990; Huang and Rusling, 1995).

From this discussion, it is clear that the peak current for PCBs increased linearly with the square root of the sweep rate ($v^{1/2}$) over the scan rate ranges. These exponents are consistent with the theoretical relation I_p vs. $v^{1/2}$ (equation 2). These results indicated the nature of the electrochemical reaction that occurred was an irreversible diffusion-controlled reduction of PCB 28, PCB 52 and PCB 101 which was limited by the rate of diffusion of the PCBs analytes from the solution to the electrode surface. The plots gave corresponding

slopes with non-zero intercepts in each PCB studied (Figure 3.3) resulting from the non-Faradaic current and uncompensated resistance.

In this work, the electrochemical behaviour of the surface of the GC electrode (GCE) was investigated in degassed aqueous 0.1 M TBAP/ACN/PBS 80:20 v/v solution and the GCE showed good electroactivity owing to the increasing currents with a potential sweep of between -2500 mV to 500 mV.

3.5 Development of the PCBs square wave analysis method

Studies on the electrochemical analysis of PCB congeners are few and as a result there is not enough information. Therefore it was necessary in this study to do a method development where all the necessary analytical parameters were investigated. Predominantly used electroanalytical methods are square wave, stripping voltammetry methods, differential pulse voltammetry and alternating current.

However, the SWV signals were found to give better and more distinct signals and therefore were chosen as the best technique for method development as a result of the high sensitivity, speed and rejection of background currents. The PCB reductions resulted in a two peak chloride reduction in each PCB analyte at lower negative potentials as shown in Figure 3.4.

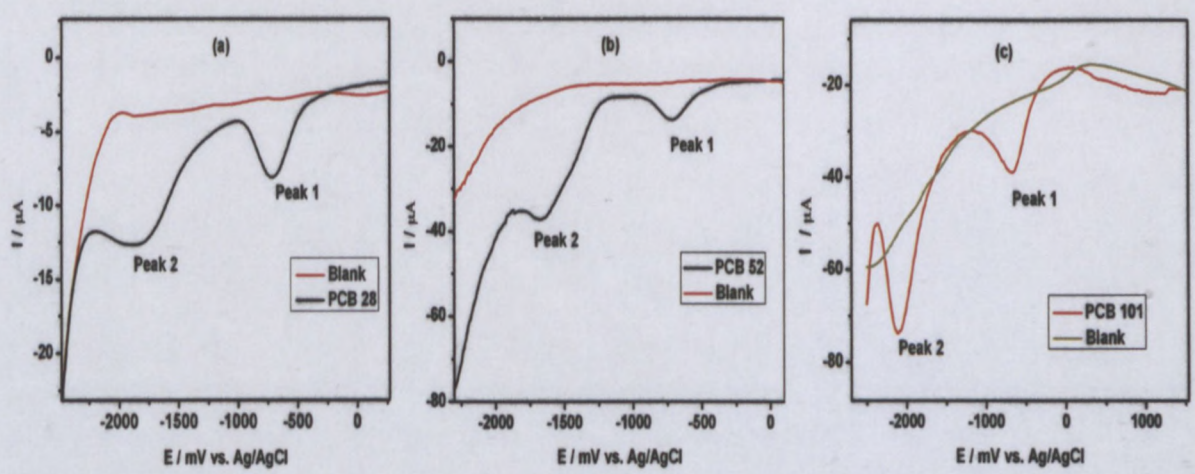

Figure 3.4: Square wave voltammetry of blank and PCB analytes in 0.1 M TBAP/ACN/PBS 80:20 v/v solution at scan rate of 20 mV/s.

For the method development study to be achieved, a calibration study was done on the PCB reductions of each analyte to compare their sensitivities. It has been reported that the reduction of PCBs starts at a potential close to -1000 mV (Huang and Rusling, 1995). In this study, the SWV signals (Figure 3.4) clearly showed reduction peaks around; -719 mV and -1910 mV (vs. Ag/AgCl) in PCB 28, -1610 mV and -625 mV (vs. Ag/AgCl) in PCB 52 and -2110 mV and -637 mV (vs. Ag/AgCl) in PCB 101, which were associated with the cathodic reductions and are within the range of the reduction potentials reported in other studies. Similar results were observed elsewhere where the irreversible behaviour suggested that PCBs were reduced to form a new product (biphenyl) (Huang and Rusling, 1995).

In order to determine the linear range, the square wave voltammograms of PCB 28, PCB 52 and PCB 101 were recorded at different concentrations in 0.1 M TBAP/ACN/PBS 80:20 v/v solution. Various concentrations of PCB 28 (0.26, 0.29, 0.32, 0.36, 0.39 ppm), PCB 52 (0.238, 0.204, 0.17, 0.102, 0.068, 0.034 ppm) and PCB 101 (10.28, 9.22, 7.94, 6.72, 4.87, 3.06 ppm) of the standard solutions were added to the working 0.1 M TBAP/ACN/PBS 80:20 v/v solution in each PCB used followed by stirring for 5 min and the system degassed for 15 mins. The current response was measured in a quiescent solution after every successive addition and recorded. The current generated as a result of the reduction was correlated to the PCB 28, 52 and PCB 101 concentrations. The reduction current generated was proportional to the concentration of PCBs in standard solution as evident in the calibration curves (Figure 3.6).

For calibration studies, the addition of 5 µL of 34.2 ppm of PCB 52 to the 0.1 M TBAP/ACN/PBS 80:20 v/v solution under diffusion controlled reactions resulted in a cathodic current from the reduction of PCB 52 observed at -625 mV (vs. Ag/AgCl) (Figure 3.5). Upon successive additions of PCB 52, the reduction peak at -400 mV (vs. Ag/AgCl) was observed to proportionally decrease with increase in PCB 52 concentration. A similar behaviour was observed with reductions in PCB 28 (Figure 3.5). Possible causes of the decrease in current observed in the reduction of PCB 28 and PCB 52 would be due to their PCB insulating properties and hydrophobicity which has been suggested to limit direct electrochemical detection of PCBs (Wei *et al.,* 2011). However, the reduction decrease with increase in concentration suggested direct proportionality of concentration with the current responses in each case.

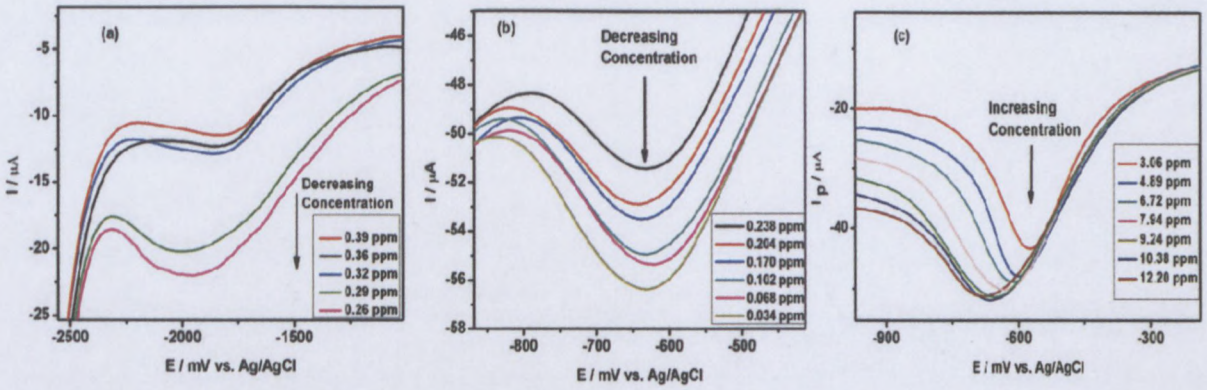

Figure 3.5: SWV curve of (a) Peak 2 of PCB 28, (b) Peak 1 of PCB 52 (c) Peak 1 for PCB 101 different concentrations with glassy carbon electrode in 0.1 M TBAP/ACN/PBS 80:20 v/v solution.

For PCB 101, the reduction peaks with increase in concentration suggested a direct proportionality of concentration with the current responses in PCB 101, which was further demonstrated with linear calibration plots (Figure 3.6). From data in Table 3.2, based on the analytical parameters deduced, peak 1 was chosen as the best peak in PCB 52 and PCB 101 for method development studies since it was the clearer of the 2 peaks in square wave voltammetry and based on its high sensitivity values (Table 3.2) and the percent relative standard deviation (% RSD). For PCB 28, the reduction was favourable with better sensitivity for peak 2 (Table 3.2) and thus preferred for method development studies.

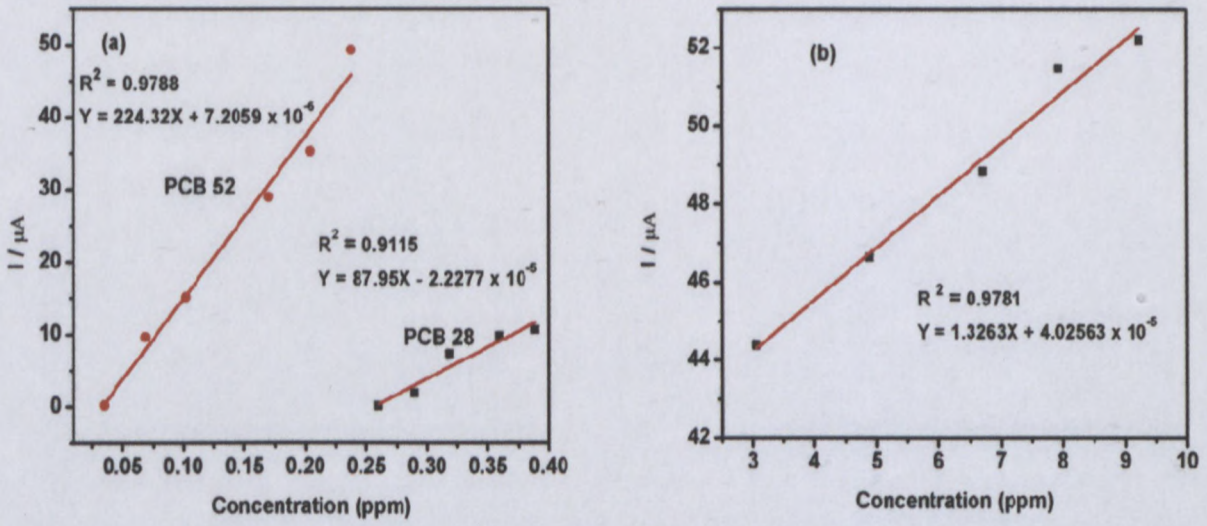

Figure 3.6: SWV calibration curves of (a) Peak 2 current vs. PCB 28, Peak 1 vs. PCB 52 (b) Peak 1 current vs. PCB 101 concentration with glassy carbon electrode in 0.1 M TBAP/ACN/PBS 80:20 v/v solution.

Based on the SWV measurements, a good linear relationship between the cathodic current response and PCB concentration was attained over the range of concentrations which varied per PCB congener analyzed in this study. The correlation coefficient values were derived with respect to each PCB congener reduction and these values showed coherent data. The limit of detections for PCB 28, PCB 52 and PCB 101 from standard solutions, calculated from 3σ/slope of the linear plot, where σ is the standard deviation of the blank measurements were determined and reported in Table 3.2 with respect to the peaks of interest.

The square wave voltammogram of GC electrode in 0.1 M TBAP/ACN/PBS 80:20 v/v solution containing different concentrations of PCB 28, 52 and 101 are shown in Figure 3.5. The cathodic peak potentials of each PCB analyte at the GC electrode were noted.

Calibration curves (Figures 3.6) based on the cathodic peak currents plotted against concentration, were found to be satisfactorily linear for analytical application (Table 3.1). The detection limits (LOD) reported here (Table 3.1) were slightly higher than those obtained using other techniques such as bioelectrochemical immunoassay techniques where LOD of 10 pg mL^{-1} (Lin, 2008) and electrochemical immunosensor using magnetic beads where LOD of 0.4 ng mL^{-1} (Centi *et al.,* 2005) were reported. However, the LODs reported in this study are within the concentration range of polychlorinated biphenyls (PCBs) reported in literature for contaminated systems which are typically in the low 1–10 ng/L range (McDonough *et al.,* 2008).

Further study involved the validation of the developed electroanalytical method which was carried out using recoveries of PCB congeners 28, 52 and 101 at two spiking levels. The % recovery results ranged from 81 % to 126 % (Table 3.1). These results were similar to the past studies of PCB recoveries done using PCB 28, 52 and 101 and were found to range from 55 % to 115 % (Goni *et al.,* 2009). The high percent recoveries are as a result of good efficiency of the extraction from the matrix and the whole analytical process (Turrio *et al.,* 2005).

Table 3.1: Electrochemical analysis of PCBs

Qualitative and voltammetric analysis of PCBs					
	PCB 52		PCB 101		PCB 28
Parameters	Peak 1	Peak 2	Peak 1	Peak 2	Peak 2
Regression coefficient (n=5)	0.979	0.948	0.978	0.975	0.912
% RSD	7.5	1.1	1.5	2.6	6.5
Limit of Detection (LOD) ($molL^{-1}$)	6.80×10^{-9}	1.46×10^{-8}	1.28×10^{-7}	2.99×10^{-7}	3.76×10^{-7}
Linear range ($molL^{-1}$)	10^{-8} to 10^{-7}	10^{-8} to 10^{-7}	10^{-7} to 10^{-6}	10^{-7} to 10^{-6}	10^{-6} to 10^{-5}
Sensitivity (μA/M)	224.37	2.48	1.33	5.66	87.95
Peak Potential (mV) vs. Ag/AgCl at 20 mV/s	-625	-1610	-637	-2110	-1910
% Recovery	115.12 ± 14.1		83.36 ± 2.4		95.91 ± 2.8

The application efficiency of a method is dependent on its reproducibility. Therefore reproducibility is a key element of an analytical method. The reproducibility of this PCB developed method was investigated in the presence of 1.0×10^{-7} M of PCB 52, 2.0×10^{-5} M of PCB 28 and 3.1×10^{-6} M of PCB 101 in 0.1 M TBAP/ACN/PBS 80:20 v/v solution. Square wave voltammetric experiments were repeatedly performed 5 times with the same GC electrode in the solution of the PCB analytes and attention paid on the respective peaks of interest. The relative standard deviation for PCB 28 was found to be 6.5 % with respect to peak 2, PCB 52 was 7.5 % with respect to peak 1 and 1.5 % with respect to peak 1 for PCB 101 confirming that the results (n = 5) were highly reproducible (Table 3.1).

3.6 Interferences to PCB detection.

In real-life situations, most of the PCBs congeners are present in wastewaters or contaminated systems with varying degree of compositions. As a result, interference from other compounds is expected. Several substances are capable of interfering with PCB response during analysis. Such substances can either affect the electrochemical reduction of polychlorinated biphenyls partially or completely. They can either be those substances that are electroactive and get reduced at the PCB reduction potentials or those substances that chemically react with PCBs during analysis thereby affecting the signal responses. However,

due to the inert nature of the PCBs, substances that react with PCBs are limited and therefore the electroactive substances are considered as possible interferences.

Some of these substances include potential organic species such as chlorophenols (Bender and Sadik, 1998) which are electroactive. Other potential substances include; 1, 3, 5-trichlorobenzene (1, 3, 5-TCB), 1, 2, 3, 4-tetrachlorobenzene (1, 2, 3, 4-TeCB), dipterex, imidacloprid, acephate (Wei *et al.,* 2011). Besides these, most metals also pose as possible interferences like Cu, Fe, Ni, Pb, Zn, since they are readily present in wastewater but since their reduction occurs in the positive potentials (Giannopoulou, 2007), they were not considered in this study.

In this study, chlorinated phenols namely 2, 4-dichlorophenol and 2, 4, 6-trichlorophenol, were investigated as one of the above organic substances. This was considered based on structural similarity and the existence of its reduction in the negative potential range. Figure 3.7 shows the square wave voltammograms in presence of PCB 28, PCB 52, PCB 101 and the two interfering compounds. Table 3.3 shows the results of the interference studies for all the PCBs used upon addition of 1:5 and 1:10 quantity of the interferences and PCB respectively, with the PCB concentration used being 4.0×10^{-7} M in each case.

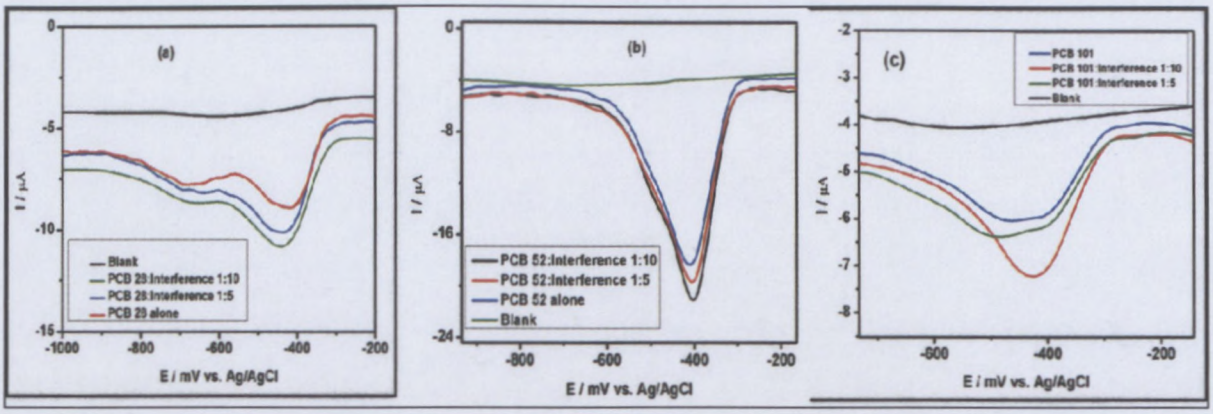

Figure 3.7: SWV of PCBs interferences in 0.1 M TBAP/ACN/PBS (80:20 v/v) solution in presence of (a) PCB 28 alone and a mixture of PCB 101 and interference (b) PCB 52 alone and a mixture of PCB 52 and interference, (c) PCB 101 alone and a mixture of PCB 101 and interference.

Table 3.2: Interference studies of 2,4-dichlorophenol and 2,4,6-trichlorophenol on PCB 28, PCB 52 and PCB 101 detection

	2,4-dichlorophenol			2,4,6-trichlorophenol		
Analyte	PCB 28	PCB 52	PCB 101	PCB 28	PCB 52	PCB 101
PCB alone (µA)	8.84	6.48	4.25	8.42	18.19	5.97
PCB Interference (1:5) (µA)	9.57	5.84	4.72	10.07	19.55	6.24
PCB interference (1:10) (µA)	10.91	5.45	4.93	10.74	21.14	7.24
% Interference (1:5)	8.2	9.8	10.99	19.60	7.50	4.50
% Interference (1:10)	23.4	15.9	15.99	27.50	16.20	21.30

From the results, it was noted that the degree of interferences increased with the increase in concentration ratio of the interfering compounds. It was also clear that the interferences are higher in the 2, 4, 6-trichlorophenol relative to 2, 4-dichlorophenol possibly due to high degree of chlorination in the 2, 4, 6-trichlorophenol. These results suggested a possible tendency that lower chlorinated molecules such as PCB 28 had higher interferences relative to the highly chlorinated molecules such as PCB 52 and PCB 101. This suggests a possible dependence of interference on degree of chlorination. The addition of the interferences caused little increase of the peak currents in each PCB reduction and interferences at given percentages were calculated with respect to the reduction peak of interest. From this study,

the interferences were seen to cause little or no meaningful interference in further applications of this developed method.

3.7 Conclusion

As previously mentioned, part of this study objectives was to develop a method for the analysis of selected PCBs congeners, which was achieved. It was concluded that electrochemical reduction constituted a simple and fast method for the reductive analysis of the polychlorinated biphenyls congeners. One of the notable findings was that the congeners of study were found to be reduced in the lower potential values in 0.1 M TBAP/ACN/PBS 80:20 v/v solution. A two step reduction was observed with two reduction peaks in each case. One of the peaks was chosen for method development based on best signal output with the highest sensitivity.

The electrochemical C-Cl bond cleavage reductions in three different PCBs were studied using CV, SWV and chemical calculations. The glassy carbon electrode used provided a good environment for the selected PCBs reduction and the interference species and was therefore suggested as a suitable electrode for PCBs electrochemical analysis. The results discussed in this study indicated an existence of irreversible diffusion-controlled reduction of PCB 28, PCB 52 and PCB 101. The transfer coefficients and peak potentials were deduced for the reduction of each chlorine in the three polychlorobiphenyls and suggested reductions occurred via a concerted mechanism. The high sensitivities achieved with this reduction process allow sensitive detection of the selected PCB congeners at low concentrations and the corresponding percent relative standard deviation (% R.S.D) values demonstrated that the reduction response was highly reproducible.

From these results, a method was developed for the analysis of PCBs with reliable analytical parameters, which allow field applications. It offers several advantages to the use of more conventional techniques with improved sensitivity and reaching very low detection limits. The method developed is simpler to use than methods already available in the literature because it makes use of reduced procedures that saves time, money and effort.

McDonough, K.M., Fairey, J.L. and Lowry, G.V. 2008. Adsorption of polychlorinated biphenyls to activated carbon: Equilibrium isotherms and a preliminary assessment of the effect of dissolved organic matter and biofilm loadings, *Water Res.*, 42: 575-584.

Muthukrishnan, A., Boyarskiy, V.P., Sangaranarayanan, M.V. and Boyarskaya, I.A. 2012. Mechanism and Regioselectivity of the Electrochemical Reduction in Polychlorobiphenyls (PCBs): Kinetic Analysis for the Successive Reduction of Chlorines from Dichlorobiphenyls. *J. Phys. Chem., C*116: 655-664.

Muthukrishnan, A., Sangaranarayanan, M.V., Boyarskiy, V.P. and Boyarskaya, I.A. 2010. Regioselective electrochemical reduction of 2, 4-dichlorobiphenyl - Distinct standard reduction potentials for carbon-chlorine bonds using convolution potential sweep voltammetry. *Chem. Phys. Lett.*, 490(4-6): 148-153.

Nicholson, R.S. and Shain, I. 1964. Theory of stationary electrode polarography: single scan and cyclic methods applied to reversible, irreversible, and kinetic systems. *Anal. Chem.*, 36: 706-723.

Rogers, K.R. and L. R. Williams, L.R. 1995. Biosensors for Environmental Monitoring: A Regulatory Perspective. *Trends Anal. Chem.* 14(7): 289-294.

Rusling, J.F. and Arena, J.V. 1985. Direct reduction of halogenated biphenyls at mercury electrodes. *J. Electroanal. Chem.*, 186: 225-235.

Skoog, D.A., West, D.M. and Holler, F.J. 1988. *Fundamentals of Analytical Chemistry.* 5th ed. New York: Saunders College Publishing.

Turrio-Baldassarri, L., Abballe, A., Casella, M., di Domenico, Iacovella, N. and La Rocca, C. 2005. Analysis of 60 PCB congeners in drinkable water samples at 10-50 pg/L level. *Microchemical Journal.* 79; 193-199.

Webster, R.D. 2004. *In situ* electrochemical-NMR spectroscopy. Reduction of aromatic halides. *Anal. Chem.,* 76(6): 1603-1610.

Wei, Y., Kong, L., Yang, R., Wang, L., Liu, J. and Huang, X. 2011. Electrochemical impedance determination of polychlorinated biphenyl using a pyrenecyclodextrin-decorated single-walled carbon nanotube hybrid. *Chem. Commun.,* 47: 5340-5342.

CHAPTER FOUR
SYNTHESIS AND CHARACTERIZATION OF POLYANILINES

4.1 Introduction

The previous chapter reviewed the relevant literature concerning PCBs, conducting polymer; polyaniline (PANI) and the methods of characterization while the current chapter deals with the chemical synthesis of polyaniline in the presence of sawdust (SD) and titanium dioxide (TiO_2) and the characterization of these polymers. Polyaniline can be synthesized by either chemical or electrochemical oxidative polymerization as a bulk powder or film. Chemical synthesis methods involve oxidation of aniline by strong oxidants, (Vivier *et al.,* 2002) such as ferric chloride ($FeCl_3$) and ammonium persulfate [$(NH_4)_2S_2O_8$] and the polymer precipitates out of the chemical reaction solution (Terje *et al.,* 1998) while electrochemical methods involve use of techniques such as potentiostatic, galvanostatic, and potential cycling methods (Guo and Li, 2005).

The oxidation of aniline is influenced by several factors such as concentration of oxidant, concentration of monomer, reaction medium, duration of the reaction, and temperature (Syed and Dinesan, 1991). For example, when the molar ratio of the oxidant and the monomer is less than or equal to 1.15, an equal composition of oxidized and reduced units is obtained. Essentially during polymerization monomers are used as starting materials to form low molecular weight oligomers (Wallace *et al.,* 2002). When the duration of the reaction is approximately 2 hours or greater, a constant yield is obtained based on the concentration of monomer indicating the complete reaction of monomer (Armes and Miller, 1988). The polymerization of aniline is also temperature dependent with variable reaction rate in the temperature range of 0-80 °C. The rate of oxidation of the aniline monomer is the rate limiting step in the polymerization reaction, and can be precisely manipulated using temperature to influence polymer composition and speed of reaction (Genies *et al.,* 1990). Aniline polymerization in an aqueous acidic medium yields the most conductive form of PANI: the emeraldine salt (ES). The ES may be converted to the corresponding emeraldine base (EB) by treatment with an alkali solution or by rinsing with a large excess of water (MacDiarmid *et al.,* 1985).

It is well documented that the chemical synthesis of polyaniline and its derivatives by $(NH_4)_2S_2O_8$ is believed to proceed, in its initial stages by a mechanism similar to that of electrochemical polymerization (Cao *et al.,* 1989; Masdarolomoor *et al.,* 2008; Bansal *et al.,* 2009). Scheme 4.1 shows the proposed mechanism of chemical polymerization of PANI with

or without dopants. In this study, pristine PANI is synthesized together with its composites. Sawdust (SD) and titanium dioxide (TiO_2) particles are used to synthesize PANI composites and in each case 1 M HCl was used as a medium.

The mechanism involves formation of the aniline radical cation and coupling of *N*- and *para*-radical cations which occurs within subsequent rearomatization of the dication of *p*-aminodiphenylamine (Bansal *et al.,* 2009). It is then oxidised to the diradical dication. Although head to tail (i.e., *N-para*) coupling is predominant, some coupling in the *ortho* position also occurs, leading to defects in conjugation in the resultant polymer (Bansal *et al.,* 2009).

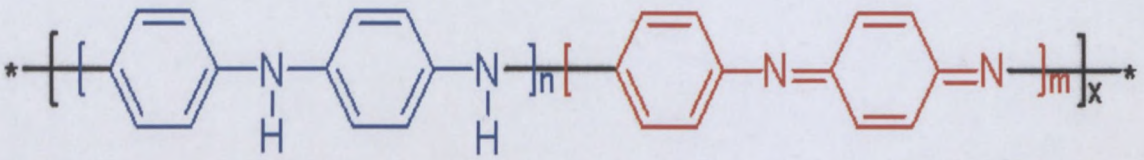

Figure 4.1: General structure of Polyaniline (PANI)

PANI exists in three different forms; leucomeraldine base (LEB), emeraldine base (EB) and pernigraniline base (PNB) (Waryo *et al.,* 2009). The molecular structure that is used to show the variation of oxidation states is shown in Figure 4.1 where, x equals half the degree of polymerization (DP). Leucoemeraldine with n = 1, m = 0 is the fully reduced state. Pernigraniline is the fully oxidized state (n = 0, m = 1) with imine links instead of amine links (Wikipedia, 2012). The emeraldine (n = m = 0.5) form of polyaniline, often referred to as emeraldine base (EB), is neutral, if doped (protonated) it is called emeraldine salt (ES), with the imine nitrogens protonated by an acid.

Other polymerization methods employed to synthesize PANI are rare methods such as enzyme–catalysed or photochemical initiated polymerization (Wallace *et al.,* 2002). It has generally been agreed that the chemical oxidative polymerization of monomers of substituted aniline is similar to that of the parent (unsubstituted) aniline and that the properties of substituted PANIs are similar to those of the parent PANI (Wallace *et al.,* 2002).

During the past two decades, PANI has been synthesized and its chemical and physical properties studied extensively under different conditions, and tremendous advances in the chemistry, electrochemistry, physics, and processing of PANI have been achieved. Currently,

attention is diverted to synthesis of composites, doped PANI materials which are believed to produce soluble and more processable PANI for various applications including adsorption.

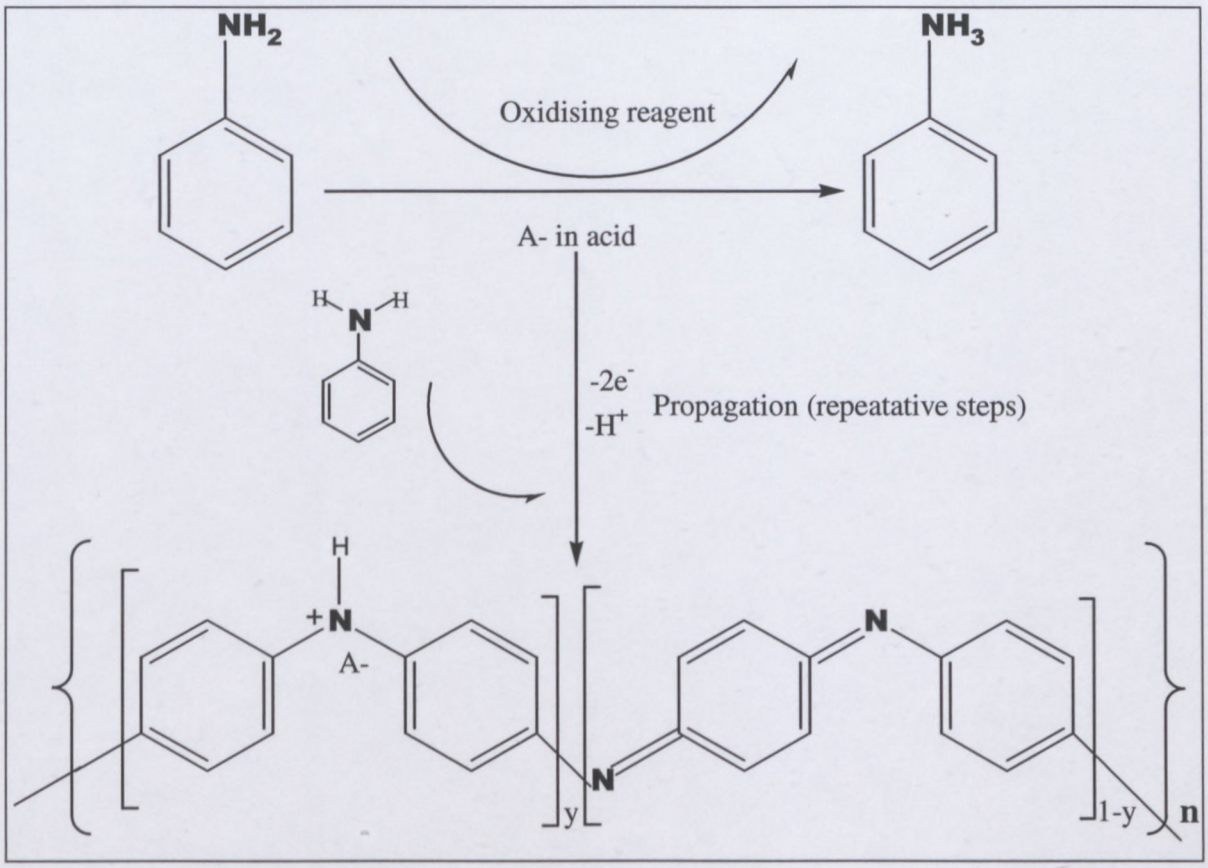

Scheme 4.1: Overall polymerization of aniline in the presence of a dopant or counter ion (A-), where A- can either be a cation, anion, biomass (surface functional groups) or organic compounds such as a dyes

The chemical composition, chemical properties, morphological and physical properties of PANI composites depends on the type of dopant, medium and interaction of PANI and dopant. Therefore, the application and efficiency of these composites are dependent on these.

These properties of the synthesized PANI composites were investigated using different methods including; spectroscopic techniques such as fourier transform infrared (FTIR), UV-visible spectroscopy, microscopic techniques such as transmission electron microscopy (TEM) and scanning electron microscopy (SEM), thermogravimetric analysis (TGA) and powder X-ray diffraction (PXRD) were also used.

4.2 Experimental method

4.2.1 Reagents and materials

The reagents used in this study included: aniline (99 % purity, Sigma Aldrich) which was doubly-distilled before use under reduced pressure and stored at a low temperature, hydrochloric acid (37 %), analytical grade ammonium persulfate ($(NH_4)_2S_2O_8$, APS), sawdust particles in the form of fine particles were used directly without additional treatment. *N,N*-dimethylformamide, (DMF) (anhydrous, 99.8 %, Analytical grade), Titanium dioxide (TiO_2) from Fluka Analytical. Deionized water; previously prepared by passing distilled water through a milli-QTM water purification system (Millipore) was used for aqueous solution preparations.

4.2.2 Synthesis of Polyanilines

Polyaniline was synthesized from 100 mL of 0.02 M aniline in 1 M HCl and stirred continuously. Then 2.5 g of ammonium persulfate (APS) was weighed and added to the solution mixture with continuous stirring. The mixture was allowed to polymerize at room temperature for 24 h. The precipitate formed was collected by filtering on a Buchner funnel using a water aspirator and washed with distilled water then left to dry at room temperature. For PANI/SD composite, 5.0 g of sawdust was first soaked in 1 M HCl and then aniline was added to the mixture. Finally 2.5 g of APS was added in the mixture and stirring was continued for 24 h at room temperature while polymerization occurred. The composites were then removed from the solution, washed thoroughly in distiiled water to remove traces of monomers and HCl and kept in readiness for characterization. For PANI/TiO_2 synthesis, TiO_2 particles were added to the mixture containing APS, aniline and HCl before polymerization occurred. Similarly for PANI/SD/TiO_2 synthesis, SD was first soaked in acid and TiO_2 added to the mixture containing APS, aniline and HCl.

4.2.3 Instrumentation

The FTIR spectra of the PANI and PANI composites were recorded using a Perkin Elmer Spectrum 100 series in the range of 400-4000 cm^{-1} at room temperature. UV–visible spectra were recorded in the 200-800 nm range using a 1 cm path length quartz cuvette and pure DMF was used as the reference on a Nicolet evolution 100 spectrophotometer. The amount of weight loss and the thermostability of PANI and PANI composites were determined from thermogravimetric analysis (TGA). Both thermogravimetric analysis (TG) and differential scanning calorimetry (DSC) were performed on a Perkin Elmer Pyris 6 system. The samples

were heated from 30 to 400 °C in air at the heating rate of 10 °C/min in a nitrogen atmosphere. The weight of the samples used was 3.0 mg in all cases. The X-ray diffraction (XRD) was performed by using a Bruker AXS D8 Advance diffractometer. The studies on the morphology, elemental composition and size distribution of the polyaniline materials were performed by using a high resolution transmission electron microscope (HRTEM) from Tecnai G2F20 X-Twin MAT (US) and the SEM images taken using a JEOL JSM-7500F scanning electron microscope.

4.2.4 Preparation of PANI composites for UV-visible studies

Samples for UV-visible studies were dissolved in *N,N*-dimethylformamide (DMF) prior to analysis and pure DMF was used as the reference. The final supernatants of each sample were analyzed in the range of 200-800 nm using a 1 cm path length quartz cuvette on a Nicolet evolution 100 spectrophotometer used to characterize the samples.

4.2.5 Preparation of PANI composites for FTIR studies

The samples were used directly by dropping on the scan plates and FTIR spectra recorded in the range 400-4000 cm^{-1} using a Perkin Elmer model Spectrum 100 series.

4.2.6 Preparation of PANI composites for SEM studies.

The PANI and PANI composite materials were thoroughly dried and kept in sealed vial containers in readiness for SEM analysis. The SEM analysis was performed on a JEOL JSM-7500F scanning electron microscope. Micrographs were obtained for samples of the composites by mounting on aluminium stubs using conductive glue and drop coating with a thin layer of carbon. Coating time was 5 min, pressure was 3 x 10^{-1} Mbar, current was 30 mA and the system was operated at 1 kV. SEM was operating with an accelerating voltage 25 kV and working distance was 15 mm. Magnifications were different for each image taken.

4.2.7 Preparation of PANI composites for TEM studies

The surface morphology of the PANI and PANI composite materials were further characterized using HR-TEM (Tecnai, G2 F20 X-Twin MAT). Specimens were prepared by suspension in DMF followed by sonication. The acceleration voltage and magnifications were different for each image taken from HR-TEM. The HR-TEM was operating at 200 kV field emission. A few drops of the dispersed material were placed on a carbon-coated copper grid

and allowed to dry by evaporation under an infrared lamp before loading the grid onto the microscope.

4.2.8 Preparation of PANI composites for XRD studies

Approximately 100 mg of the PANI and PANI composite materials were ground to a fine powder. All powder samples were characterized using a Bruker-Axs D8 advance XRD with Cu Kα radiation operated at 40 kV and 40 mA. The XRD spectra were recorded in the range of 10 ° to 90 °C.

4.2.9 Preparation of PANI composites for TGA/DSC studies

Prior to measuring, samples were ground to fine particles in a pestle and mortar. Equal amounts of 3 mg of each of the materials were then weighed in an analytical balance and run in the TG and DSC analyzers at the heating rate of 10 °C/min in a nitrogen atmosphere from 30 ° to 400 °C.

4.3 Results and discussion

4.3.1 Chemical synthesis of PANIs

Polyanilines synthesized in this study had colour variations from green to cream as can be seen in the photos (Figure 4.2). All the compounds were in powder forms. The colour variations have been explained extensively in the literature as a result of protonation and deprotonation.

It can be seen that four colour transitions appeared during chemical oxidative polymerization of PANI (Figure 4.3), which reflects the conversion of different oxidation states of PANI. In the leucomeraldine base (LB), PANI existed in a reduced state with pale yellow appearance which transformed to green in pernigraniline oxidized base (POB) and appears dark green in the neutral emeraldine base (EB). Further oxidation resulted in the pernigraniline base (PB) state which corresponds to the purple appearance.

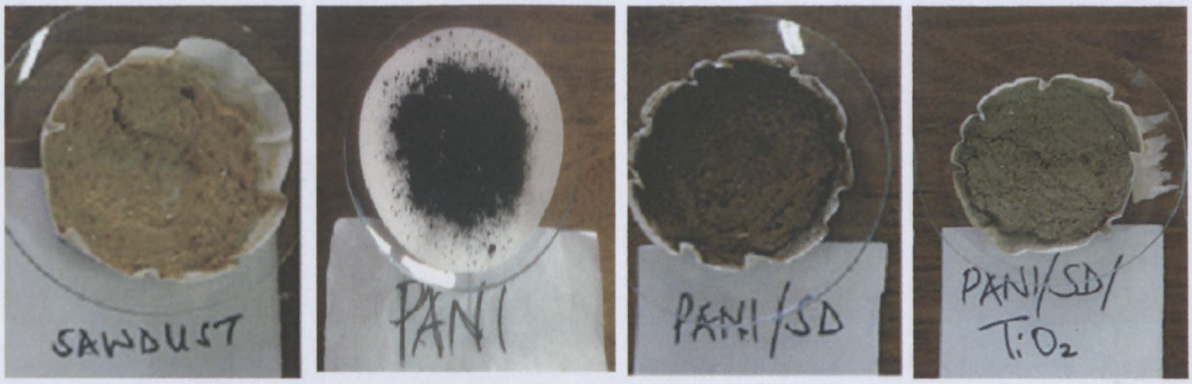

Figure 4.2: Images of SD, PANI, PANI/SD and PANI/SD/TiO_2 after synthesis.

In this study, the appearance of the synthesized materials was as follows; acid treated sawdust was light brown in colour, pure PANI possessed a dark green colour and was powdery with fine granules while the PANI/SD had a typical brown colour with course granules owing to the coating of sawdust particles, PANI/TiO_2 had a light green colour (image not shown) while PANI/SD/TiO_2 was light green in colour as shown in Figure 4.2.

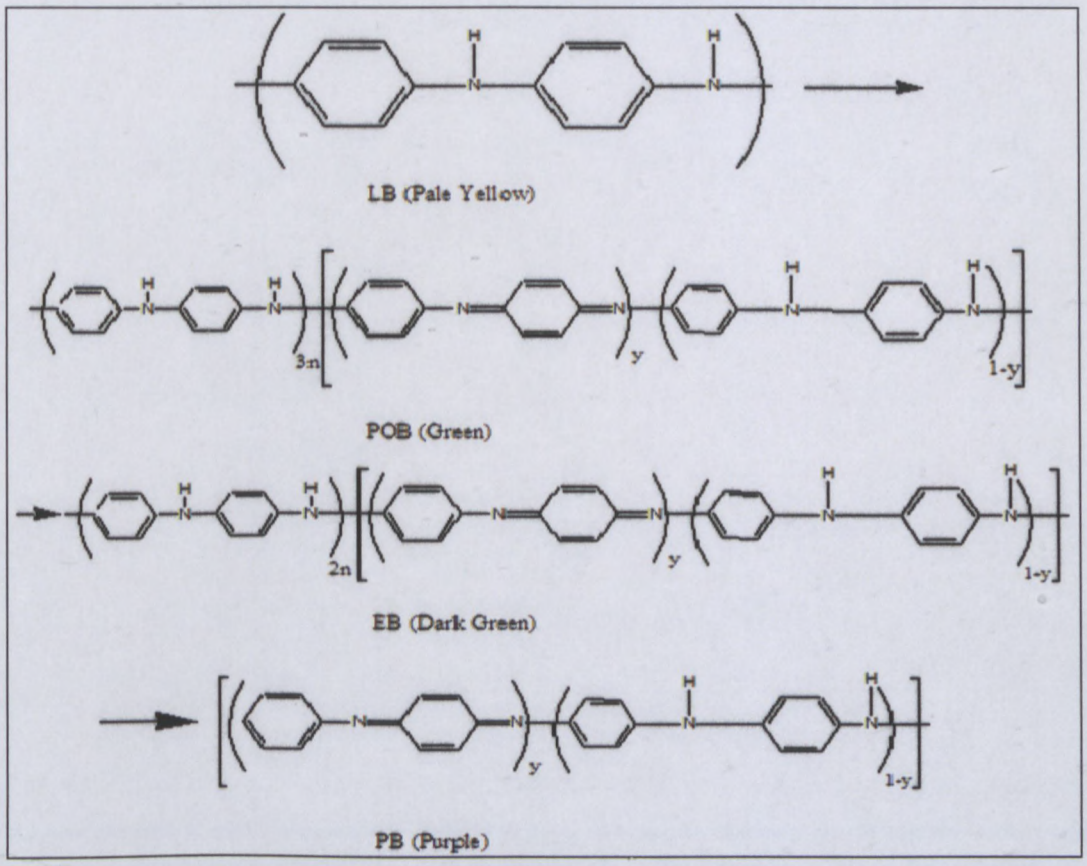

Figure 4.3: Various colour changes during polyaniline synthesis.

The green coloured products obtained were indicative of formation of polyaniline that is in its emeraldine redox state (Wallace *et al.,* 2002). Emeraldine base is normally regarded as the most useful form of polyaniline due to its high stability at room temperature and the fact that, upon doping with acid, the resulting emeraldine salt form of polyaniline is highly electrically conducting (MacDiarmid, 2001).

4.3.2 Spectrophotometric characterization of Polyanilines

The PANIs synthesized were characterized by spectroscopy to confirm the type of products synthesized and to elucidate their structures. These spectroscopic characterizations were done using FTIR and UV-visible techniques. It has been reported in the literature that different dopants affect the PANI backbone properties differently therefore it was essential to characterize these PANI composites to understand this. The structural elucidation gave an insight into the mechanism of polymerization as well as the possible chemical interactions the polymer and the polymer composites had. Four materials were employed in this work. These include, PANI, PANI/TiO_2, PANI/SD and PANI/SD/TiO_2. All the materials used were characterized without any prior modifications.

4.3.2.1 Fourier Transform Infrared analysis (FTIR)

The FTIR studies were carried out to elucidate the chemical functional groups of PANI and its composites, where the effect of change in the environment of PANI was noted in the presence of SD and TiO_2 particles. Specifically, changes in the nitrogen functional group bands were expected with the introduction of SD and TiO_2 into the polymer. Figure 4.4 shows the FTIR spectra for (a) PANI and PANI/TiO_2, (b) PANI/SD and (d) PANI/SD/TiO_2 composites.

The main characteristic peaks of the pure PANI (Figure 4.4 a (i)) were assigned as follows: 1400 cm^{-1} and 1500 cm^{-1} were attributed to C-C stretching of the benzenoid and C=N stretching of the quinoid rings respectively. These characteristics bands were similarly reported in other studies (Furukawa *et al.,* 1988; Quillard *et al.,* 1994). The characteristic absorption band around 1193 cm^{-1} (MacDiarmid *et al.,* 1985) related to the C–N stretching in the bipolaron structure was observed (Khiew *et al.,* 2004). The peak at 1280 cm^{-1} corresponding to C–N stretching of secondary amine in polymer main chain was clearly observed, which was similarly reported (Hatchett *et al.,* 1999) elsewhere. The existence of the absorption band at 805 cm^{-1} was interpreted as originating from out of plane bending vibration of C–H, which is formed in the aromatic ring structure during the protonation of HCl

doped PANI (Han *et al.,* 2002). These results indicate that the pure PANI was highly doped and existed in the conducting emeraldine salt form.

For the PANI composites showed in Figure 4.4 a (ii) and Figure 4.4 b, the FTIR spectra were almost identical to that of the pure PANI with some bands having slight red shifts. Shifts to higher energy for the C-N stretch initially at 1193 cm^{-1} for pure PANI was observed at 1210 cm^{-1} (PANI/SD), 1197 cm^{-1} (PANI/TiO_2) and 1198 cm^{-1} (PANI/SD/TiO_2) for each composite (Table 4.1). In addition to these, C-N stretching observed at 1280 cm^{-1} for pure PANI was shifted to slightly higher energy at 1290 cm^{-1} (PANI/SD), 1296 cm^{-1} (PANI/TiO_2) and 1297 cm^{-1} (PANI/SD/TiO_2) for each composite (Table 4.1). These red shifts indicated that some interactions existed between SD and TiO_2 with nitrogen sites of PANI directly influencing the vibration of C-N bonds since intensity of these bands also increased in all PANI composites.

The aromatic C-H stretching bands at 805 cm^{-1} in pure PANI shifted to higher wave numbers of 807 cm^{-1} (PANI/SD), 818 cm^{-1} (PANI/TiO_2), 817 cm^{-1} (PANI/SD/TiO_2) for each composite relative to pristine PANI mainly due to the introduction of SD and TiO_2 into the pure PANI matrix that caused significant reductions in the intensity of the aromatic peak.

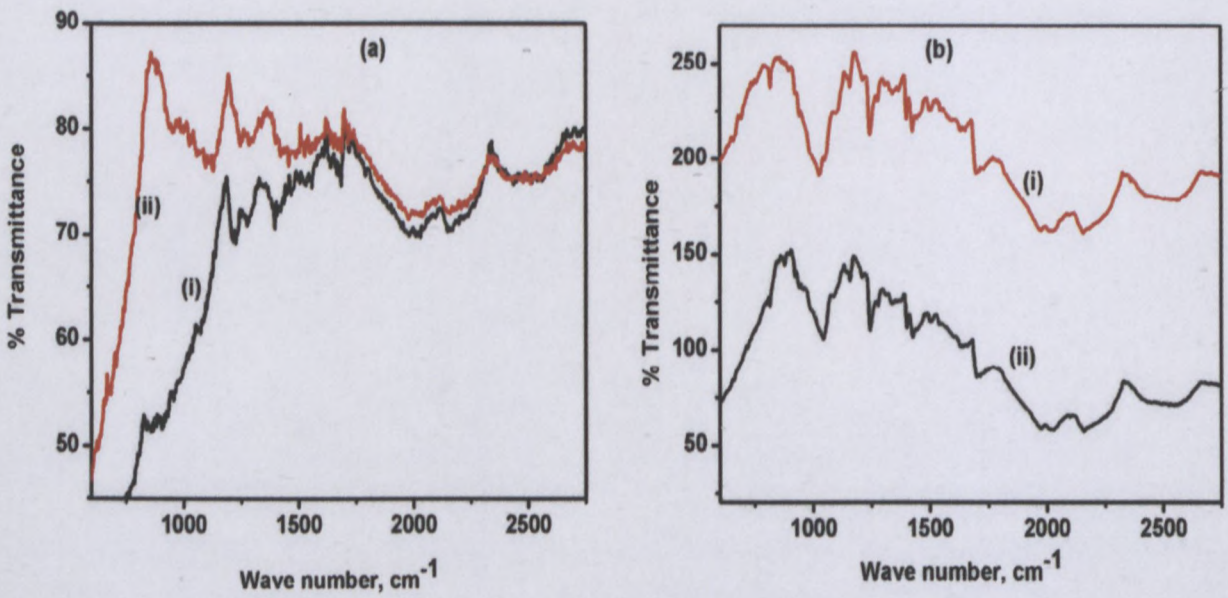

Figure 4.4: FTIR spectra of (a) (i) PANI, (ii) PANI/TiO_2; (b) (i) PANI/SD (ii) PANI/SD/TiO_2 composites.

It was noted that the characteristic bands of PANI at 1400 and 1500 cm^{-1}, respectively were least affected by the introduction of SD and TiO_2 during the formation of PANI composites as shown by the small shifts (Table 4.1).

Table 4.1: Comparison of FTIR absorption bands of PANI and PANI composites synthesized in this study.

	PANI	PANI/SD	PANI/TiO_2	PANI/SD/TiO_2
C-H bending (cm^{-1})	805	807	818	817
C-N stretching (cm^{-1})	1193	1210	1197	1198
C-N stretching (cm^{-1})	1280	1290	1296	1297
Aromatic C-C (Benzenoid) (cm^{-1})	1400	1400	1401	1401
Aromatic C=N (Quinoid) (cm^{-1})	1500	1500	1500	1500

The shift in the characteristic FTIR frequencies of PANI in the composites clearly suggested the formation of composites with substantial interaction between the polymer chain, SD and TiO_2 particles.

4.3.2.2 UV-visible analysis

The UV–visible spectra provided information about the existence of π-conjugation in conducting polymers and the optical band gap. These band gaps tell whether the polymer is conducting, semiconducting or insulating. Figure 4.5 shows the UV-visible spectra of PANI and its composites.

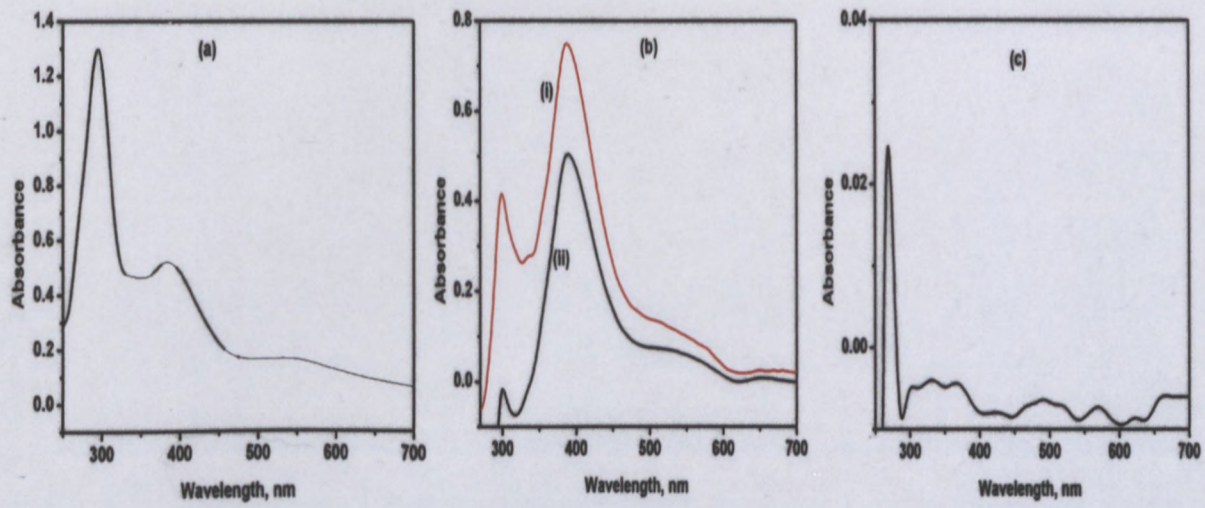

Figure 4.5: UV spectra of (a) PANI, (b) (i) PANI/SD, (ii) PANI/SD/TiO_2 and (c) PANI/TiO_2

The absorption bands at 294 and 386 nm in PANI (Figure 4.5 (a)) were attributed to π-π* transitions in the benzenoid structure (Li *et al.,* 2004; Ram *et al.,* 2005), which are typical of all the analyzed materials. These bands exhibited red shifts (bathochromic shift) to 299 nm in PANI/SD, 388 nm in PANI/SD and 389 nm in PANI/SD/TiO_2 as observed in Figure 4.5 in the final polymer composites. In the case of PANI/TiO_2, a lower wavelength was observed at 270 nm suggesting a reduced band gap of the π-π* transitions in the benzenoid structure. The shoulder at 526 nm in PANI describes the benzenoid to quinoid ring excitonic transition (Xia *et al.,* 1995). This corresponds to the n-π* transitions of quinine-imine groups (Stejskal *et al.,* 2004). This shoulder experiences a red shift to 545 nm in PANI/SD and 537 nm in PANI/SD/TiO_2. However, in PANI/TiO_2 (Figure 4.5 c) the shoulder was not observed indicative of complete interaction of TiO_2 with the quinoid ring resulting in a reduced band gap of n-π* transitions.

The presence of a peak and a shoulder in the PANI spectra was indicative of the presence of two types of chemically non-equivalent rings in the polymer chain, namely the benzenoid and the quinoid rings (Rannou *et al.,* 1998). From the spectra of the composites, it was observed that the intensity of the π–π* transition peak and excitonic transition peak increased with red shifts compared to that of pristine PANI.

However, this increase was quite high in the excitonic transition peak and rather low in the π–π* transition peak. This suggested that SD and TiO_2 particles had some interactions with quinoid rings on the polymer and these affected the excitonic transition peak and resulted in a possible complexation. These interactions reduce the band gap of π–π* transition of rings which existed in the polymer structure and thus electron transitions occur with lower energy. This explained the behaviour of PANI/SD/TiO_2 spectra which showed red shifts relative to PANI and PANI/SD as shown in Figure 4.5 (b) (i). However, in the PANI/TiO_2 composite spectra (Figure 4.5 (c)) the effect of TiO_2 on the environment of PANI was greater with the PANI and TiO_2 interaction reducing the band gap of π–π* transition of rings which existed in the PANI structure, and electron transitions occurred with low energy.

4.3.3 Morphological properties

A morphological study defines materials structural relationships and surface chemistry. It provides the knowledge of materials shape, sizes and orientation. This study involves all the synthesized materials as discussed in the next sections. The characterization of polymers is an important step since it provides useful parameters in determining the mechanical and structural properties and compatibility of polymers.

4.3.3.1 Scanning electron micrograph (SEM)

The morphology of the neat and composite powders and the qualitative dispersion of the TiO_2 and sawdust (SD) particles in the composites were examined by SEM. All the electron micrographs were obtained from powder specimens of these materials. SEM micrographs of PANI and its composites are shown in Figure 4.6 a, b, c, d and e respectively. SEM observations showed the differences in morphology of PANI, PANI/SD, PANI/TiO_2 and PANI/SD/TiO_2 composites.

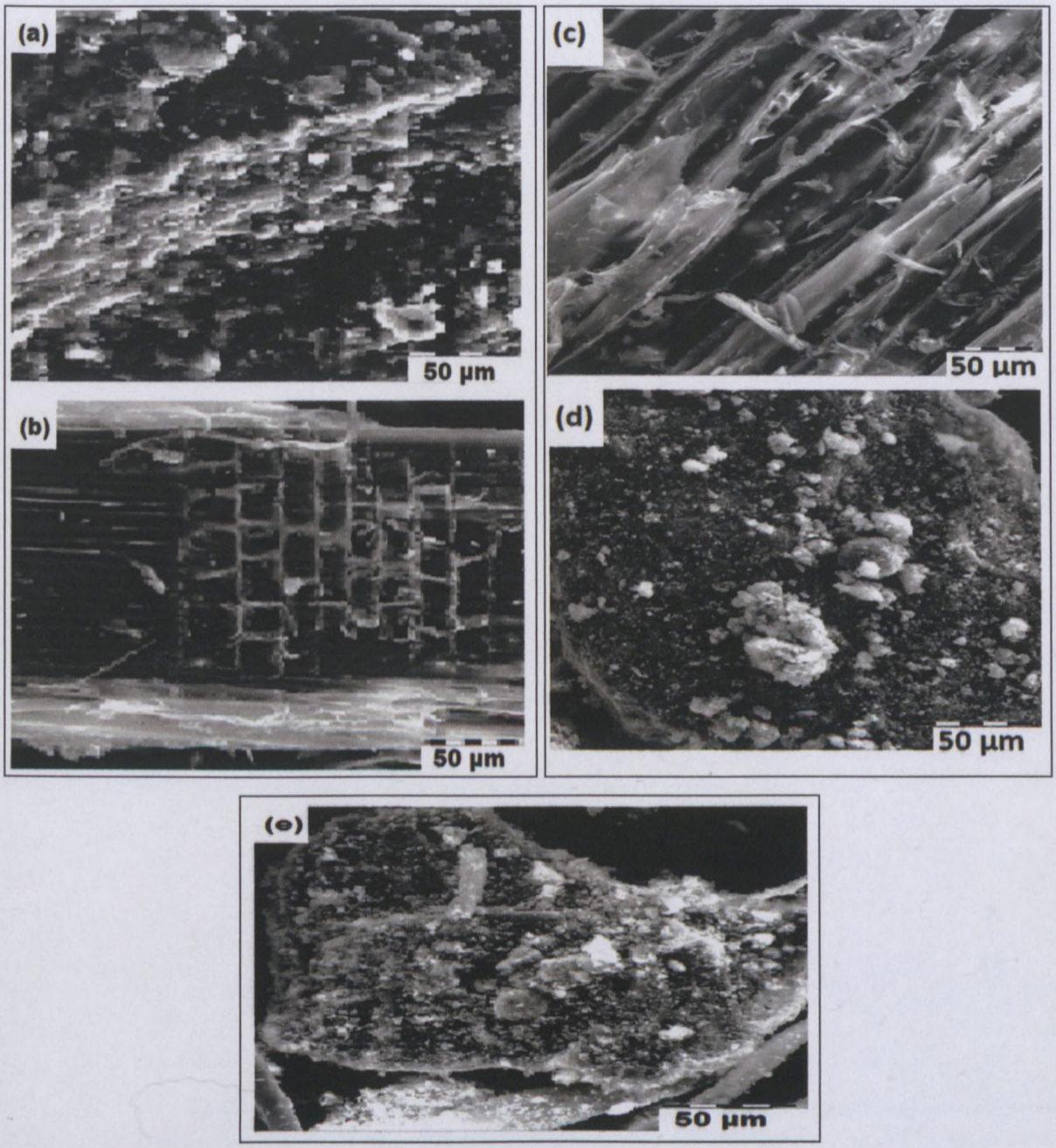

Figure 4.6: SEM micrographs of (a) PANI (b) acid treated SD (c) PANI/SD, (d) PANI/TiO_2 and (e) PANI/SD/TiO_2.

The SEM of cross-sections of neat PANI is shown in Figure 4.6 a. PANI powder appeared to have numerous honeycombed structures with observable pores within the polymer matrix. These observations were similar to those reported elsewhere (Chao *et al.,* 2005). The micrograph depicting the morphology of the neat PANI powder revealed plain, homogeneous and condensed powder surfaces.

The SEM micrograph of PANI/SD composite powders showed aligned rod-like structures with uniform distribution of sawdust particles in the PANI powder matrices with no apparent aggregations. This could be a result of strong interactions between polymer molecules and sawdust particles. In the case of PANI/TiO_2 composites, Figure 4.6 d revealed that the composite particles had cauliflower shapes which were highly dispersed with dark spheres of TiO_2 aggregated (Pham *et al.,* 2009) in the PANI/TiO_2 hybrid particles. The TiO_2 particles were observed as white in colour and piled up within the PANI matrix. Also, the micrograph confirmed the underlying distribution of TiO_2 in the PANI matrix by the presence of the big particles dispersed in the polymer matrix, which consequently contributed to the formation of the pores with an increase in the specific surface of the composite material.

For the acid treated SD micrograph (Figure 4.6 b), a regular network pattern was observed which disappeared in the subsequent composite formations. Figure 4.6 e show larger pores of sawdust which gets reduced with coating of PANI/SD (Figure 4.6 c). Introduction of TiO_2 particles in the PANI/SD composite made the PANI/SD/TiO_2 composite smaller, resulting in a composite with cauliflower shape and caused changes in morphological structure heaped composites with the pores structure maintained as shown in Figure 4.6 e.

The micrographs of the composites clearly indicated that the TiO_2 and sawdust particles were well dispersed in the respective composites (Figure 4.6 b–d). This suggests that the interaction between polymer molecules, SD and TiO_2 particles overcame the van der Waals interaction between TiO_2 particles, which would have otherwise resulted in TiO_2 aggregation. These interactions may be due to charge transfer from the nitrogen atom of the quinoid units of the polymer to sawdust and TiO_2 particles (Zengin and Kalayci, 2010). Therefore, TiO_2 and sawdust (SD) particles were homogeneously dispersed in the polymer matrices confirming the existence of uniformity in the PANI composite materials.

Although the morphology of the composites did not differ much from the pure PANI, when TiO_2 was added, the grain size of composite became smaller, which led to the changes in morphological structure heaped composites from loose cotton to firm gravel in appearance. This indicated that the TiO_2 particles had a nucleation effect on the polymerization, leading to a homogeneous polyaniline shell around them (Salem *et al.,* 2009). The porosity observed in

the pure PANI structure was retained in all the composites even with the introduction of SD and TiO_2.

The dark region is related to the conductive polyaniline phase, while the bright region was related to non-conducting polyaniline and polyaniline composite phases. It was observed that polyaniline content was markedly localized in the polyaniline composites matrix.

4.3.3.2 Transmission electron microscopy (TEM)

In the present work, samples of the prepared PANI composites were characterized by TEM as described in section 4.2.7. Figure 4.7 shows the TEM micrographs of (a) pure PANI, (b) acid treated SD, (c) PANI/SD, (d) PANI/TiO_2 and (e) PANI/SD/TiO_2 particles.

From Figure 4.7, it was observed that the shapes of the polymer composites varied. Acid treated SD had rod like structures which were clustered, PANI had networked rod structures, PANI/SD had spherical shaped structures, PANI/TiO_2 had spherical aligned powders and PANI/SD/TiO_2 had aggregated rod like structures, respectively.

In both PANI/SD and PANI/TiO_2 (Figure 4.7 c and d), the distribution of particles sizes was observed being approximately 30 nm. It was possible that these large particles were aggregates of smaller particles that coagulated together during the drying of dispersions for TEM. The micrographs showed that the presence of TiO_2 and SD particles caused changes in morphology of the PANI in the respective composites. In both cases, the products appeared to be composed of highly amorphous particles with high surface area.

The TEM image of the PANI/SD/TiO_2 composites in Figure 4.7 e showed smeared dark spheres due to the doped PANI, which was similar to the results obtained by Wei *et al.*, 2007. It was observed that TiO_2 and PANI were well dispersed in the composites, and the surfaces of the PANI/TiO_2 composites were strongly affected by the TiO_2 aerogel structure and consequently modified the morphology of PANI significantly.

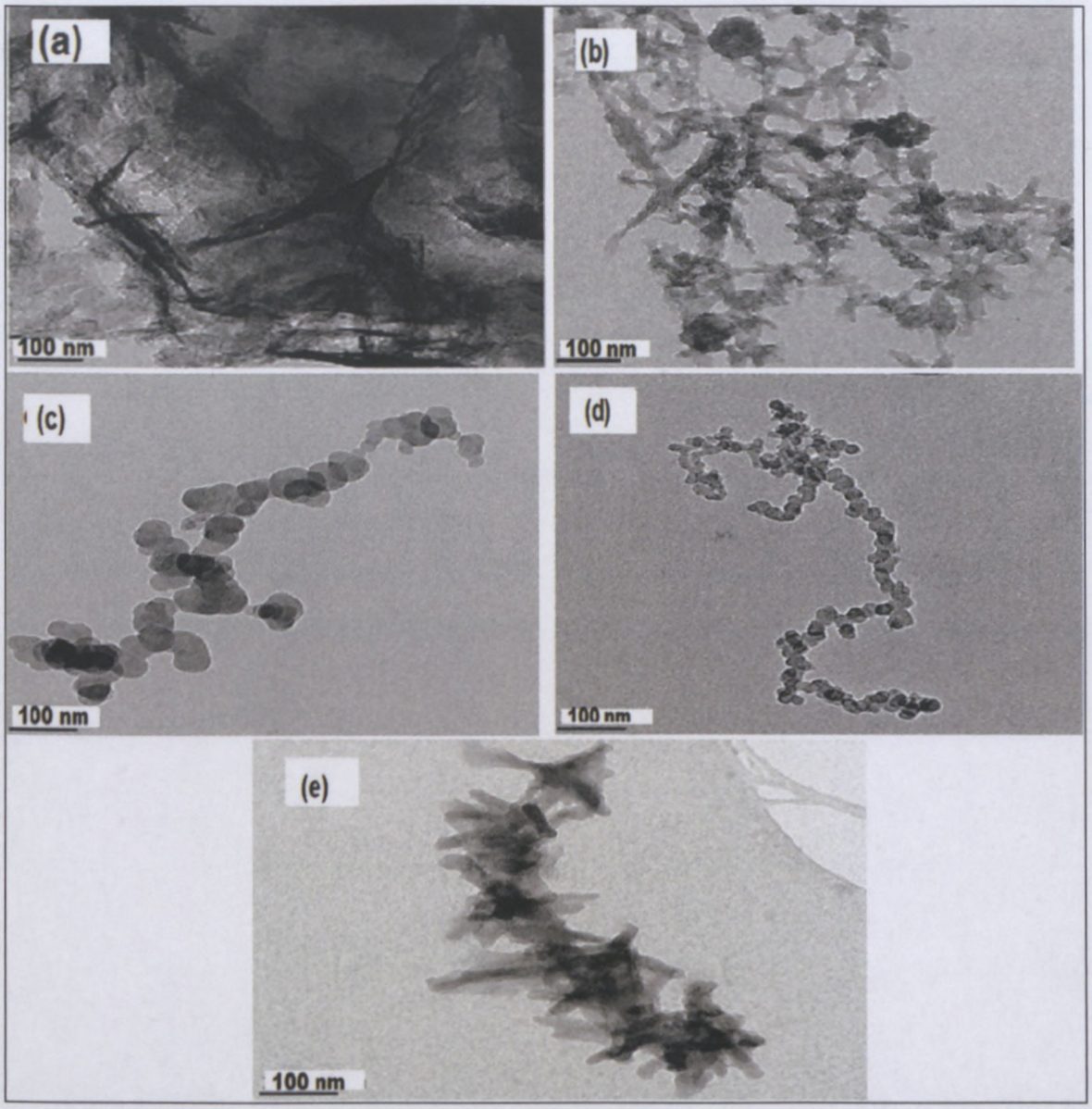

Figure 4.7: TEM micrograh of (a) acid treated SD (b) pure PANI, (c) PANI/SD (d) PANI/TiO_2 and (e) PANI/SD/TiO_2 particles. Micrographs obtained at 100 keV at a magnification of 100 nm.

The surfaces of the PANI/SD/TiO_2 hybrid particles were different from those of the pure PANI due to the interpenetration of PANI in TiO_2 structure as shown in Figure 4.7 e. The resultant PANI/SD/TiO_2 material therefore showed well dispersed particles of SD and TiO_2 around the polyaniline backbone structure.

4.3.3.3 Elemental composition of the materials using EDX

The chemical element composition of the polymer composites was investigated with an energy dispersive X-ray (EDX) spectrometer. Observing the EDX spectra while varying the electron beam energy helped to provide information on the chemical elements present in

each material. For all materials a copper grid was used as the sample holder. Therefore peaks at 1.0, 8.0 and 9.0 keV were observed resulting from the copper element.

(a) PANI/TiO_2 composite material

The incorporation of titanium oxide in the polymer was confirmed by the Energy Dispersive X-Ray (EDX) analysis (Refer Appendix A). The EDX spectrum of the chemically prepared composite material also showed a signal of carbon (C) at 0.2 keV and nitrogen (N) at 0.3 keV. The signal of oxygen (O) at 0.35 keV indicated that the PANI powder was doped by the HCl (Cl^-) ions from the acid. The presence of the important peak of titanium (Ti) located at 5.0 and 4.8 keV showed that the composite contains Ti^{4+} ions resulting from TiO_2. The presence of Ti and O was attributed to TiO_2 in the composite, and the strong signals of C and N are attributed to PANI in the composite. Therefore, we consider that the TiO_2 particles were incorporated in the polymer during the *in situ* polymerization of aniline, which led to the formation of PANI/TiO_2.

(b) PANI/SD composite material

The incorporation of SD in the polymer was confirmed by the EDX analysis. The EDX spectrum of the chemically prepared composite material also showed signals of nitrogen (N) at 0.2 keV and the presence of the intense peaks of carbon located at 0.1 keV (Refer Appendix B). These strong signals of C and N were attributed to PANI in the composite. The peak due to carbon was also attributed to SD. The signals of oxygen (O) at 0.3 keV indicated that the SD was doped by the HCl acid. Other elements (Ca, Si, and P) were characteristic of the presence of traces of impurities in the formed PANI/SD composite. These results suggested that SD particles were incorporated in the polymer during the *in situ* polymerization of aniline, which led to the formation of PANI/SD composite material.

(c) PANI/SD/TiO_2 composite material

The incorporation of both TiO_2 and SD particles in the polymer was confirmed by the EDX analysis. The EDX spectrum of the chemically prepared composite material showed signals of nitrogen (N) at 0.2 keV and the presence of the intense peaks of carbon located at 0.1 keV (Refer Appendix C). The signals of chlorine (Cl) at 2.5 keV and oxygen (O) at 0.3 keV indicated that the SD was doped by the HCl acid. The presence of the peaks of titanium (Ti) located at 4.8 and 5.0 keV showed that the composite contains Ti^{4+} ions resulting from TiO_2. Other elements (Ca, Si, S, Na and P) were characteristic of the presence of traces of impurities in the PANI/SD/TiO_2. These results suggested that SD and TiO_2 particles were

incorporated in the polymer during the *in situ* polymerization of aniline which led to the formation of PANI/SD/TiO_2.

(d) PANI composite material

The constituent elements in this polymer were confirmed by the EDX analysis. The EDX spectrum of the chemically prepared composite material showed signals of nitrogen (N) at 0.15 keV and the presence of the intense peaks of carbon located at 0.1 keV (Refer Appendix D). These signals were attributed to the presence of PANI polymer. The signal of oxygen (O) at 0.2 keV indicated that the PANI was doped by the HCl acid. Other elements (Na, Si, S and Ca) were characteristic of the presence of traces of impurities in the PANI.

(e) Acid treated SD material

The elemental composition in SD was confirmed by the EDX analysis, which showed the presence of the intense peaks of carbon located at 0.2 keV (Refer Appendix E). This was characteristic of the SD material. The signals of chlorine (Cl) at 2.5 and of oxygen (O) at 0.4 keV were as a result of the SD treatment in the HCl. Other element such as silicon (Si) was characteristic of the presence of traces of impurities in the SD.

4.3.4 Powder X-ray Diffraction patterns (PXRD)

XRD was used to identify the hybrid nature of the polymer materials in which crystalline orientation of synthesized polymers was studied. Figure 4.8 shows the powder X-ray diffraction patterns of acid treated SD, PANI/SD, PANI, PANI/TiO_2 and PANI/SD/TiO_2 composites. Pure PANI powders exhibited two broad peaks at 2θ angles of 20 ° and 26 °, which indicated that PANI contained some crystalline domains (Pan *et al.,* 2005). These peaks may be assigned to the scattering from PANI chains at interplanar spacing (Feng *et al.,* 2000). The PANI characteristic peak at 26 ° was associated to the amorphous structure of PANI (Zhang *et al.,* 2002).

In the diffraction patterns of acid treated SD and PANI/SD, broad diffraction peaks were observed both at around 15 ° and 24 ° which were associated with the amorphous structure of the two materials. From the PXRD pattern of the PANI/TiO_2 hybrid powder (Figure 4.8), major diffraction peaks at 24 °, 37 °, 47 °, 53 °, 61 °, 68 ° and 75 ° were observed which were associated with the presence of TiO_2 phase (Pham *et al.,* 2009). In the PANI/TiO_2 hybrid particles, the interpenetration of PANI into the TiO_2 network helped in the enhancement of the degree of crystallinity of PANI/TiO_2.

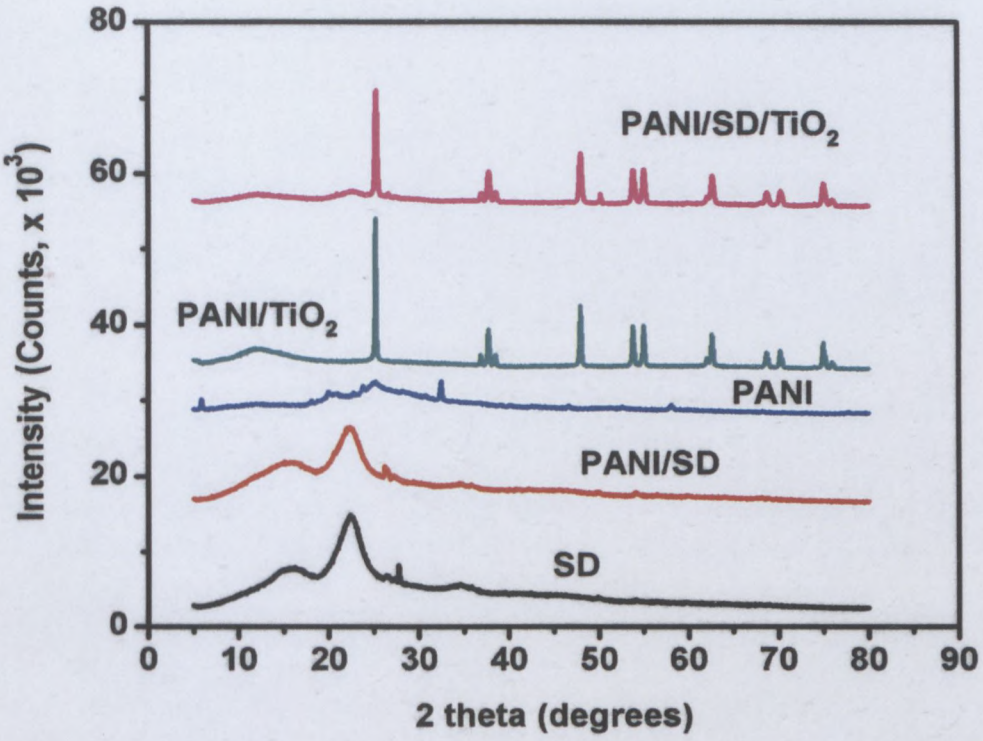

Figure 4.8: Powder X-ray diffraction patterns of acid treated SD, PANI/SD, PANI, PANI/TiO_2 and PANI/SD/TiO_2 composite.

From the PANI/TiO_2 patterns in Figure 4.8, weak narrow diffraction peaks were observed. This suggests that the peak at 2θ ~ 26 ° is weak for the PANI/SD/TiO_2 composite when in fact it is quite a strong peak. A similar observation is found for PANI/TiO_2. This suggests enhanced crystallinity for the composites containing TiO_2 and not decreased crystallinity as was cited (Xia and Wang, 2002). In PANI/SD/TiO_2 patterns, the diffraction peak original broad at 26 ° in pure PANI was weak, narrow and associated with crystalline structures. However, the effects of SD and TiO_2 in the PANI/SD/TiO_2 composite with TiO_2 might have been more predominant than SD causing the material to be crystalline.

According to Figure 4.8, it is clear that the aniline monomers polymerized in presence of sawdust and TiO_2 affected not only the final morphology but also the layer structure of polyaniline. This was confirmed by the transformation of the amorphous structure of PANI to crystalline PANI/TiO_2 and PANI/SD/TiO_2 while a distortion in crystal structure of PANI was evident due to inclusion of SD during the polymerization reaction with sawdust leading to transformation of the crystalline PANI into the amorphous phase; PANI/SD. By comparing the PXRD patterns of the composite and pure PANI, it was confirmed that PANI retained its structure even though it was distorted during the polymerization reaction.

4.3.5 Thermal properties

This is the characteristic of a material that determines how it reacts when it is subjected to excessive heat, or heat fluctuations over time. Thermogravimetric analysis was employed for this purpose since it provides information about the thermal properties of the polymers, and the amount of material incorporated in them.

4.3.5.1 Thermogravimetric analysis (TGA/DSC)

The thermal stability of the composites was analyzed using TGA and DSC analysis. Figure 4.9 (a-d) represents the TG-DSC curves of the polyanilines. From these figures it was observed that the PANIs showed two-step mass loss processes which were similar to the observation made by Gupta & Umare, 1992 and Khor *et al.*, 1990. The first process around 60 to 140 °C was attributed to the expulsion of water and dopant from the PANI matrix. The second step mass loss initiation between 160 and 400 °C varied depending on the composite. This step was due to the degradation of the PANI backbone. The first weight loss at 60 °C provided the weight composition of PANI versus the dopant (SD and TiO_2) components, and the second weight loss provided information regarding the influence of the SD and TiO_2 on the thermal properties of the polymer composites relative to pure PANI.

Figure 4.9 shows the TGA traces of PANI and PANI composites. The onset of the decomposition for thermogram was 150 °C. Most of the weight losses occurred between 160 and 400 °C (Table 4.2). The degradation of the polymer composites occured at 20 °C lower than the degradation temperature of pure PANI suggesting that the composites influenced the structure and thermal stability of PANI (Wang *et al.,* 2006).

The thermal stability comparison of the PANI composites showed an increasing trend from PANI/SD, PANI/SD/TiO_2 to PANI/TiO_2 composite, which was from none TiO_2 containing to TiO_2 containing composites (Figure 4.9). The weight losses in these composites between 30-150 °C were thought to be due to the presence of unremoved water molecules as moisture in polymers, PANI composites and acid dopants (Ghorbani *et al.,* 2012). The onset of the decomposition of PANI and PANI/SD were 150 °C and 260 °C respectively while that for PANI/TiO_2 and PANI/SD/TiO_2 were 260 °C in each case.

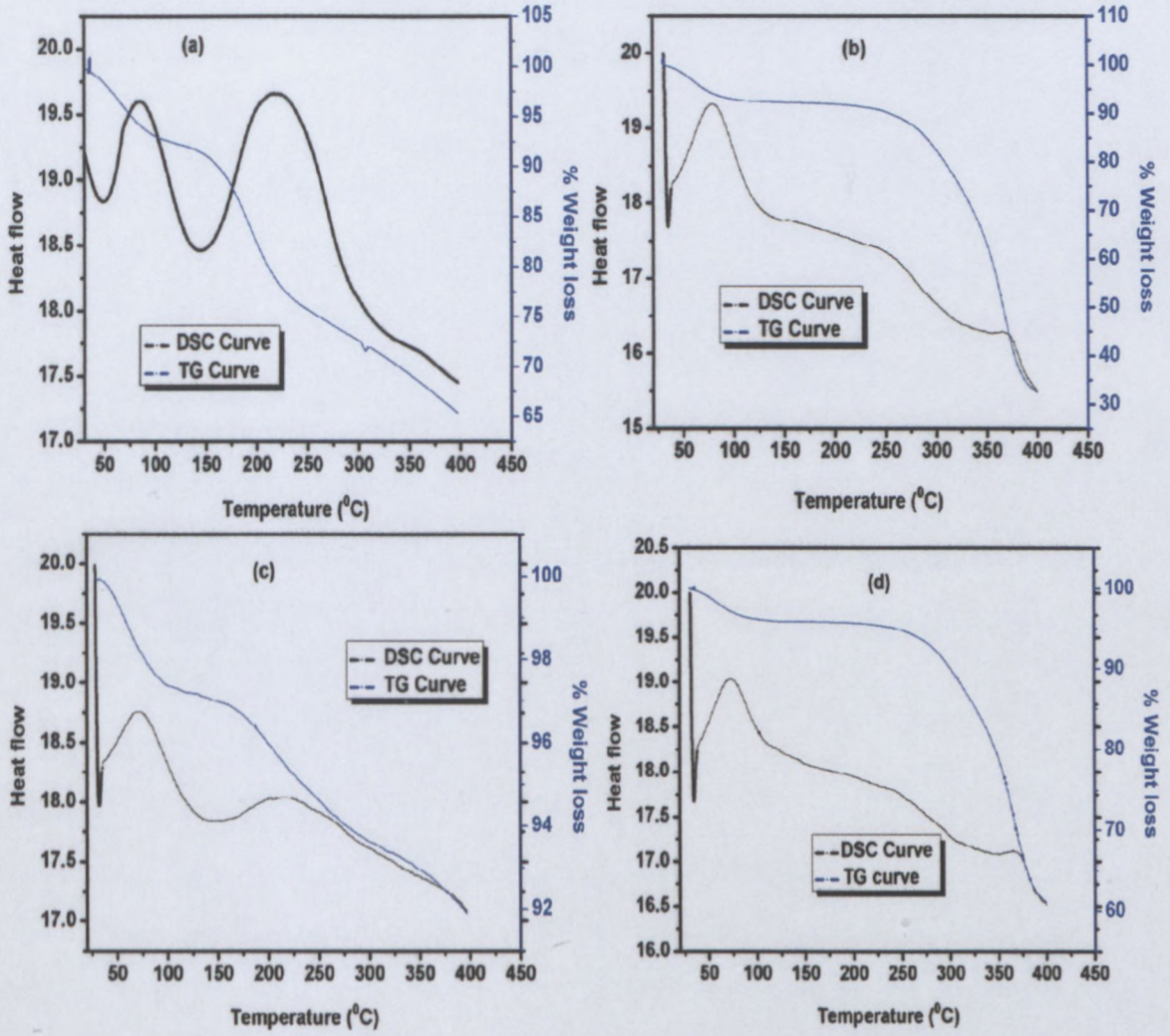

Figure 4.9: Thermogravimetric curves (TG curves) and corresponding differential scanning curves (DSC curves) for (a) pure PANI, (b) PANI/SD, (c) PANI/TiO_2 and (d) PANI/SD/TiO_2 composites.

In comparison to PANI, PANI/SD initial degradation occurred at a higher temperature, this suggested more heat stability than the pure PANI owing to the SD contained in the composite while for PANI/TiO_2 and PANI/SD/TiO_2 higher thermal stability was observed with PANI/TiO_2. For PANI/SD, beyond 260 °C, the degradation was proportional to the amount of SD in the composite. The TGA curve of the PANI/TiO_2 hybrid particles (d) is shown in Figure 4.9. It shows slightly different thermal decomposition behaviour than that of the PANI.

The maximum thermal decomposition rate of the PANI/TiO_2 hybrid particles occurred at only 380 °C even though large-scale thermal decomposition persisted from 300 to 400 °C. The difference in temperature can be explained by the strong interaction between TiO_2 and PANI due to the interpenetrating structure of the PANI/TiO_2 hybrid particles. The thermal

degradation of PANI composites followed similar trends because the polymer component went through the same thermal degradation cycle. The degradation of polyaniline and its composites occured in steps which involved elimination or removal of various components of the composites within the materials. This is discussed further in Table 4.2 as percentage loss of various components.

Table 4.2: Summary of the degradation products during thermal analysis

Material	% content		
	H_2O (30-150 °C)	SD/SO_4^{2-} (260-380 °C/160-220 °C)	PANI-Backbone (100%-(H_2O + SD/SO_4^{2-})
PANI	10.0	25.0	65.0
PANI/SD (5:8)	10.0	55.0	35.0
PANI/SD/TiO_2	5.0	29.7	65.3
PANI/TiO_2	5.0	2.0	93.0

From the TGA results, it was clear that the presence of the SD and TiO_2 particles in the structure of PANI chains contributed to the enhancement of thermal stability in the composites with PANI/TiO_2 and PANI/SD/TiO_2 being more stable to heat due to contribution from SD and TiO_2 in the final structure.

The DSC curves of PANIs are also depicted in Figure 4.9. PANI and its composites under nitrogen atmosphere displayed endothermic peaks during the DSC measurement. In all these curves, endothermic peaks were observed at lower temperatures of 85 °C (PANI), 77 °C (PANI/SD), 67 °C and 72 °C (PANI/SD/TiO_2), and were ascribed to the loss of water or release of moisture content and other combined small molecules, (Luo *et al.*, 2006) which was consistent with the TGA result. The second thermal event was related to the decomposition of amine units of the PANI molecules with corresponding endothermic peaks at 219 °C (PANI), 325 °C (PANI/SD), as similarly discussed elsewhere (Kittur *et al.*, 2002). This was also associated with a considerable weight loss in TGA measurement. In the case of PANI/TiO_2 and PANI/SD/TiO_2 the second peak were observed at 225 °C (Fig. 4.9 c) and 375 °C (Fig. 4.9 d) respectively. This could be due to the strong interaction between TiO_2 and PANI due to the interpenetrating structure of the PANI/TiO_2 and PANI/SD/TiO_2 hybrid particles.

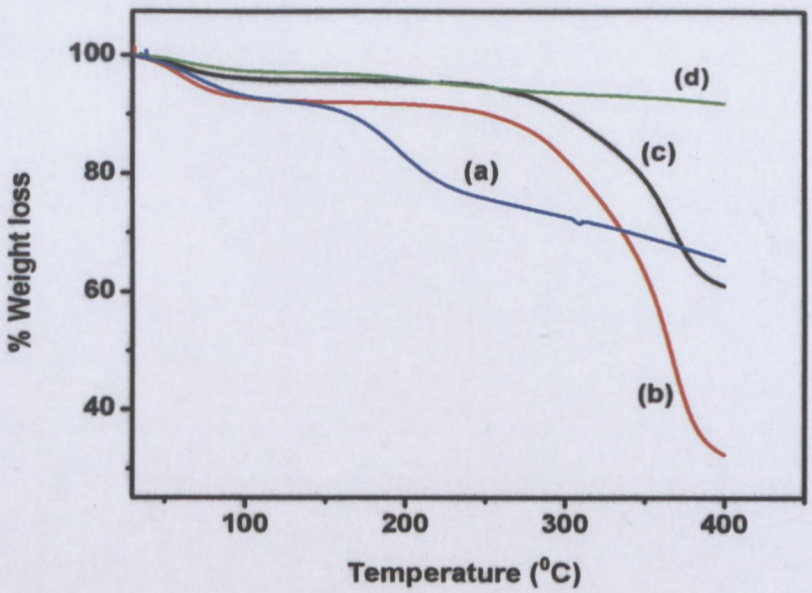

Figure 4.10: Comparison of thermal degradation of (a) PANI, (b) PANI/SD, (c) PANI/SD/TiO_2 and (d) PANI/TiO_2.

In Figure 4.10 comparison was further made for the TG decomposition of each polymer as shown. Thermal stability in the composites was clearly depicted with the least degraded material being PANI/TiO_2 relative to other composites. In PANI/TiO_2 a single step loss was clearly observed. As the heat was constantly supplied weight loss due to degradation was minimal. Comparison of the PANI and PANI composites showed that PANI was less stable than the PANI composites.

4.4 Conclusion

Polyaniline composites were successfully synthesized through *in situ* polymerization and characterized by powder X-ray diffraction (PXRD), scanning electron microscopy (SEM), Fourier transform infrared (FTIR) and UV-Vis spectroscopy and the results were compared with pristine polyaniline.

UV-visible spectra of these polymers revealed that the polymers exhibited two UV-visible absorption bands corresponding to the two types of chemically non-equivalent rings in the polymer chain, benzenoid and quinoid groups respectively. The FTIR spectra of PANI showed characteristics peaks which were observed in all the composites. However, the absorption bands of the composites were found to shift to higher wave numbers as compared to those observed in pure PANI. The observed shifts were attributed to the interaction between the SD, TiO_2 and PANI molecular chains. The PANI composites had

increased intensity of the peaks as a result of close proximity of SD and TiO_2 at nitrogen sites to the aromatic hydrogens. It was clear that the formation of PANI/TiO_2, PANI/SD and PANI/SD/TiO_2 composites distorted the PANI chains structure. The FTIR and UV-visible spectra revealed similar behaviour in the polyaniline composites suggesting that the PANI backbone remained intact in the final composites.

The TGA data provided the thermostability trends with the approximate composition of materials in the composites. The TGA data suggested that PANI composites were more thermally stable than pristine PANI due to the presence of sawdust and titanium dioxide particles at the nitrogen sites. Further studies showed that the thermal stability increased in the order PANI < PANI/SD < PANI/SD/TiO_2 < PANI/TiO_2. The enhanced thermal stability of the composites was ascribed to the interaction between PANI, titanium dioxide and sawdust particles that restricts thermal motion of the PANI in the composites.

The SEM micrographs depicting morphology of the neat PANI revealed homogenous distribution of SD and TiO_2 in polyaniline matrix. The shift in characteristic FTIR frequencies of polyaniline and its composite suggested the formation of composites. The micrographs of the composites revealed that TiO_2 and SD particles were well dispersed in the composites. The polyaniline and its composites exhibited pore like structures indicating good porosity that may be useful in applications such as adsorption studies as adsorbent materials. Similar outcome for TEM results showed that in all the materials synthesized which varied depending on the evidence that the PANI/SD/TiO_2 were well dispersed with structures showing the pores.

From the PXRD analysis the degree of crystallinity of the synthesized materials were further assessed where the pure PANI was determined to be crystalline as the Bragg diffraction peaks for $2\theta \sim 26$ ° appeared in its diffraction pattern. These diffraction peaks were affected differently and became weak with the inclusions of TiO_2 and SD particles in the PANI/SD, PANI/TiO_2 and PANI/SD/TiO_2 hybrid materials. The PXRD studies confirmed the presence of SD and TiO_2 phase in the composites.

From this study, it was clear that all the chemically synthesized polymers exhibited properties typical of polyaniline and the results from the spectroscopic, morphological and thermal characterization confirmed successful formation of the respective polymers.

4.5 References

Armes, S.P. and Miller, J.F. 1988. Optimum reaction conditions for the polymerization of aniline in aqueous solution by ammonium persulphate. *Synth. Met.*, 22: 385-393.

Bansal, V., Bhandari, H., Bansal, M.C. and Dhawan, S.K. 2009. Electrical and optical properties of poly (aniline-co-8-anilino-1-napthalene sulphonic acid) -A material for ESD applications. *Indian J. Pure Appl. Phys.*, 47: 667-675.

Cao, Y., Andreatta, A., Heeger, A.J. and Smith, M. 1989. Synthesis of Acid doped Conducting polyaniline. *Polymer*, 30: 2305.

Chao, D., Chen, J., Lu, X., Liang Chen, L., Zhang, W. and Wei, Y. 2005. SEM study of the morphology of high molecular weight polyaniline. *Synth. Met.*, 150: 47-51.

Feng, W., Sun, E., Fujii, A., Wu, H., Niihara, K. and Yoshinno, K. 2000. Synthesis and Characterization of Photoconducting Polyaniline-TiO_2. Nanocomposite. *Bull. Chem. Soc. Jpn.*, 73: 2627-2633.

Furukawa, Y., Ueda, F., Ohydo, Y., Harada, I., Nakajima, T. and Kawagoe, T. 1988. Vibrational spectra and structure of polyaniline. *Macromolecules*, 21: 1297-1305.

Genies, E.M., Boyle, A., Lapkowski, M. and Tsintavis, C. 1990. Polyaniline: A historical survey. *Synth. Met.*, 36: 139-182.

Ghorbani, M. and Eisazadeh, H. 2012. Synthesis and characterization of chemical structure and thermal stability of nanometer size polyaniline and polypyrrole coated on rice husk. *Synth. Met.*, 162: 527-530.

Goldstein, J., Newbury, D., Echlin, P., Joy, D., Romig Jr., A., Lyman, C., Fiori, C. and Lifshin, E. 1992. Scanning electron microscopy and X-ray microanalysis: A text for biologists, materials scientists, and geologists. 2nd ed. New York: Plenum Press.

Guo, D.J. and Li, H.L. 2005. Well-dispersed multi-walled carbon nanotube/polyaniline composite films. *J. Solid State Electrochem.*, 9: 445-449.

Gupta, M.C. and Umare, S.S. 1992. Studies on poly (omethoxyaniline). *Macromolecules,* 25: 138-142.

Han, M.G., Cho, S.K., Oh, S.G. and Im, S.S. 2002. Preparation and characterization of polyaniline nanoparticles synthesized from DBSA micellar solution. *Synth. Met.*, 126(1): 53-60.

Hatchett, D.W., Josowicz, M. and Janata, J. 1999. Acid doping of polyaniline: spectroscopic and electrochemical studies. *J. Phys. Chem.* B103: 10992-10998.

Khiew, P.S., Huang, N.M., Radiman, S. and Ahmad, M.S. 2004. Synthesis of NiS nanoparticles using a sugar–ester nonionicwater-in-oil microemulsion. *Mater. Lett.*, 58: 516-521.

Khor, S.H., Neoh, K.G. and Kang, E.T. 1990. Synthesis and characterization of some polyaniline–organic acceptor complexes. *J. Appl. Polym. Sci.*, 40(11-12): 2015-2025.

Kittur, F.S., Prashanth, H., Sankar, K.U. and Tharanathan, R.N. 2002. Characterization of chitin, chitosan and their carboxymethyl derivatives by differential scanning calorimetry. *Carbohydr. Polym.*, 49(2): 185-193.

Li, X., Wang, G., Li, X. and Lu, D. 2004. Surface properties of Polyaniline/nano-TiO_2 composites. *Appl. Surf. Sci.,* 229: 395-401.

Luo, K., Shi, N. and Sun, C. 2006. Thermal transition of electrochemically synthesized polyaniline. *Polym. Degrad. Stab.,* 91: 2660-2664.

MacDiarmid, A.G., Chiang, J.C., Halpern, M., Huang, W.S., Mu, S.L., Somasiri, N.L.D., Wu, W.Q., and Yaniger, S.I. 1985. 'Polyaniline': Interconversion of metallic and insulating forms, *Mol. Cryst. Liq. Cryst.,* 121: 173-180.

MacDiarmid, A.G. 2001. Synthetic Metals: A Novel Role for Organic Polymers (Nobel Lecture). *Angew. Chem. Int. Ed.*, 40: 2581-2590.

Masdarolomoor, F., Innis, P.C. and Wallace, G.G. 2008. Electrochemical synthesis and characterization of polyaniline/ poly (2-methoxyaniline-5-sulfonic acid) composites. *Electrochem. Acta*, 53: 4146-4155.

Pan, W., Yang, S.L., Li, G. and Jiang, J.M. 2005. Electrical and structural analysis of conductive polyaniline/polyacrylonitrile composites. *Eur. Polym. J.*, 41: 2127-2133.

Pham, Q.M., Pham, D.H., Kim, J.S., Kim, E.J. and Kim, S. 2009. Preparation of polyaniline-titanium dioxide hybrid materials in supercritical CO_2. *Synth. Met.,* 159(19-20): 2141-2146.

Quillard, S., Louarn, G., Lefrant, S. and MacDiarmid, A.G. 1994. Vibrational analysis of polyaniline: A comparative study of leucoemeraldine, emeraldine, and pernigraniline bases. *Phys. Rev.* B50(17): 12496-12508.

Ram, M.K., Yavuz, O., Lahsangah, V. and Aldissi, M. 2005. CO gas sensing from ultrathin nano-composite conducting polymer film. *Sens. Actuators*, B106: 750-757.

Rannou, P., Gawlicka, A., Berner, D., Pron, A., Nechtschein, M. and Djurado, D. 1998. Spectroscopic, structural and transport-properties of conductive polyaniline processed from fluorinated alcohols. *Macromolecules,* 31(9): 3007-3015.

Salem, M.A., Al-Ghonemiy, A.F. and Zaki, A.B. 2009. Photocatalytic degradation of Allura red and Quinoline yellow with Polyaniline/TiO_2 nanocomposite. *Appl. Catal. B: Environ.*, 91: 59-66.

Stejskal, J., Hlavata, D., Holler, P., Trchova, M., Prokes, J. and Sapurina, I. 2004. Polyaniline prepared in the presence of various acids: a conductivity study. *Polym. Int.,* 53: 294-300.

Syed, A.A. and Dinesan, M.K. 1991. Polyaniline-A novel polymeric material. *Talanta*, 38: 815-837.

Terje, A., Skotheim, R.L.E. and John, R.R. 1998. *Handbook of conducting polymers.* 2nd ed. New York: Marcel Dekker.

Vivier, V., Cachet-Vivier, C., Michel, D., Nedelec, J.Y. and Yu, L.T. 2002. Voltamperommetric study of chemically made polyaniline powder with cavity microelectrode technique. *Synth. Met.*, 126: 253-262.

Wallace, G.G., Spinks, G.M. and Teasdale, P.R. 2002. *Conductive electroactive polymers: intelligent materials systems.* 2nd ed. Boca Raton, FL: CRC Press.

Wang, S., Tan, Z., Li, Y., Sun, L. and Zhang, T. 2006. Synthesis, characterization and thermal analysis of polyaniline/ZrO_2 composites. *Thermochim. Acta.,* 441: 191-194.

Waryo, T.T., Songa, E.A., Matoetoe, M.C., Ngece, R.F., Ndangili, P.M., AlAhmed, A., Jahed, N.M., Baker, P.G.L. and Iwuoha, E.I. 2009. Functionalisation of polyaniline nanomaterials for amperometric biosensing, Nanostructured Materials for Electrochemical Biosensors, New York: Nova Science Publishers.

Wei, C., Zhu, Y., Yang, X. and Li, C. 2007. One-pot synthesis of polyaniline-doped in mesoporous TiO_2 and its electrorheological behaviour. *Mater. Sci. Eng. B: Solid-State Mater. Adv. Technol.*, 137(1-3): 213-216.

Wikipedia. 2012. Polyaniline. http://en.wikipedia.org/wiki/Polyaniline [12 August 2012].

Xia, H. and Wang, Q. 2002. Ultrasonic Irradiation: A novel approach to prepare conductive polyaniline/nanocrystalline titanium oxide composites. *Chem. Mater.*, 14: 2158-2165.

Xia, Y., Wiesinger, M. and MacDiarmid, A.G. 1995. Camphor sulfonic acid fully doped polyaniline emeraldine salt: conformations in different solvents studied by an ultraviolet/visible/near-infrared spectroscopic method. *Chem. Mater.*, 7(3): 443-445.

Xu, J.C., Liu, W.M. and Li, H.L. 2005. Titanium dioxide doped polyaniline. *Mater. Sci. Eng.*, C25: 444-447.

Zengin, H. and Kalayci, G. 2010. Synthesis and characterization of polyaniline/activated carbon composites and preparation of conductive films. *Mater. Chem. Phys.*, 120: 46-53.

Zhang, Z., Wei, Z. and Wan, M. 2002. Nanostructures of polyaniline doped with inorganic acids. *Macromolecules*, 35(15): 5937-5942.

CHAPTER FIVE
EXTRACTION STUDIES

5.1 Introduction

The extraction studies involve the use of techniques such as adsorption in removing PCBs from wastewaters. Adsorption is the process through which a substance, originally present in one phase, is removed from that phase by accumulation at the interface between that phase and a separate (solid) phase. Adsorption is a simple and efficient method to remove organics from wastewater. Adsorption is a well-known separation process and is widely used to remove certain classes of chemical pollutants from wastewaters, especially those that are practically unaffected by unconventional biological treatments (Ai *et al.,* 2010). In most adsorption studies, activated carbon has been the most widely used adsorbent due to its large specific surface area and predominant proportion of micropores. Activated carbon adsorption has been considered suitable insofar as PCBs are very apolar pollutants (Sotelo *et al.,* 2002). An example of activated carbon use was observed in a study that showed that in the presence of influent particulates, PCB removal was significantly better (99 %) in a biological activated carbon (AC) column compared to the 62 % obtained in an otherwise identical granulated activated carbon (GAC) column (Ghosh *et al.,* 1999). However, high regeneration cost and poor mechanical rigidity of activated carbon limit its wider applications.

Other adsorbents such as bentonite have showed good results for the sorption of PCBs (Kastáneka *et al.,* 1995). The bentonite may function as a recyclable surfactant support for the adsorption and subsequent combustion of organic pollutants (Shen, 2002). Hydroxy-intercalated and several pillared bentonite showed high sorption capacity, although they seem to be less efficient than GAC (Matthes and Kahr, 2000). A chemical activation of elutrilithe was developed, and showed a superior affinity and capacity compared to the classical existing sorbents (Vansant, 1999). Fly ash has also been used in the removal of PCBs from an aqueous solution (Nollet *et al.,* 2003). Sawdust on the other hand can be used as an alternate adsorbent to commercially available carbon due to its low cost and good efficiency.

Polymeric adsorbents, especially hyper-cross-linked resin, have been considered as a practical alternative to activated carbon (Qu *et al.,* 2010). The wide variation in functionality, surface area, porosity and the ease of regeneration has made the use of polymeric resins as alternative to activated carbon for removal of specific pollutants from wastewater (Lin, 2009; Sahin *et al.,* 2009). Compared with classical adsorbents such as the silica gels, alumina and

the activated carbons, the macroporous polymer are more attractive alternatives because of their wide range of pore structures and surface characteristics (Kunin, 1976). Various polymeric adsorbents have been investigated and different adsorption mechanisms have been proposed (Li *et al.,* 2001; Li *et al.,* 2002; Pan *et al.,* 2008; Huang *et al.,* 2009). The use of these polymeric adsorbents for the treatment of effluents containing benzenoid compounds has been widely studied (He and Huang, 1995). Some of the polymeric adsorbents include polyaniline which has been applied as adsorbent in various media. For example, polyaniline coated sawdust (PANI/SD) hybrid has been effectively used in removal of metals (Ansari and Raofie, 2006a; Ansari and Raofie, 2006b), anions (Ansari *et al.,* 2009) and dyes (Ayad and Abu El-Nasr, 2010; Ansari and Mosayebzadeh, 2011) from wastewaters. There are also examples of adsorbing trace naphthalene compounds with polymeric adsorbents for drinking water preparation (Walther *et al.,* 1984; Dore *et al.,* 1986) among others. It is in this respect that a polyaniline composite is considered in this study for extraction purposes.

Most adsorbents used in adsorption normally have challenges as a result of improper solid waste disposal after remediation process. As a result of these challenges, this study focused on combining a polymer which is porous, easy to prepare and environmentally stable, biomass which is cheap and a catalyst to degrade the pollutant in order to help overcome problems of solid wastes and possible related hazards. In addition to that the solid waste containing TiO_2 in this case can be reused by application in other uses such as pigments (Barletta *et al.,* 2006) in paint manufacture since TiO_2 forms white pigments.

Polychorinated biphenyls have been remediated in wastewater through various adsorption means. Some of the notable methods have involved use of activated carbon adsorption which has been frequently used to remove apolar pollutants from wastewater (Sotelo *et al.,* 2002). However, the activated carbon has proved expensive relative to application of agricultural wastes (Sotelo *et al.,* 2002). In other examples, Yoon *et al.,* 2006 recently demonstrated that PCB 166 preferentially accumulated on type TOG activated carbon in regions rich in aromatic carbon functional groups. Research has shown that the adsorption capacity of non-coplanar hydrophobic organic compounds (HOCs) was lower than that of co-planar compounds of similar hydrophobicity on various forms of black carbon (Jonker and Koelmans, 2002; Cornelissen *et al.,* 2004). The adsorption attenuation was attributed to steric hindrances, presumably brought about by the twisting of biphenyl rings with respect to one another as more chlorine is added to the structure.

In this chapter, attention is paid to the extraction studies of selected polychlorinated biphenyl congeners of interest (PCB 28, PCB 52 and PCB 101). The use of pristine PANI powder as

adsorbent, however, could be limited by the polymer surface area and complicated by diffusion processes. This drawback necessitated the need for further functionalization of PANI using TiO_2 and coating of sawdust, which forms part of the current study objective. Efforts have been made to investigate the potential and use of PANI/SD/TiO_2, as a low cost adsorbent replacing activated carbon for the removal of PCBs using the adsorption technique and various adsorption parameters monitored. Differences in the adsorption of PCBs onto PANI/SD/TiO_2 with different surface chemistry are expected.

5.2 Material and Reagents

PCBs used in the adsorption experiments included IUPAC no. PCB 28 (2, 4, 4'-trichlorobiphenyl), PCB 52 (2, 2', 5, 5'-tetrachlorobiphenyl) and PCB 101 (2, 2', 4, 5, 5'-pentachlorobiphenyl). The 3 PCBs used were purchased from Dr. Ehrenstorfer (Augsburg, Germany) as mixed solution in isooctane for PCB 52 and as fine solid for PCB 28 and PCB 101. These congeners were chosen to cover the tetra- through penta-homologue groups and include congeners previously studied by others such as PCB 52 (Jonker and Koelmans, 2002). All PCB stocks were prepared freshly in 0.1 M TBAP/ACN/PBS 80:20 v/v solution before use. Acetonitrile (HPLC grade), phosphate buffer (PBS), pH 7.4, Analytical grade argon (Afrox, South Africa) was used to degas the system. Tetrabutylammonium perchlorate, (TBAP; Sigma Aldrich, electrochemical grade) and used without further purification. Deionized water was used for aqueous solution preparations. The PANI/SD/TiO_2 was dried to constant mass and used as the adsorbent material without any further treatment.

5.3 Materials and Instrumentation

Square wave voltammetry electrochemical experiments were carried out using a BAS 100W electrochemical analyzer from Bioanalytical systems inc. (West Lafayette, IN) with conventional three electrode system consisting of a glassy carbon electrode (GCE) as the working electrode (A = 0.071 cm^2) and a platinum wire (3 mm diameter) from Sigma Aldrich. Ag/AgCl (3 M NaCl) electrodes from BAS were used as auxiliary and reference electrodes, respectively.

All experimental solutions were purged with high purity argon gas and blanketed with argon atmosphere during measurements. The experiments were carried out at room temperature (25 °C). Alumina micropowder and polishing pads were obtained from Buehler, IL, USA and were used for polishing of the GCE. All potentials were quoted with respect to Ag/AgCl.

5.4 Extraction procedures

The PANI/SD/TiO_2 used in this research was sieved prior to use in order to remove dust and course particulate matter. The stock solutions of the PCBs were made in acetonitrile and methanol; for the concentration of PCB 28 and PCB 101 as 3.8 x 10^{-3} M and 3.1 x 10^{-6} M respectively. Stock solution for PCB 52 was used as purchased, 3.4 x 10^{-5} M. The adsorption experiments were performed in closed batch systems prepared in 10 mL glass beakers and sealed with parafilm. The isotherms were run by taking different concentrations of PCB 28 (2.8 x 10^{-4} M), PCB 52 (6.7 x 10^{-7} M) and PCB 101 (6.0 x 10^{-5} M) at room temperature in neutral solution. These concentrations were selected after preliminary investigations. Parallel experiments were also performed without adding PANI/SD/TiO_2 particles (control).

For each experimental run, 10 mL of PCB of known concentration and 0.05 g of the synthesized PANI/SD/TiO_2 were taken in a 50 mL glass beaker since glass do not interfere with PCBs solutions. The mixture solution was left unstirred for 15 min at room temperature. 0.5 mL of the samples was withdrawn at time intervals of 15 min for 1.75 h and supernatant liquid portions centrifuged for 10 min. The supernatant was then brought into an electrochemical cell and the equilibrium concentrations of the PCBs (PCB 28, PCB 52 and PCB 101) determined through PCB reduction with electrochemical analysis; square wave voltammetry (SWV) technique, using an electrochemical analyzer (BAS 100W). The adsorbed amounts of PCB were calculated using the equation:

$$q_t = \left(\frac{C_0 - C_e}{m} \right) V \quad \text{.....Equation 1}$$

Where C_o and C_e are the initial and equilibrium concentrations of PCB ($molL^{-1}$), *m* is the mass of PANI/SD/TiO_2 (g), q_t is the amount adsorbed ($mol\ g^{-1}$) and V is the volume of solution (L).

5.5 Results and Discussion

The experiment was done at different time intervals between 0 to 120 min with a fixed adsorbent dose of 0.05 g PANI/SD/TiO_2. Figure 5.1 depicts that the uptake of PCBs by PANI/SD/TiO_2 was quite rapid initially, gradually slowed down and then reached equilibrium. From the plot it was evident that a substantial amount was adsorbed within 0 to 15 min of contact time with PANI/SD/TiO_2 in all the PCBs analysed relative to subsequent periods thereafter. PCB 28 reached equilibrium much earlier at 45 min while 75 min was taken for the attainment of equilibrium for PCB 52, with PCB 101 attained its equilibrium adsorption after 90 min. Adsorption was observed at a faster rate for PCB 28 compared to PCB 52 and PCB 101 which suggested a possible preference of adsorption in the lower chlorinated congeners

5.4 Extraction procedures

The PANI/SD/TiO_2 used in this research was sieved prior to use in order to remove dust and course particulate matter. The stock solutions of the PCBs were made in acetonitrile and methanol; for the concentration of PCB 28 and PCB 101 as 3.8 x 10^{-3} M and 3.1 x 10^{-6} M respectively. Stock solution for PCB 52 was used as purchased, 3.4 x 10^{-5} M. The adsorption experiments were performed in closed batch systems prepared in 10 mL glass beakers and sealed with parafilm. The isotherms were run by taking different concentrations of PCB 28 (2.8 x 10^{-4} M), PCB 52 (6.7 x 10^{-7} M) and PCB 101 (6.0 x 10^{-5} M) at room temperature in neutral solution. These concentrations were selected after preliminary investigations. Parallel experiments were also performed without adding PANI/SD/TiO_2 particles (control).

For each experimental run, 10 mL of PCB of known concentration and 0.05 g of the synthesized PANI/SD/TiO_2 were taken in a 50 mL glass beaker since glass do not interfere with PCBs solutions. The mixture solution was left unstirred for 15 min at room temperature. 0.5 mL of the samples was withdrawn at time intervals of 15 min for 1.75 h and supernatant liquid portions centrifuged for 10 min. The supernatant was then brought into an electrochemical cell and the equilibrium concentrations of the PCBs (PCB 28, PCB 52 and PCB 101) determined through PCB reduction with electrochemical analysis; square wave voltammetry (SWV) technique, using an electrochemical analyzer (BAS 100W). The adsorbed amounts of PCB were calculated using the equation:

$$q_t = \left(\frac{C_0 - C_e}{m} \right) V \quad \text{.....Equation 1}$$

Where C_o and C_e are the initial and equilibrium concentrations of PCB (molL^{-1}), *m* is the mass of PANI/SD/TiO_2 (g), q_t is the amount adsorbed (mol g^{-1}) and V is the volume of solution (L).

5.5 Results and Discussion

The experiment was done at different time intervals between 0 to 120 min with a fixed adsorbent dose of 0.05 g PANI/SD/TiO_2. Figure 5.1 depicts that the uptake of PCBs by PANI/SD/TiO_2 was quite rapid initially, gradually slowed down and then reached equilibrium. From the plot it was evident that a substantial amount was adsorbed within 0 to 15 min of contact time with PANI/SD/TiO_2 in all the PCBs analysed relative to subsequent periods thereafter. PCB 28 reached equilibrium much earlier at 45 min while 75 min was taken for the attainment of equilibrium for PCB 52, with PCB 101 attained its equilibrium adsorption after 90 min. Adsorption was observed at a faster rate for PCB 28 compared to PCB 52 and PCB 101 which suggested a possible preference of adsorption in the lower chlorinated congeners

studied relative to the high substituted congener (PCB 101). Similarly, relationship where a lower adsorption capacity for the highly chlorinated PCB mixtures, in comparison with the less chlorinated ones, was observed elsewhere (Pirbazari and Weber, 1981). An observation of preferential coplanar sorption was also reported elsewhere for PCB interaction with humic substrates (Uhle *et al.,* 1999).

In this study, the adsorption capacities were calculated as 8.09 mg g^{-1} (PCB 28), 4.58 mg g^{-1} (PCB 52) and 3.76 mg g^{-1} (PCB 101) as shown in Table 5.1. From studies of partition coefficients, the adsorption of PCBs (PCB 21 and PCB 173) was reported to increase as the lipophilic character of the compounds increase (Nollet *et al.,* 2003). Since solubility decreases with the number of chlorines attached to the biphenyl molecule. This is similar to the results observed in this study with PCB 28 tending to be more lipophilic relative to PCB 52 and PCB 101 and adsorbs faster as shown in Figure 5.1.

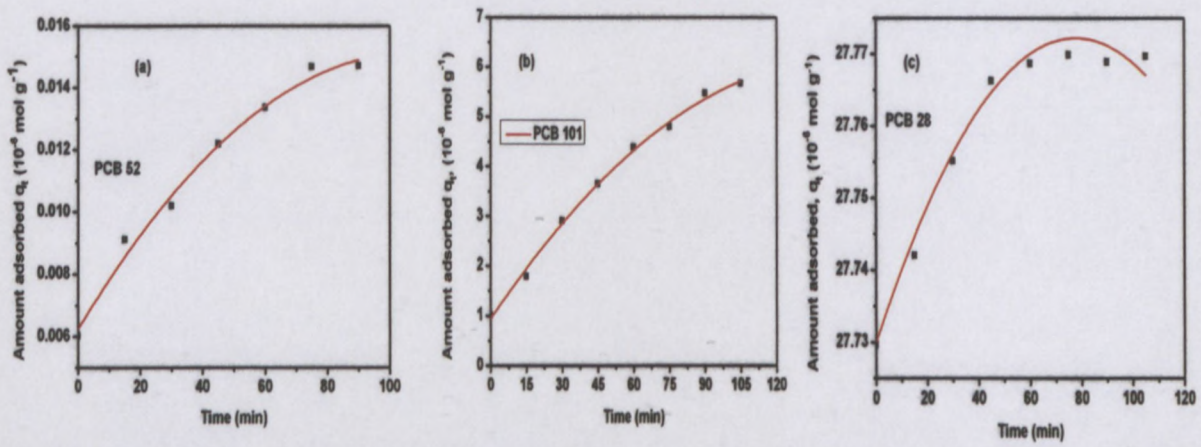

Figure 5.1: Effect of contact time on adsorption of PCBs onto PANI/SD/TiO_2 (0.05 g PANI/SD/TiO_2, 25 °C, 1.75 h).

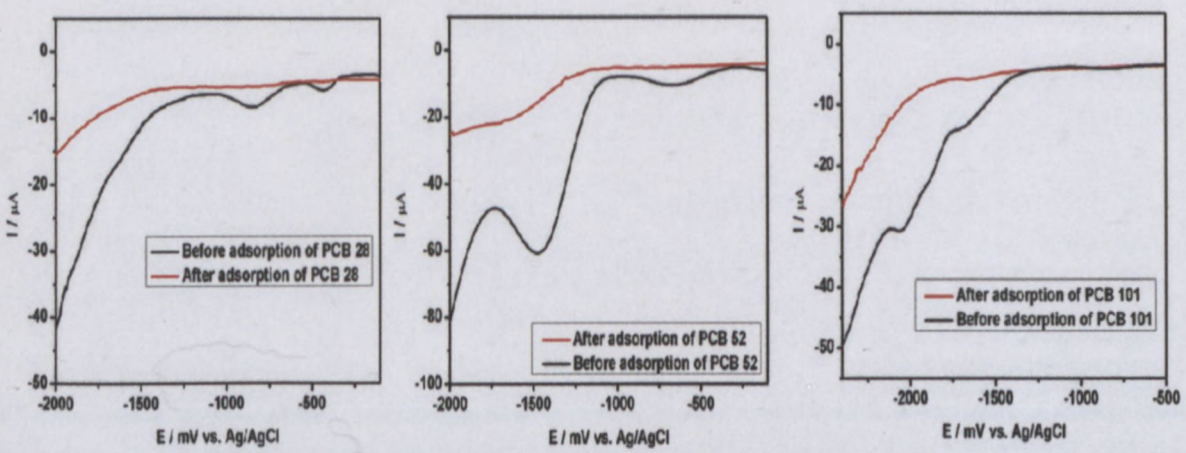

Figure 5.2: Comparison of SW voltammogram before and after adsorption studies for each PCB used.

The extraction study was further compared before and after adsorption. The result of these behaviours is shown in the voltammograms (Figure 5.2) for the each analyte. From the results it was observed in all the cases that after adsorption there were no reduction peaks in the voltammogram suggesting a possible adsorption of all PCB analytes on the adsorbent material, PANI/SD/TiO_2 and therefore the analytes were absent in the aqueous solution. This confirms the potential of the synthesized adsorbent materials to adsorb the PCB analyte species which satisfies part of the study objective.

5.5.1 Kinetics of adsorption

According to the kinetic data obtained from the experiments, pseudo-second-order and an intraparticle diffusion equation was used to explain the adsorption mechanism. The validities of these four kinetic models were checked and depicted in Figure 5 (a-c) which was based on linearized equations;

(a) Pseudo-second-order equation:

$$\frac{t}{q_t} = \frac{1}{k_2 q_e^2} + \frac{t}{q_e} \quad \text{.....Equation 2}$$

Where q_e and q_t are the amounts of PCB adsorbed (mole g^{-1}) at equilibrium and at time t (min), k_2 is the rate constant and t is the adsorption time (min). For the pseudo-second-order model used in PCB 28 and PCB 52, a plot t/qt versus t should give a straight line and q_e and k_2 can be determined from the slope and intercept of the plot respectively.

(b) Intraparticle diffusion equation:

$$q_t = k_1 t^{0.5} + C \quad \text{.....Equation 3}$$

Where C is the intercept, related to the thickness of the boundary layer and k_1 is the intraparticle diffusion rate constant. For all the models evaluated, the determination coefficient R^2 was applied to determine which of the kinetic models best fitted the data. Regarding the intraparticle diffusion model used in PCB 101, the values of constants C were obtained from the intercept of the straight line plot of qt versus $t^{0.5}$. For this model, it is essential that when the intraparticle diffusion is the sole rate limiting step (Bia *et al.*, 2012), a plot of q_t vs. $t^{0.5}$ is a straight line passing through the origin.

Other kinetic model equations applied include;

(c) Pseudo-first-order equation:

$$\log(q_e - q_t) = \log q_e - \frac{k_1 t}{2.303} \quad \text{.....Equation 4}$$

Where q_e and q_t are the amounts of PCB adsorbed (mole g^{-1}) at equilibrium and at time t (min), k_1 is the rate constant of pseudo-first order sorption and t is the adsorption time (min).

(d) Elovich equation:

$$q_t = b + aInt \quad \text{.....Equation 5}$$

Where q_t is the amount of PCB adsorbed (mole g^{-1}) at time t (min), b and a are the desorption constant (g mol^{-1}) and initial sorption rate (mol g^{-1} min^{-1}) respectively and t is the adsorption time (min).

Based on linear regression (R^2) values, the adsorption kinetics of PCBs onto PANI/SD/TiO_2 can be described well by pseudo-second order and intraparticle diffusion models (Figure 5.3). Comparison of other two kinetic models (Equations 4 and 5) did not yield better results compared to Equation 2 and 3 (Table 5.1). The corresponding kinetic parameters and the correlation coefficients are summarized in Table 5.1.

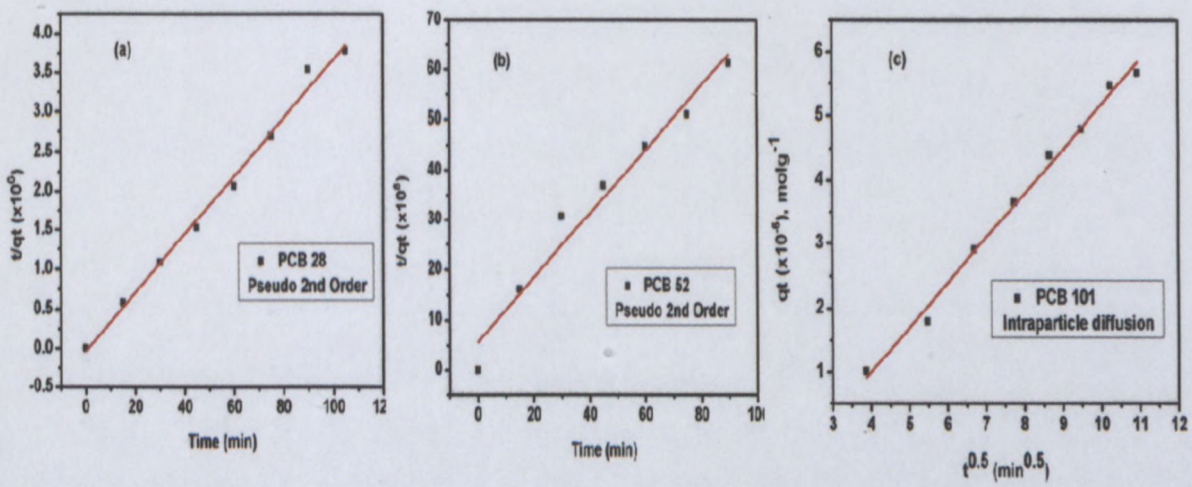

Figure 5.3: Graphical representation of various adsorption kinetic models used.

Results of the kinetic models used showed good correlation coefficients for pseudo-second-order kinetic model and supported the fact that adsorption of PCB congeners (PCB 28 and PCB 52) onto functionalized polyaniline coated sawdust follows a pseudo-second-order model (Figure 5.3). This kinetic model is associated with a chemisorption mechanism as

stated in the literature by Pirbazari and Weber, 1981 for a study on PCBs on carbon. In the case of PCB 101, the kinetic model that explained the nature of the adsorption process was found to be intraparticle diffusion model which suggested a possible diffusion limited step during adsorption.

For our kinetic data, R^2, and the quantity adsorbed at equilibrium q_e were calculated and estimated as shown in Table 5.1. The linear fits obtained by applying the pseudo second order model with the determination coefficient values ranged from 0.991 (PCB 28) to 0.962 (PCB 52) indicating that the behaviour was better approximated to the pseudo-second-order kinetics and for PCB 101 intraparticle diffusion model, it was found to fit with coefficient value of 0.992. For this model the rate constant (k_2) decrease with increasing chlorination, which could be attributed to the increased number of chloride ions available for adsorption. In both adsorption kinetics and isotherm studies, the models with the best fit data (Table 5.1 bold fonts) with the highest coefficient of correlations were preferred and considered in the adsorption studies of PANI/SD/TiO_2.

Table 5.1: Summary of the kinetic and isotherm parameters for adsorption of PCBs

Parameter	PCB 28	PCB 52	PCB 101
Pseudo first –order			
k_1/min	0.023	0.007	0.015
$Q_{e\ cal}$ (mol g^{-1})	1.890×10^{-5}	6.212×10^{-6}	4.540×10^{-5}
R^2,	0.916	0.928	0.846
Pseudo second-order			
k_2 ($gmol^{-1}$ min^{-1})	**2.41×10^{2}**	**91.95**	286.73
$Q_{e\ cal}$(mol g^{-1})	**2.770×10^{-5}**	**1.570×10^{-5}**	1.880×10^{-5}
R^2	**0.991**	**0.962**	0.848
Intraparticle Diffusion			
k_1 (mol $g^{-1}min^{-0.5}$)	4×10^{-9}	1×10^{-9}	**6.950×10^{-7}**
C (mol g^{-1})	3×10^{-9}	6×10^{-9}	**1.770×10^{-6}**
R^2,	0.892	0.910	**0.992**
Elovich a	1×10^{-8}	7×10^{-9}	2×10^{-6}
b	3×10^{-5}	1×10^{-9}	2×10^{-5}
R^2	0.845	0.855	0.907
Langmuir (R^2)	**0.999**	0.986	**0.954**
Freundlich (R^2)	0.955	**0.994**	0.910
Adsorption Capacity (mg g^{-1})	**8.090**	**4.580**	**3.760**

5.5.2 Adsorption equilibrium

Results of adsorption equilibrium for PCB 28, PCB 52 and PCB 101 are shown in Figure 5.4. The experimental results were analyzed by linear Langmuir and Freundlich isotherm models, two widely used models. Generally, Freundlich isotherm is empirical, whereas the Langmuir isotherm is based on different hypotheses. Langmuir model is the simplest theoretical model for monolayer adsorption onto a surface with finite number of identical sites. It is originally developed to represent chemisorptions on a set of distinct, localized adsorption sites (Abdullah *et al.,* 2009). The equation is applicable to homogeneous adsorption where adsorption process has equal activation energy, based on the following basic assumptions: (i) molecules are adsorbed at a fixed number of well-defined localized sites, (ii) each site can hold one adsorbate molecule, (iii) all sites are energetically equivalent, (iv) there is no interaction between molecules adsorbed on neighbouring sites.

The expression of the equation for Langmuir isotherm is given by;

$$\frac{C_e}{q_e} = \frac{C_e}{q_{\max}} + \frac{1}{kq_{\max}} \quad \text{.....Equation 4}$$

Where q_e is the amount adsorbed per mass of adsorbent (mg g^{-1}), q_{max} is the monolayer capacity (mg g^{-1}), C_e is the equilibrium concentration (mg L^{-1}) and k is a constant that is related to the energy of adsorption. Thus, a plot of C_e/q_e versus C_e is expected to give a straight line of slope $1/q_{max}$ and intercepts $1/kq_{max}$. Figure 5.2 shows the obtained results. The values for the correlation coefficients strongly supported the assumption that the adsorption data follows the Langmuir model of sorption since the Langmuir equation provided an accurate description of the experimental data, which was confirmed by the high values of the correlation coefficients.

The Freundlich expression is an empirical equation applicable to non-ideal sorption on a heterogeneous surface as well as multilayer sorption (Abdullah *et al.,* 2009). For the Freundlich isotherm, a linear expression form for the equation is given by;

$$\log q_e = \frac{1}{k_f} + \frac{1}{n} \log C_e \quad \text{.....Equation 5}$$

Therefore, a plot of ln q_e versus ln C_e should be a straight line of slope 1/n and intercept $1/k_f$ where q_e is the amount adsorbed per mass of adsorbent, k_f is the Freundlich constant, C_e is the equilibrium concentration and 1/n is interpreted as a heterogeneity factor (Ferreira *et al.,* 2004).

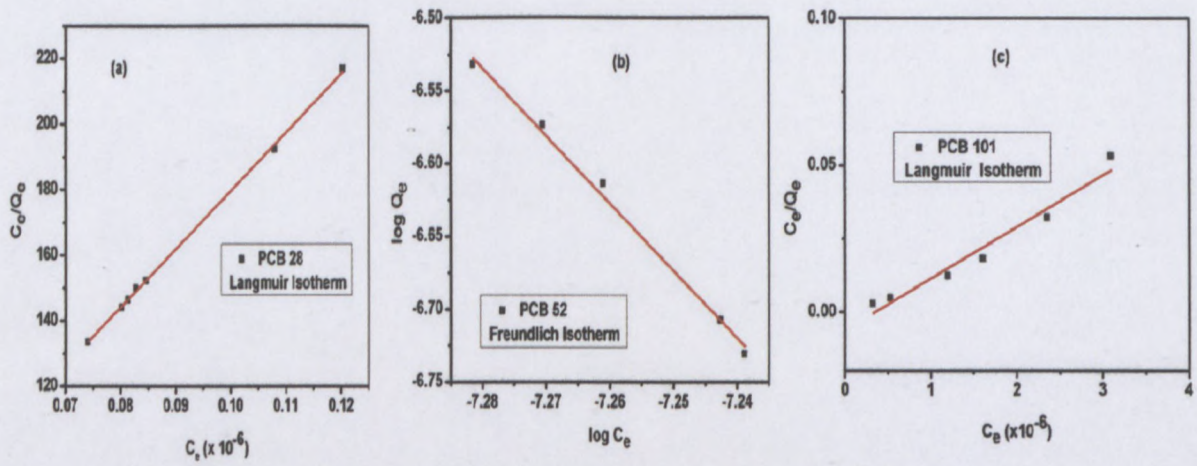

Figure 5.4: Langmuir and Freundlich isotherms as applied to the PCB adsorption.

The Langmuir equation did not reproduce equilibrium data satisfactorily for PCB 52 which could be attributed to the energetic heterogeneity of the PANI/SD/TiO_2 as similarly reported by Sotelo *et al.*, 2002. However, a better reproduction was obtained for PCB 28 and PCB 101, indicating that the ranges of adsorption energy for these compounds were narrower than that for PCB 52. The Freundlich isotherm led to reasonably good results for the PCB 52 (Figure 5.4) which was similar to results of PCB 52 adsorption onto fly ash (Sotelo *et al.*, 2002).

5.6 Conclusion

This study determined the potential of PANI/SD/TiO_2 to extract PCBs from contaminated media. PCBs adsorption followed a pseudo second order kinetic model for PCB 28 and PCB 52 whereas the PCB 101 adsorption obeyed intraparticle diffusion model. PANI/SD/TiO_2 adsorbent was used successfully for removal of selected PCB congeners. The adsorption capacity for the lower chlorinated PCB 28 was higher than the adsorption capacity for PCB 52 and PCB 101. Even though not all the 209 PCB congeners were tested, the results so far with three selected congeners strongly support the promising ability of the PANI/SD/TiO_2 to effectively extract various PCB congeners and give some insights into adsorption behaviour of PCBs on PANI/SD/TiO_2. For large-scale field applications of the PANI/SD/TiO_2 system, however, its reactivity under various practical conditions relevant in natural systems, where the technology is ultimately intended to be implemented, should be eventually confirmed. These include pH, temperature, co-existing natural organic matter, and adsorbent dosage.

A systematic study is needed to better understand the relationship between PANI/SD/TiO_2 adsorbent and PCB adsorption. The potential of the synthesized adsorbent to remediate PCBs was assessed with outstanding results. From the results discussed above it is clear that PANI/SD/TiO_2 can be used to remove PCBs from wastewaters.

5.7 References

Abdullah, M.A. Chiang, L. and Nadeem, M. 2009. Comparative evaluation of adsorption kinetics and isotherms of a natural product removal by Amberlite polymeric adsorbents. *Chem. Eng. J.*, 146: 370-376.

Ai, L., Jiang, J. and Zhang, R. 2010. Uniform polyaniline microspheres: A novel adsorbent for dye removal from aqueous solution. *Synth. Met.*, 160: 762-767.

Ansari, R. and Mosayebzadeh, Z. 2010. Removal of Eosin Y, an anionic dye, from aqueous solutions using conducting electroactive polymers. *Iran. Polym. J.*, 19(7): 541-551.

Ansari, R. and Raofie, F. 2006a. Removal of Lead Ion from aqueous solutions using sawdust coated by polyaniline. *CODEN ECJHAO E-Journal of Chemistry,* 3(10): 49-59.

Ansari, R. and Raofie, F. 2006b. Removal of Mercuric Ion from aqueous solutions using sawdust coated by polyaniline. *CODEN ECJHAO E-Journal of Chemistry,* 3(10): 35-43.

Ansari, R., Khoshbakht Fahim, N. and Fallah Delavar, A. 2009. Removal of Nitrite Ions from aqueous solutions using conducting electroactive polymers. *The Open Process Chemistry Journal,* 2: 1-5.

Ayad, M.M. and Abu El-Nasr, A. 2010. Adsorption of cationic dye (Methylene Blue) from water using polyaniline Nanotubes Base. *J. Phys. Chem.,* C114: 14377-14383.

Bartletta, M., Gisario, A., Rubino, G. and Tagliaferri, V. 2006. Electrostatic spray deposition (ESD) of 'self organizing' TiO_2-epoxy powder paints: Experimental analysis and numerical modelling. *Surface & Coatings Technology*, 201: 3212-3228.

Bia, G., De Pauli, C.P. and Borgnino, L. 2012. The role of Fe (III) modified montmorillonite on fluoride mobility: Adsorption experiments and competition with phosphate. *J. Environ. Manage.*, 100: 1-9.

Cornelissen, G. and Gustafsson, O. 2004. Sorption of phenanthrene to environmental black carbon in sediment with and without organic matter and native sorbates. *Environ. Sci. Technol.,* 38(1): 148-155.

Dore, M., Simon, P., Deguin, A. and Victor, J. 1986. Removal of nitrate from drink water by ion exchange-impact on the chemical quality of treated water. *Water Res.,* 20(2): 221-232.

Ferreira, S.L.C., Andrade, H.M.C. and dos Santos, H.C. 2004. Characterization and determination of the thermodynamic and kinetic properties of the adsorption of the molybdenum (VI)-calmagite complex onto activated carbon. *J. Colloid Interface Sci.*, 270: 276-280.

Ghosh, U., Weber A.S., Jensen, J.N. and Smith, J.R. 1999. Granular activated carbon and biological activated carbon treatment of dissolved and sorbed polychlorinated biphenyls. *Water Environ. Res.,* 71(2): 232-240.

He, B.L. and Huang, W.Q. 1995. Ion Exchangers and Polymeric Adsorbents, Shanghai Scientific and Technical Education, Shanghai: 439-452.

Huang, J., Yan, C. and Huang, K. 2009. Removal of p-nitrophenol by a water-compatible hypercrosslinked resin functionalized with formaldehyde carbonyl groups and XAD-4 in aqueous solution: A comparative study. *J. Colloid Interface Sci.*, 332(1): 60-64.

Jonker, M.T.O. and Koelmans, A.A. 2002. Sorption of polycyclic aromatic hydrocarbons and polychlorinated biphenyls to soot and soot-like materials in the aqueous environment: mechanistic considerations. *Environ. Sci. Technol.*, 36: 3725-3734.

Kastánek, F., Kuncováa, G. and Demnerová, K. 1995. Laboratory and pilot-scale sorption and biodegradation of polychlorinated biphenyls from ground water. *Int. Biodeterior. Biodegrad.*, 35(1-3): 287-300.

Kunin, R. 1976. The use of macro reticular polymeric adsorbents for the treatment of waste effluents. *Pure & Appl. Chem.,* 46: 205-211.

Li, A.M., Zhang, Q.X., Chen, J.L., Fei, Z.G., Chao, L. and Li, W.X. 2001. Adsorption of phenolic compounds on Amberlite XAD-4 and its acetylated derivative MX-4. *React. Funct. Polym.,* 49(3): 225-233.

Li, A.M., Zhang, Q.X., Zhang, G.C., Chen, J.L., Fei, Z.H. and Liu, F.Q. 2002. Adsorption of phenolic compounds from aqueous solutions by a water-compatible hypercrosslinked polymeric adsorbent. *Chemosphere*, 47(9): 981-989.

Lin, S.H. and Juang, R.S. 2009. Adsorption of Phenol and its derivatives from water using synthetic resins and low cost natural adsorbents: A review. *J. Environ. Manage.*, 90: 1336-1349.

Matthes, W. and Kahr, G. 2000. Sorption of organic compounds by A1 and Zr-hydroxy-intercalated and pillared bentonite. *Clays clay miner.,* 48(6): 593-602.

Nollet, H., Roels, M., Lutgen, P., Van der Meeren, P. and Verstraete, W. 2003. Removal of PCBs from wastewater using fly ash. *Chemosphere,* 53: 655-665.

Pan, B.J., Pan, B.C., Zhang, W.M., Zhang, Q.X., Zhang, S.R. and Zheng, S.R. 2008. Adsorptive removal of phenol from aqueous phase by using a porous acrylic ester polymer. *J. Hazard. Mater.*, 157: 293-299.

Pirbazari, M. and Weber, W.J. 1981. Adsorption of polychlorinated biphenyls from water by activated carbon. In: Cooper N.J. (ed.) Chemistry Water Reuse, vol. 2. USA: Ann Arbor Science: 309-339.

Qu, X., Tian, M., Liao, B. and Chen, A. 2010. Enhanced electrochemical treatment of phenolic pollutants by an effective adsorption and release process. *Electrochim. Acta*, 55: 5367-5374.

Sahin, M., Gorcay, H., Kir, E. and Sahin, Y. 2009. Removal of calcium and magnesium using polyaniline and derivatives modified PVDF cation-exchange membranes by Donnan dialysis. *React. Funct. Polym.,* 69: 673-680.

Shen, Yun-Hwei. 2002. Removal of phenol from water by adsorption–flocculation using organobentonite. *Water Res.*, 36(5): 1107-1114.

Sotelo, J.L., Ovejero, G., Delgado, J.A. and Martinez, I. 2002. Comparison of adsorption equilibrium and kinetics of four chlorinated organic from water onto GAC. *Water Res.*, 36: 599-608.

Uhle, M.E., Chin, Y.P. and Aiken, G.R. 1999. Binding of polychlorinated biphenyls to aquatic humic substrates: The role of substrate and sorbate properties on partitioning: *Environ. Sci. Technol.*, 33: 2715-2718.

Vansant, E.F. 1999. New composite adsorbents for the removal of pollutants from waste waters. *Stud. Surf. Sci. Catal.*, B120: 381-396.

Walther, H.J., Kaeding, J. and Fecimer, P. 1984. Capacity of macroporous adsorber polymers in the elimination of organic micro contaminants. *Acta. Hydrochim. Hydrobiol.*, 12(2): 173-181.

Yoon, T.H., Benzerara, K., Ahn, S., Luthy, R.G., Tyliszczak, T. and Brown, G.E. 2006. Nanometer-scale chemical heterogeneities of black carbon materials and their impacts on PCB sorption properties: soft X-ray spectromicroscopy study. *Environ. Sci. Technol.,* 40(19): 5923-5929.

CHAPTER SIX
CONCLUSION AND RECOMMENDATION

6.1 Conclusion

This chapter deals with conclusions of the results presented in this study and makes further recommendations for electrochemical analysis and remediation research. This study has been directed towards the development of an electrochemical method of analysing PCBs using square wave voltammetric (SWV) technique and application in the remediation of PCBs from contaminated solutions using low cost adsorbent, TiO_2 functionalised polyaniline coated sawdust (PANI/SD/TiO_2). The approach taken involved optimization of supporting electrolyte used and determination of a suitable potential window of study. From this study, 0.1 M TBAP/ACN/PBS 80:20 v/v solution was used as supporting electrolyte and a potential window of 500 mV to -2500 mV was proposed as the best conditions. Glassy carbon electrode (GCE) was also proposed as a suitable electrode for the reduction of PCBs (PCB 28, PCB 52 and PCB 101). The results from the method development gave lower limits of detection which made the method an approachable alternative compared to the other techniques reported in the literature.

Another approach which was taken in the study was to chemically prepare PANI and its composites (PANI/SD, PANI/TiO_2 and PANI/SD/TIO_2) for property comparisons relative to the material of interest, i.e. PANI/SD/TiO_2. Morphology and stability of these materials was investigated and results showed that the introduction of SD and TiO_2 to the structure of PANI improved its surface and stability properties for other applications.

The success of the characterization studies was observed with the various techniques employed in the previous discussions. UV-visible and infrared spectroscopic studies showed that SD and TiO_2 particles affected the quinoid units along the polymer backbone and indicated strong interactions, otherwise known as the doping effect between SD and TiO_2 particles and the quinoidal sites of PANI. From the SEM and TEM micrographs, the morphology of the neat PANI revealed homogenous surfaces while the micrographs of the composites clearly indicated uniform dispersion within the materials, which contributed to the enhanced application of the PANI/SD/TiO_2 composite as adsorbents. The thermostability measurements showed an increase in stability in the order of PANI < PANI/SD < PANI/SD/TiO_2 < PANI/TiO_2. From these observations, PANI/SD/TiO_2 and PANI/TiO_2 were deduced as good candidates for applications such as adsorption that can withstand temperature changes. The PXRD studies also confirmed the presence of SD and TiO_2

particles in the PANI/SD/TiO_2 composite with the degree of crystallinity in PANI changing from crystalline to armphous in the resulting composites formed.

The work presented here opens an entirely new approach in the analysis and remediation of PCBs in the environment through the development of a simple, sensitive and user friendly electrochemical method coupled with the synthesis of novel adsorbent material, which is environmentally friendly.

6.2 Future work and Recommendation

The following aspects of the development of an electroanalytical method of PCB analysis and remediation studies need further investigation:

- Though, bare GCE was used for my work, future studies to further establish how other modified GCE would perform.

- This study considered reduction due to chlorine loss generally but further investigation on the selectivity of reduction is necessary to define the order of reaction and provide an understanding of the chlorine regio-selectivity during the electrochemical reduction process.

- In order to obtain a comprehensive understanding of the reductive cleavage of PCBs, it is essential to carry out further extensive computational studies in conjunction with the bulk electrolysis.

- More work on the optimization of the adsorption studies to be considered by varying different parameters such as pH, initial concentration, dose of adsorbent, size of adsorbent particle and working temperature. This would possibly improve the performance of the adsorption process and make it more reliable than reported here.

- This work focused on the potential of the new material, PANI/SD/TiO_2 to extract PCBs from aqueuos solutions. However, batch isotherms and column tests should be done to determine PANI/SD/TiO_2 properties for enhanced PCB adsorption.

APPENDICES

Appendix A: EDX spectrum for PANI/TiO_2

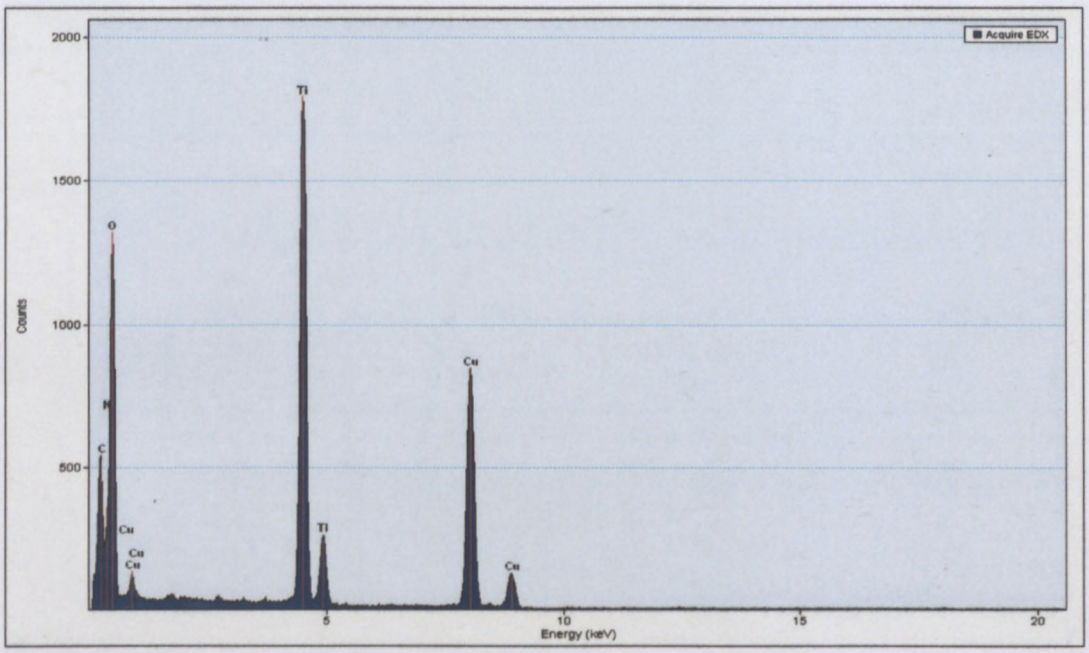

Appendix B: EDX spectrum for PANI/SD

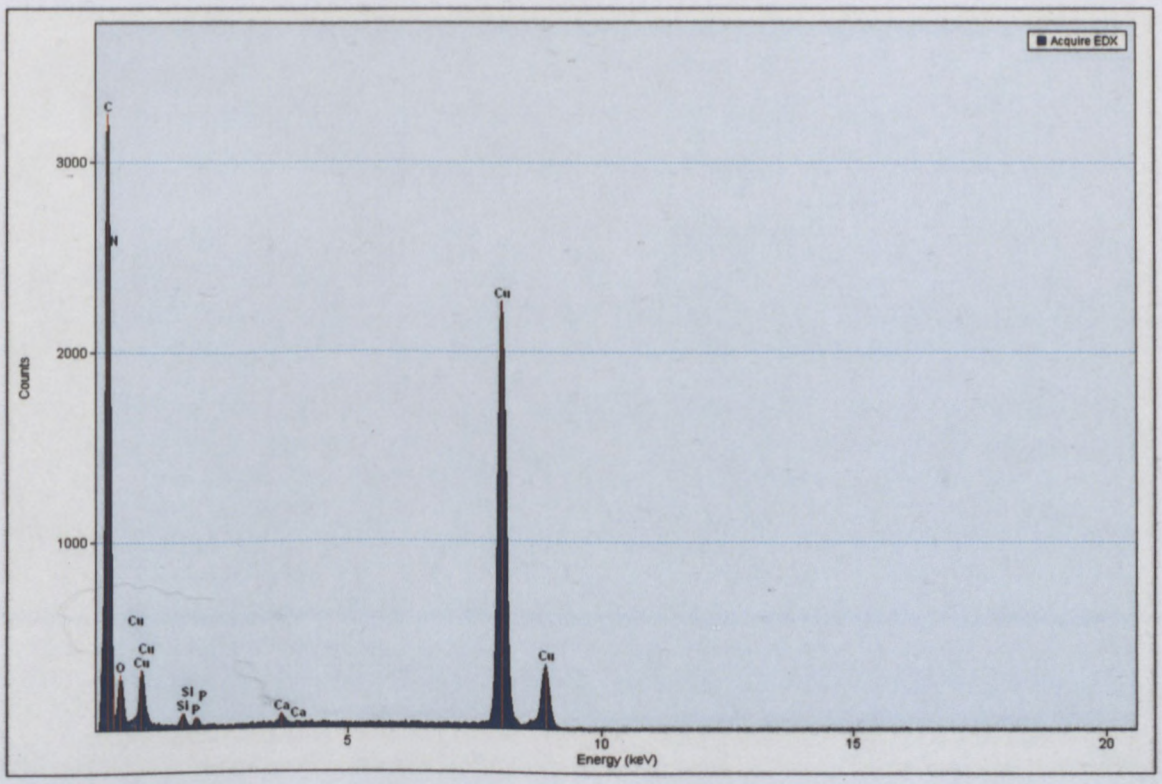

Appendix C: EDX spectrum for PANI/SD/TiO_2

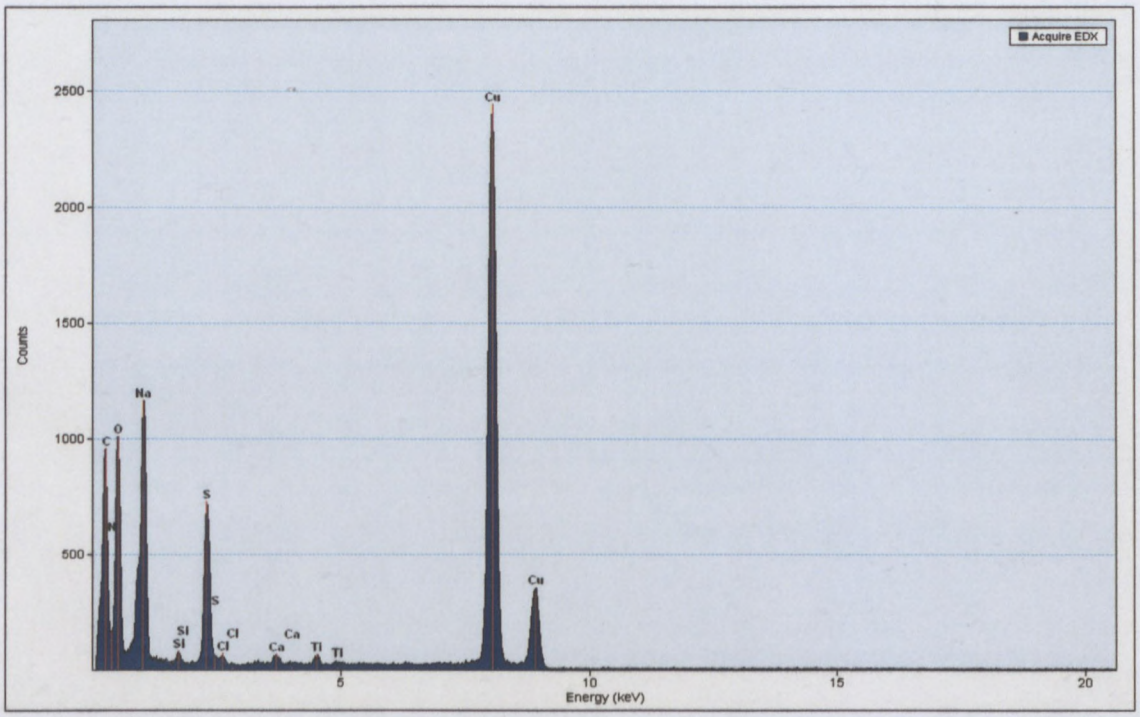

Appendix D: EDX spectrum for PANI

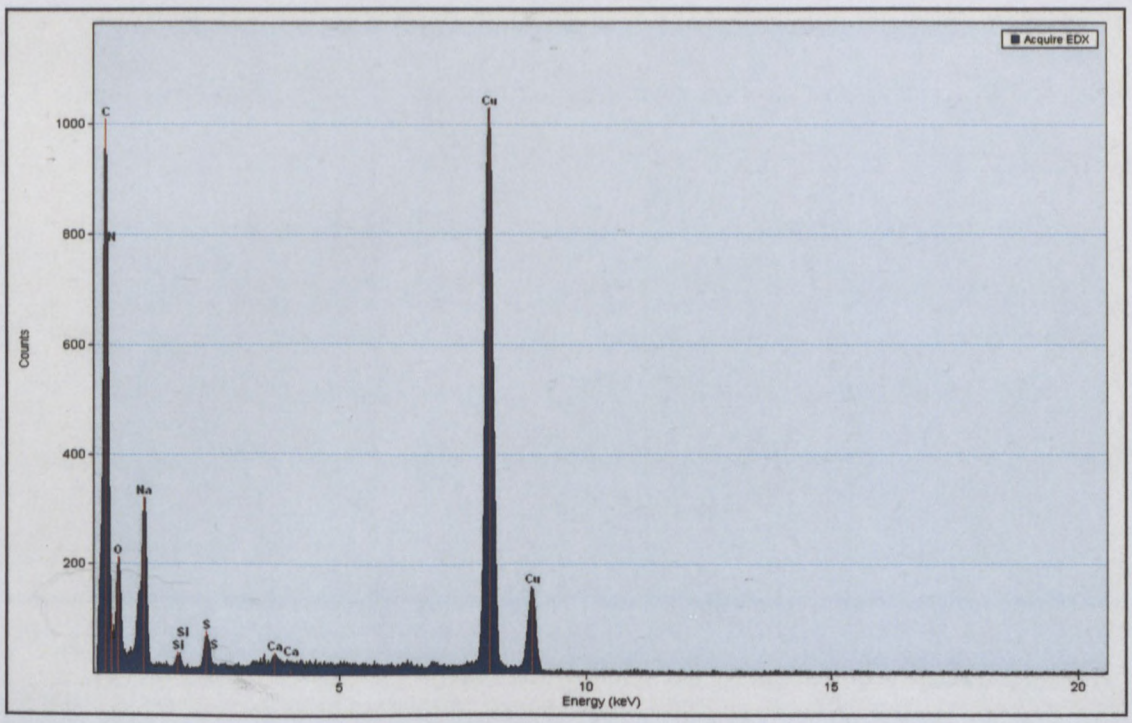

Appendix E: EDX spectrum for acid treated sawdust